POLITECNICO DI MILANO

Scuola di Ingegneria Civile, Ambientale e Territoriale

Corso di Laurea in Environmental and Geomatic Engineering

LOW-COST GNSS RECEIVERS FOR GEODETIC LOCAL MONITORING

Relatore: Chiar.mo Prof. Ludovico Biagi

Correlatore: Ing. Marco Negretti

Tesi di Laurea di:
GREC Florin Cătălin
Matr. 813510

Anno academic 2014/2015

Abstract

Landslides cause fatalities and property damage throughout the world. To reduce the impact, real-time and near-real-time landslide monitoring systems must be developed and used. The purpose of local monitoring is to detect when hill slopes are primed for sliding and can provide early indications of rapid, catastrophic movement.

For certain applications, latency of the monitoring results is not a crucial point. In other cases only small latencies are acceptable: for example, a suspected Alpine landslide that insists on villages. In these cases, continuous quasi real time monitoring by permanent stations is required. Here, a typical monitoring configuration is given by a GNSS permanent station, outside the monitored area, in a stable site and several permanent stations in the monitored area. Data can be processed and the results can be monitored in a quasi-continuous way by automated procedures. In these situations, the use of low cost GNSS receivers could be interesting because it can significantly increase the number of monitored points without notably increasing the network cost. This investigation is the scope of our work and several experiments have been set up and performed/will be performed to assess them.

To reach our goals, geodetic and low cost receivers are teamed up: Leica GR10 as reference station and single - frequency u-blox 7P receivers. The author discovered few of the shortcomings of u-blox receiver: lack of antenna calibrations, multipath-prone, gaps of few seconds in the raw data and big number of cycle slips. 3 experiments have been planned and performed in Como and Milano. Once the acquisition phase was completed data was processed with commercial (Leica GeoOffice), academic (Bernese) and free and open source software (goGPS and RTKLIB). The results are compared in the final step of the project, accuracy and reliability of solutions are discussed. All experiments proved that u-blox is capable in detecting displacements at centimetre level, in few cases even below 1 cm. Moreover, better accuracy is obtained if length of the baseline is considered and not the coordinates separately.

The outline of the dissertation is as follows:

- Chapter 1 stands as an introduction for this research, motivation, objectives and questions are presented.
- Chapter 2 presents an overview about GNSS systems. The main updates applied to GPS (L5 signal) and Galileo (latest launching missions) are listed. It presents also SBAS systems.

- Chapter 3 discusses the type of GNSS receivers today on the market with emphasize on the geodetic receivers and evaluation kit (EVK) used for this thesis. The challenges faced by u-blox are briefly reported.
- Chapter 4 introduces the double differencing technique on phase observations. Strategies followed by Bernese, Leica Geo Office (LGO), goGPS and RTKLIB are discussed in detail.
- Chapter 5 describes the research approach and the three experiments performed to reach the objectives stated in the Introduction.
- Chapter 6 is responsible for presenting the pre-processing stage, processing stage and results of each of the three experiments conducted in the field, and to validate the applicability of u-blox NEO-7P for landslide monitoring
- Chapter 7 concludes the research with a series of conclusions and recommendations for future work.

Acknowledgements

This thesis would not have been possible without the help of few people that in a way or another contributed to my work.

I would like to express my deep gratitude to Professor Ludovico Biagi, my research supervisor, for his patient, guidance, enthusiastic participation and thorough explanations. Moreover, I would like to thank him for providing me with the most favourable work conditions throughout the period of my research and for helping me to solve all administrative problems.

I would like to express my appreciation to Maria Grazia Visconti for helping me in mastering Bernese GPS Software and Leica Geo Office. Her extensive knowledge about these scientific software proved to be very useful for my work.

I would also like to thank to Marco Negretti for his continuous assistance in keeping my progress on schedule. I am grateful for providing me the instrumental setup required to conduct the field tests in Como.

My regards to Gabriele Colosimo for proofreading and evaluating my thesis in his quality of external co-examiner.

I would like to thank to Frank Pache for giving me the opportunity to follow an internship in Leica Geosystems, in the Networked Reference Stations department. This internship increased my knowledge about GNSS technology and proved to be a solid foundation for my thesis.

Thanks to Youssef Tawk and Christian Waese for everything they taught me about Leica GR10 and Leica GRX1200 receivers. Moreover, based on the training provided by them I could use with success Spider QC software in analysing and interpreting better the data used for this research.

I would like to thank Mirko Reguzzoni and Riccardo Barzagli for their assistance with the collection of data for Milano Prova experiment.

Last but not least, I am grateful to my family for their unconditional love, support, encouragement, prayers and confidence in me.

Contents

List of Figures

List of Tables

Table of Acronyms

APME A Posteriori Multipath Estimator

APV Approaches with Vertical guidances

ARP Antenna Reference Point

ASCII American Standard Code for Information Interchange

ATX Antenna Exchange Format

BDS BeiDou

BIH Bureau International de l'Heure

BPSK Bi-phase shift key

C/A Coarse Acquisition

CDMA Code Division Multiple Access

CGCS200 China Geodetic Coordinate System 2000

CODE Centre for Orbit Determination in Europe

CORS Continuously Operating Reference Station

CRC Cyclic redundancy check

CS Commercial Service

CTP Conventional Terrestrial Pole

DD double differences

DGPS Differential GPS

DGNSS Differential GNSS

DoD Department of Defense

DTM Digital Terrain Model

ECEF Earth-Centred Earth-Fixed

EGNOS European Geostationary Navigation Overlay Service

ESSP European Satellite Services Provider

FAA Federal Aviation Administration

FARA Fast Ambiguity Resolution Approach

FDMA Frequency Division Multiple Access

FEC Forward Error Correction

FOC Full Operational Capability

FOSS Free and Open Source Software

FTP File Transfer Protocol

GAGAN GPS and GEO Augmented Navigation

GEO Geostationary Earth Orbit

GIC Ground Integrity Channel

GIS Geographic Information System

GLONASS Global Navigation Satellite System

GNSS Global Navigation Satellite Systems

GPS Global Positioning System

HOW Handling Word

ICD Interface Control Document

IERS International Earth Rotation Service

IGS International GPS Service

IGSO Inclined Geosynchronous Satellite Orbit

IOD Issue of Data

IONEX Ionosphere Map Exchange format

IOV In Orbit Validation

IRP International Reference Pole

IRM International Earth Rotation Service Reference Meridian

ITRF International Terrestrial Reference Frame

ITRS International Terrestrial Reference System

LAN Local Area Network

LAMBDA Least-Squares Ambiguity Decorrelation Adjustment

LGO Leica Geo Office

MEO Medium Earth Orbit

MIL-STD Military Standard

MIT Massachusetts Institute of Technology

MSAS Multi-functional Satellite Augmentation System

NAVSTAR Navigation Satellite Timing and Ranging

NMEA National Marine Electronics Association

NOAA/NGS National Oceanic and Atmospheric Administration/National Geodetic Survey

NPA Non-Precision Approaches

NTRIP Networked Transport of RTCM via Internet Protocol

OCXO Oven Controlled Crystal Oscillator

OS Open Service

PCC Phase Centre Corrections

PCF Program Control File

PCO Phase Centre Offset

PCV Phase Centre Variations

PDOP Position Dilution of Precision

PPP Precise Point Positioning

PRN Pseudo-Random Noise

PRN Pseudo Random Noise

QZSS Quasi Zenith Satellite System

RINEX Receiver Independent Exchange Format

RIMS Ranging and Integrity Monitoring Stations

RTCM Radio Technical Commission for Maritime Services

RTK Real Time Kinematic

SBAS Satellite Based Augmentation Systems

SNR Signal to Noise Ratio

SoL Safety of Life Service

SPS Standard Positioning Service

TCXO Temperature Compensated Crystal Oscillator

TEC Total Electron Content

TLM Telemetry Word

TPS Total Station

USB Universal Serial Bus

UTC Coordinate Universal Time

UTM Universal Transverse Mercator

WAAS Wide Area Augmentation System

WAD Wide Area Differential

Chapter 1. Introduction

1.1. Motivation

Landslides are a serious geologic hazard common to almost every country in the world. Is defined as the movement of a mass of rock, debris, or earth down a slope (Crude, 1991). Almost every landslide has multiple causes. Slope movement occurs when forces acting down – slope (mainly due to gravity) exceed the strength of the earth materials that compose the slope. Landslides can be initiated in slopes already on the verge of movement by rainfall, snowmelt, changes in water level, stream erosion in ground water, earthquakes, volcanic activity, disturbance by human activities, or any combination of these factors. Landslides can move slowly (millimetres per year) or can move quickly and disastrously, as is the case with debris flow.

It is estimated that in the United States, they cause in excess of $1 billion in damages and from about 25 to 50 deaths each year. In Italy, landslides kill or injure people almost every year. Information exists on the direct damage to the population caused by different natural hazards, including landslides: the most recent catalogue covers a 68 years' time window, from 1941 to 2010, and lists 3139 landslide events that have resulted in deaths, missing persons, injured people and homelessness (Salvati et al., March 2010).

Length of period (yr)	59 (1950-2008)
Deaths (a)	4077
Missing persons (b)	26
Injured people (c)	2019
Fatalities (a+b)	4103
Evacuees and homeless people	177 376
Largest number of fatalities in an event	1952
Total number of events	2204

Table 1. 1: *Statistics of landslide and flood events with deaths, missing persons and injured people in Italy, for period 1950 – 2008 (after Salvati et al.).*

Figure 1.1 shows the location of 2533 sites that suffered one or more landslide events with direct consequences to the population of Italy, in the 1359 year period 650 – 2008. Map in the upper-right corner shows density of landslide sites per square kilometre, in five classes.

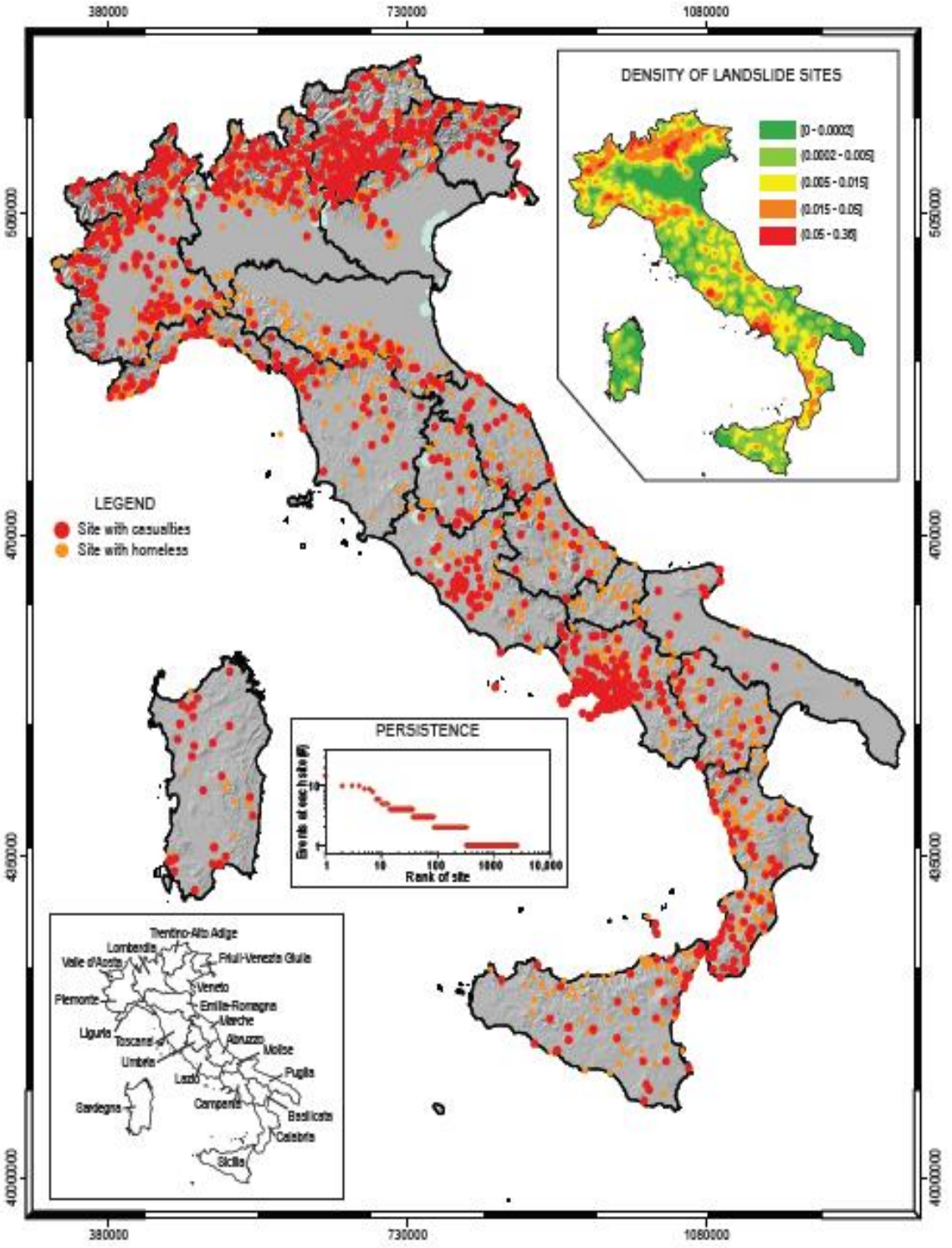

Fig. 1. 1: *Map showing the location of 2533 sites affected by landslide events with direct consequences to the population of Italy. Map in the upper-right corner shows density of landslide sites per square kilometre (after Salvati et al.).*

In Romania, landslides represent a common natural hazard, threatening property, infrastructures and human lives. Luckily, the number of deaths associated with landslides is very low but tends to increase because the frequency of events increases as well, mainly due to deforestation in hilly region and climate change between 1962 and 2000. The surface

exposed to the landslide risk is 800 000 ha, where are located 50 000 households in which live 250 000 people. Area with the highest risk is located in the southern and south-western Carpathian arc (Maftei, R., Tudor, E., Vina, G., Porumbescu, C.,). Bălteanu et al. computed a Landslide Susceptibility Index (based on many variables) and it may range from 0 to 10, where 0 - 2 range is no susceptibility and 7 – 10 range is very high susceptibility. The no susceptibility class represents 39.2 % of the territory and the very high susceptibility class reaches 13.4 % (see Figure 1.2).

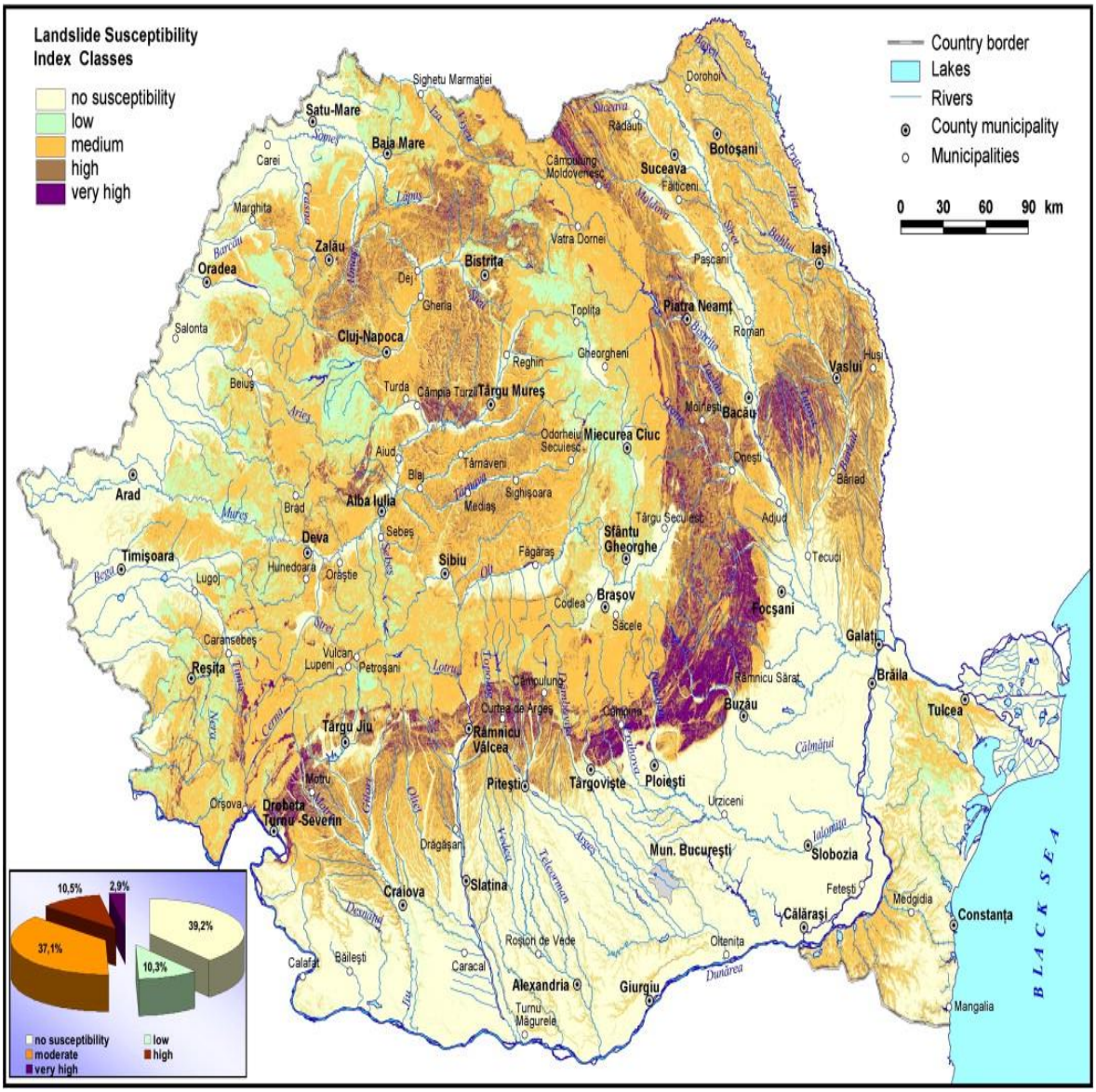

Fig. 1. 2: *Landslide susceptibility classes in Romania (after Bălteanu et al.).*

The monitoring of landslides areas is a multi-disciplinary approach which leads to the estimation of the slope development and safety measures. Globally, landslides cause hundreds of billions of dollars in damages and hundreds of thousands of deaths and injuries

each year. Because of this reasons, more and more techniques that can help in reducing the number of casualties and the amount of material losses were developed. In the past, these have been monitored by geotechnical instruments such as accelerometers and displacement transducers. Nowadays, new techniques have been developed and consists in geodetic and geotechnical measurements.

According to Braun, the geodetic monitoring methods, these can be divided into point and area. In point methods, specific points are monitored. When the spatial position of these monitored targets move between measurements sessions, after comparing with the other points, conclusions about the slope are formulated. This method works well if there is a good coverage in the whole territory. In 'area' methods the entire critical zone is surveyed and the measured points are selected on the very faults and within a regular grid (Braun, J., Hanek, P., 2014).

In both cases, the campaign sessions include classical terrestrial measurements using total stations or levels and more new technique, GNSS (Global Navigation Satellite Systems) survey sessions. The measurements with GNSS are easier than terrestrial methods, but the accuracy of position mainly depends on the observation time, atmosphere conditions, unobstructed view of sky, number of satellites and transformation of coordinates intro reference system (Raska, Popisil, 2011). A good monitoring system is one with an early warnings and high reliability. Among the possible choices, GNSS can be an option for observing the displacements of earth surface and inform in time the residents of an area prone to landslides due to its accuracy and real-time monitoring, providing optimal observation conditions.

No doubt, pricey geodetic and geotechnical instrumentation is available as well as for surface and subsurface deformations and also the triggering influences like precipitation. For economic reasons, however, all these techniques are not used in too many situations for obvious reasons. At the same time, the worldwide number of sites with an urgent need for monitoring is increasing. Thus, cost effective geodetic approaches are requested and constitute the basis of the research questions of this thesis.

1.2. Research Questions

This research aims to evaluate the performance of low - cost GNSS receivers for static in near real – time processing. An integrated monitoring system (see Figure 1.3) is much more

complex and consists in both hardware and software parts. In landslide monitoring, geodetic methods are applied together with geotechnical methods using, among others, inclinometers, declinators, extensometers, accelerometers and hydrostatic levelling instruments to measure deformations, stresses and forces (Braun, J., Hanek, P., 2014). For the purpose of this research, these aspects are not important and all attention will be shifted to geodetic methods by low - cost sensors.

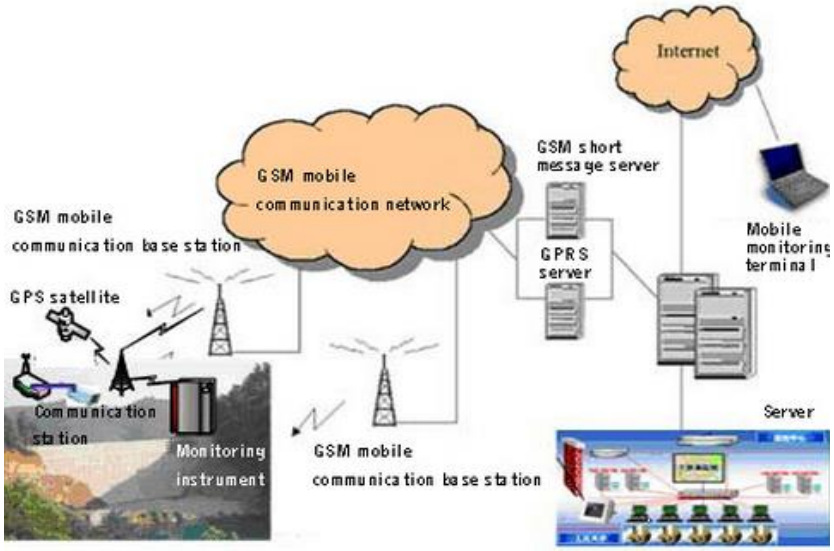

Fig. 1 3: *Integrated monitoring system.*

The slow movement of a landslide is about few millimetres a year. However, in active area the movements reach centimetre level. Therefore, we decided to focus on movements of 1-2 centimetres, which leads to the first question of this project:

What accuracy can low cost sensors reach when used for monitoring purposes?

Accuracy is not the only performance parameter that should be checked. Many times the geometry of the constellations, atmosphere, environment, electronic noise and other causes can significantly degrade the final position accuracy (presence of outliers). Thus, one would be interested in reliability of the monitoring system, i.e. probability during the period of operation that an error might result in a computed position error exceeding a maximum allowed value. All this leads to another question:

How reliable are the results obtained? How many outliers (false alarms) are expected for unity of time?

The increase of number of dangerous sites and the high cost of geodetic and geophysical sensors translate into high monitoring costs. In addition to this constraints, when a landslide event take places all the instruments placed in the active area will be lost; again, the need of low cost sensors arises.

Which are the main problems and how can they be overcome?

One of the characteristics of a low cost GNSS receiver is its capacity of acquiring signal emitted only on L1 frequency. This is a major setback especially for removing ionosphere delays: since Iono free combination cannot be used, models or IGS products have to be considered. Moreover, multipath is another source of errors and its behaviour is site dependent, therefore very difficult to deal with.

A secondary issue that needs to be stressed is related to the chosen processing software. Assuming the best low cost GNSS receiver is used, there is still another part that has to be addressed, namely the solution for processing the raw data.

The available software on the market can be classified in two groups: Free and Open Source Software and commercial software. Inside these two categories, a further classification can be made: the software can be or not a scientific one, usually developed in a university or research institute. Table 1.2 gives a better view over the main GNSS processing software available today.

FOSS		**Commercial**	
Scientific	**Non scientific**	**Scientific**	**Non scientific**
GAMIT (developed in MIT)	goGPS, RTKLIB	Bernese GPS software	Leica Geo Office,

Table 1. 2: *GNSS software market situation.*

Nowadays, FOSS software are better and better bridging more and more the gap with costly, commercial software. Consequently, a new question had to be answered:
Are GNSS FOSS software at the same level with a commercial one?

1.3. Research Objectives

The duration of this master research has been limited to 6 months. Thus, the work has focused on the above questions, rather than attempting to cover all aspects of landslide monitoring by means of GNSS technology.

This research has the following objectives:

Objective 1: Experimentally study and compare the performance of a low cost GNSS receiver with the professional grade GNSS receivers.

The price of the monitoring unit is an important factor that should be considered in such application. The challenge is to have a robust GNSS equipment which records continuously movements on the surface and can give results with an accuracy of about 1 – 2 centimetre or even sub centimetre range in order to detect even the slow movements of earth surface in a slide area.

This kind of accuracy can be obtained only from evaluation of carrier phase measurements over a certain time span. Usually, a time window of approx. 15 – 60 min is considered (Gunther, 2008).

Objective 2: Experimentally study a more efficient method to process raw data.

A wide variety of GNSS post processing software are going to be used both commercial and Free and Open Source Software (FOSS). Then, the results will be compared and discussed in detail. Of particular interest is to check how good does the Kalman filter performs compared to the traditional Least-Square Adjustment. Experiments in different environments will be carried out to identify the reliability of the u-blox sensors in locations with and without error sources. To fully accomplish this objective, the thesis should state if FOSS programs can give results close enough to commercial software, which processing parameters should be used (cut-off angle, ionosphere models and so on) and what can be done to improve more the processing.

Objective 3: Discover if the detected variations agree with the imposed ones.

In other words, we want to evaluate if and at what level of precision there is a correspondence between controlled displacements and position variations detected by the low – cost sensor. For this, an experiment consisting in moving the antenna on a sliding device 5 mm after every 3 hours was planned and executed.

Constraint 1: The site location.

Some of the experiments have to be performed in location with error sources and not clear – sky condition. In the real world, the sensors have to be installed in the critical area no

matter how the relief and the surrounding environment look like. Therefore, if the monitoring takes place in area with multipath sources or forests the results are expected to be influenced and distorted by these. For the present research, most of the experiments were performed in area with acceptable observation conditions to exploit at maximum the capabilities of u-blox. However, in future few short tests will be performed in more harsh testing environments.

Constraint 2: An active landslide site.

An actual landslide would not be monitored because of three main reasons: (1) before investing money and time in landslides monitoring by means of low-cost sensors these devices must be first tested under laboratory conditions to be sure they are reliable and accurate enough for such application, (2) in the near vicinity of the research place there is no landslide monitored by geodetic, pricey sensors therefore there is no reference for confronting the results of the low – cost sensor, (3) although the u-blox sensors are low – cost devices is still not acceptable to monitor a landslide and lose the receiver and the data, in case the event take places.

Constraint 3: Shortcomings of u-blox receivers.

For this research, u-blox NEO 7P has been chosen. This is a low – cost sensor, produced by the Swiss company u-blox, capable of tracking GPS, GLONASS, BeiDou and QZSS system. Low-cost receivers use narrow-band filters to limit the sampling frequency. It results in noisier code, Doppler and carrier phase measurements. Additionally, high-end receivers usually use patented multipath mitigation techniques to remove the effect of multipath measurements, such as vision correlators from Novatel (Fenton, et al., 2005) or the A Posteriori Multipath Estimator (APME) technique from Septentrio (Sleewaegen, et al., 2005). This leads to more precise pseudorange measurements.

Additionally low-cost receivers are usually equipped with low performance Temperature Compensated Crystal Oscillator (TCXO) whereas high-end receivers usually use very stable Oven Controlled Crystal Oscillator (OCXO) or higher – grader oscillators. More stable oscillators allow longer integration time.

Constraint 4: u-blox 7P cannot track in the same time GLONASS and GPS.

A receiver capable to track in the same time more satellite systems will offer better solution because of the increased number of observations and because of the improvement of the geometry of the satellites. Unfortunately, the tested device is not capable of tracking simultaneous more than 1 constellations. Not long ago, a new generation of u-blox, 8M, was released and this offer the option to track more than one satellite constellation in the same time.

Constraint 4: Antenna calibration of u-blox.

At this moment Phase Centre Variations (PCV) and Phase Centre Offset (PCO) of u-blox antenna are not included in the standard Antenna Exchange Format (ATX) calibration file that may be included in GNSS software. This means that the results will be affected by some errors caused by lack of antenna calibration. However, their magnitude should not be more than 1 centimetre (Bernese GPS software user manual). This kind of errors are not critical in applications like landslide monitoring where one expects to see displacements at centimetre level. For Precise Point Positioning (PPP) the antenna offset has to be known. Efforts in this direction have been made by Schwieger & Wanninger (2006) in their investigations about accurate positioning using low – cost GPS sensors.

1.4. Thesis Outline

The outline of the dissertation is as follows:

- Chapter 1 stands as an introduction for this research, motivation, objectives and questions are presented.
- Chapter 2 presents an overview about GNSS systems. The main updates applied to GPS (L5 signal) and Galileo (latest launching missions) are listed. It presents also SBAS systems.
- Chapter 3 discusses the type of GNSS receivers today on the market with emphasize on the geodetic receivers and evaluation kit (EVK) used for this thesis. The challenges faced by u-blox are briefly reported.
- Chapter 4 introduces the double differencing technique on phase observations. Strategies followed by Bernese, Leica Geo Office (LGO), goGPS and RTKLIB are discussed in detail.
- Chapter 5 describes the research approach and the three experiments performed to reach the objectives stated in the Introduction.

- Chapter 6 is responsible for presenting the pre-processing stage, processing stage and results of each of the three experiments conducted in the field, and to validate the applicability of u-blox NEO-7P for landslide monitoring
- Chapter 7 concludes the research with a series of conclusions and recommendations for future work.

Chapter 2. Review of GNSS

This chapter provides an overview of GNSS technologies and the way the positioning is performed. It begins with a short description of the Global Positioning System and an overview of the L1 C/A signal. At the moment, there are 4 global navigation systems fully operational or under development: NAVSTAR-GPS, GLONASS, Galileo and BeiDou.

2.1. Global Positioning System (GPS)

The GPS is a satellite-based system that can be used to locate positions anywhere on the earth. Operated by the U.S. Department of Defense (DoD), NAVSTAR (NAVigation Satellite Timing and Ranging) GPS provides continuous, real-time, 3-dimensional (3-D) positioning, navigation and timing worldwide. Any person with a GPS receiver can access the system, and it can be used for any application that requires location coordinates.

The broadcast ephemeris describes a position of transmitting antenna phase centre of given satellite in the WGS84 Earth-Centred Earth-Fixed (ECEF) reference frame, this is the reference system for the GPS and it is compatible with the International Terrestrial Reference System (ITRS). WGS84 is based on a consistent set of constants and model parameters that describe the Earth's size, shape, and gravity and geomagnetic field; is defined as follows:

- The origin is located at the centre of the Earth's body,
- The Z-axis is the direction of the IERS Reference Pole (IRP). This direction corresponds to the direction of the BIH Conventional Terrestrial Pole (CTP),
- The X-axis is defined by the intersection of the IERS Reference Meridian (IRM) and the equatorial plane,
- The Y-axis completes a right-handed, ECEF orthogonal coordinate system.

The defining parameters of WGS84 are the semi-major axis of the WGS84 ellipsoid and the flattening factor of the Earth:

Semi-major axis: $a = 6\,378\,137.0$ m

Flattening: $f = 1/298.257223563$

2.1.1. GPS segments

The GPS system consists of three segments:

1) the space segment: the GPS satellites themselves,

2) the control system, operated by the U.S. military,

3) the user segment, which includes both military and civilian users and their GPS equipment.

a. Space Segment: The GPS Constellation

The first GPS satellite was launched by the U.S. Air Force in early 1978. There are now at least 24 MEO satellites orbiting the earth at an altitude of about 20 200 km. The high altitude insures that the satellite orbits are stable, precise and predictable, and that the satellites' motion through space is not affected by atmospheric drag. These 24 satellites make up a full GPS constellation; however, today there are more than 30 satellites in orbit.

The GPS satellites are powered primarily by sun-seeking solar panels, with NiCad batteries providing secondary power. On board each GPS satellite are four atomic clocks, only one of which is in use at a time. These highly accurate atomic clocks enable GPS to provide the most accurate timing system that exists.

Satellite Orbits

There are at least four satellites in each of 6 orbital planes (see Figure 2.1). Each plane is inclined 55 degrees relative to the equator, which means that satellites cross the equator tilted at a 55 degree angle. The system is designed to maintain full operational capability even if two of the 24 satellites fail.

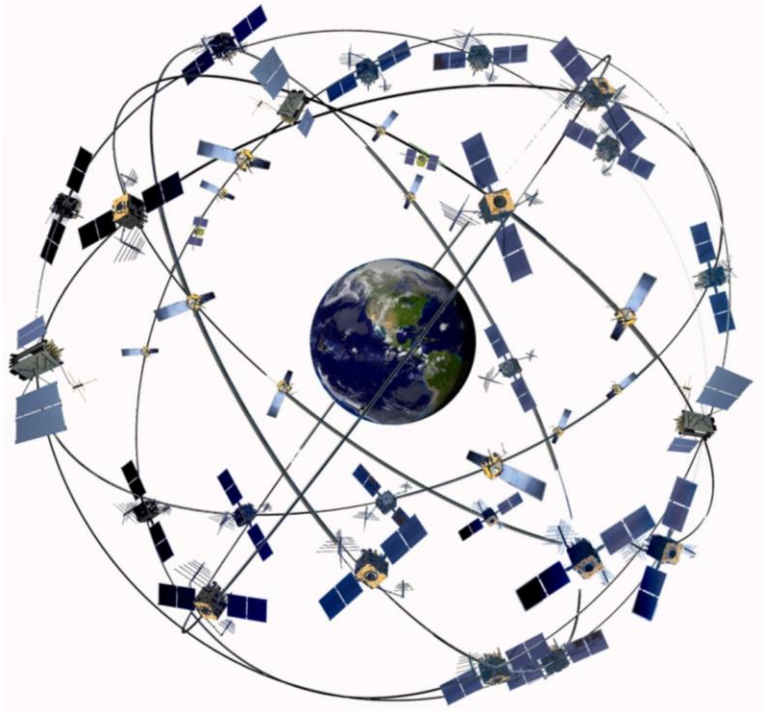

Fig. 2. 1: *GPS constellation (http://www.frazeology.com/gps-turns-40/).*

GPS satellites complete an orbit in approximately 12 hours, which means that they pass over any point on the earth about twice a day. The satellites rise (and set) about four minutes earlier each day.

b. Control Segment: U.S. DoD Monitoring

The U.S. Department of Defense maintains a master control station at Falcon Air Force Base in Colorado Springs, CO. There are about twelve other monitor stations located in Hawaii, Ascension Island, Diego Garcia and Kwajalein. The observation of each control station to each satellite are sent to the control centre located at the Master station. By complex modelling applied to the received observations, the control centre predicts the orbit and clock offset of each satellite for the next 24 hours. Any discrepancies between predicted orbits and actual orbits are transmitted back to the satellites. The satellites can then broadcast these corrections, along with the other position and timing data, to the users so that a GPS receiver on the earth can precisely establish the location of each satellite it is tracking.

The position of the control stations materialize the reference frame and are used to estimate the orbits of the satellites and their clocks. A message is put together and sent up to the satellite. This message contains information needed by the satellite to inform the end user about its location and clock.

Ground control stations continuously track GPS satellites, estimate clock and orbit, keep GPS time and upload data that describe clock and orbit for each space vehicle. Among periodical operations, small manoeuvres to maintain orbit, small clock corrections and major relocations to compensate for any failure can be mentioned.

c. User Segment: Military and Civilian GPS Users

The U.S. military uses GPS for navigation, reconnaissance, and missile guidance systems. Civilian use of GPS, developed at the same time as military applications, was being established, and has expanded far beyond original expectations. There are civilian applications for GPS in almost every field, from surveying to transportation to natural resource management to agriculture. Most civilian uses of GPS, however, fall into one of four categories: navigation, surveying, mapping and timing.

2.1.2. Fundamentals of satellite positioning

A GPS receiver calculates its position by a technique called satellite ranging, which involves the measure of the distance between the GPS receiver and the in view GPS satellites. The range

(the range a receiver calculates is actually a pseudorange, or an estimate of range rather than a true range) or distance, is measured as elapsed travel time. The position of each satellite is known, and the satellites transmit their positions as part of the "messages" they send via radio waves. The GPS receiver on the ground is the unknown point, and can compute its position based on the information it receives from the satellites.

The first step in measuring the distance between the receiver and one satellite requires measuring the time it takes for the signal to travel from the satellite to the receiver. Once the receiver knows how much time has elapsed, it multiplies the travel time of the signal times the speed of light (because the satellite signals travel at the speed of light, approximately 300 000 kilometres per second) to compute the distance. Distance measurements to four satellites are required to compute a 3-dimensional (latitude, longitude and altitude) position.

$$\rho = \Delta t * c \tag{2.1}$$

where

ρ: pseudorange between satellite and receiver

Δt: travel time

c: speed of light, 300 000 km/s

Equation 2.1 is true when the satellites clocks are perfectly synchronized with GPS time, which is practically impossible, or to know the offset of each clock with respect to GPS time.

The offset between satellites clocks (t^s) and GPS time (t^{GPS}) is defined as follows:

$$dt^s = t^s - t^{GPS} \tag{2.2}$$

The offset of satellites clocks can be accurately enough described by a polynomial of second order in time:

$$dt^s(t^{GPS}) = dt_0^S + a^s t^{GPS} + b^s t_{GPS}^2 \tag{2.3}$$

Because the receiver clock experiences an offset, dt_R equation 2.1 becomes:

$$P_R^S(t) = c\Delta t = c\tau + c\,(dt_R - dt^s) \tag{2.4}$$

where

τ: is the travel time

Δt: is the measured time

In order to measure the travel time of the satellite signal, the receiver has to know when the signal left the satellite and when the signal reached the receiver. Knowing when the signal reaches the receiver is easy, the GPS receiver just "checks" its internal clock when the signal arrives to see what time it is. To know when the signal leave the satellite all GPS receivers are synchronized with the satellites so they generate the same digital code at the same time. When the GPS receiver receives a code from a satellite, it can look back in its memory bank and remember when it emitted the same code. This little trick allows the GPS receiver to determine when the signal left the satellite.

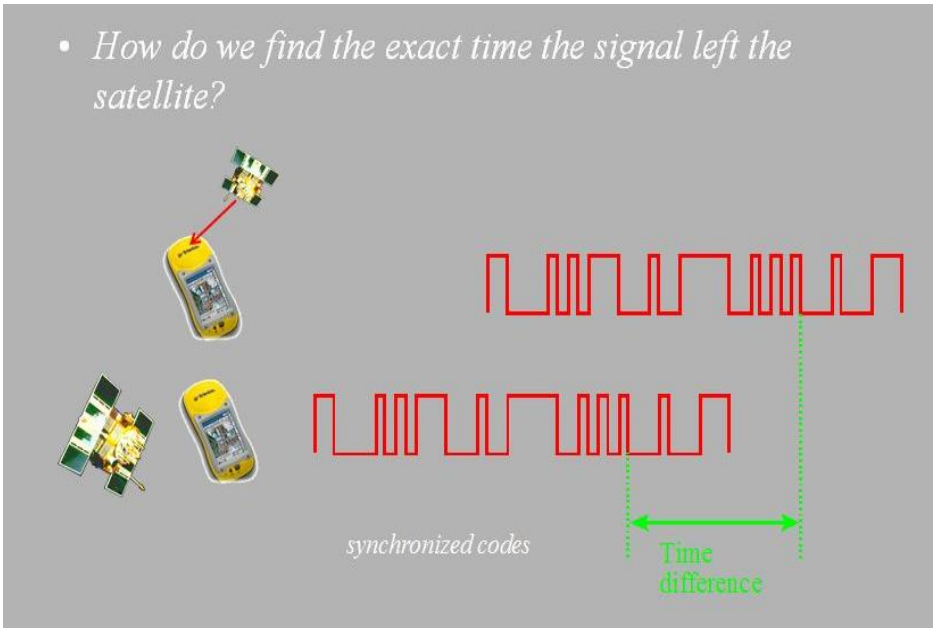

Fig. 2. 2: *Travel time of satellite signals.*

Once the receiver has the distance measurements, it is basically a problem of geometry. At least four satellites are necessary to determine the four unknowns: X, Y, Z and dt_R. If the receiver knows where the four satellites are, and how far it is from each satellite, it can compute the location of its antenna through 3D multi-trilateration. Here is an illustration of how it works.

1). The GPS receiver "locks on" to one satellite and calculates the range to be 20 200 km. This fact helps narrow the receiver location down, but it only tells us that we are somewhere on a sphere which is cantered on the satellite and has a 20 200 km radius. Many of the locations on that sphere are not on earth, but out in space.

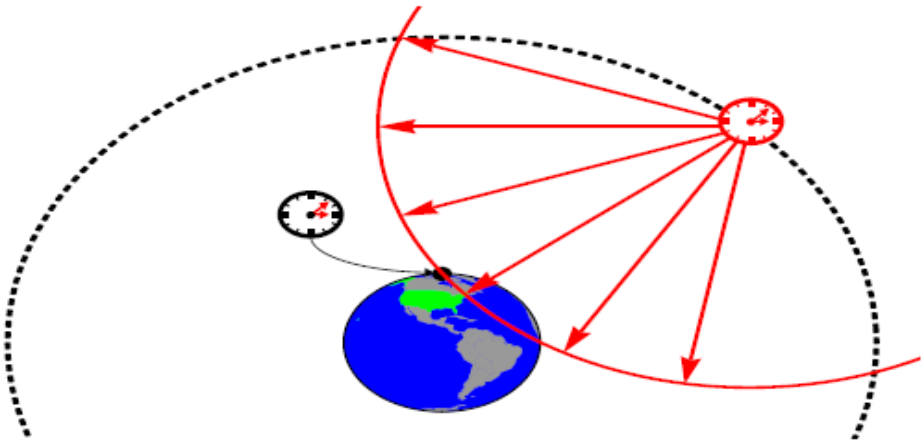

Fig. 2. 3: *One satellite in view (red clock): sphere.*

2). Now, consider that the receiver picks up a signal from a second satellite and calculates the range between the receiver and the satellite. That means we are also somewhere on a sphere with a certain radius with the second satellite at the centre. When the two spheres intersect, a circle is formed, so we must be somewhere on that circle.

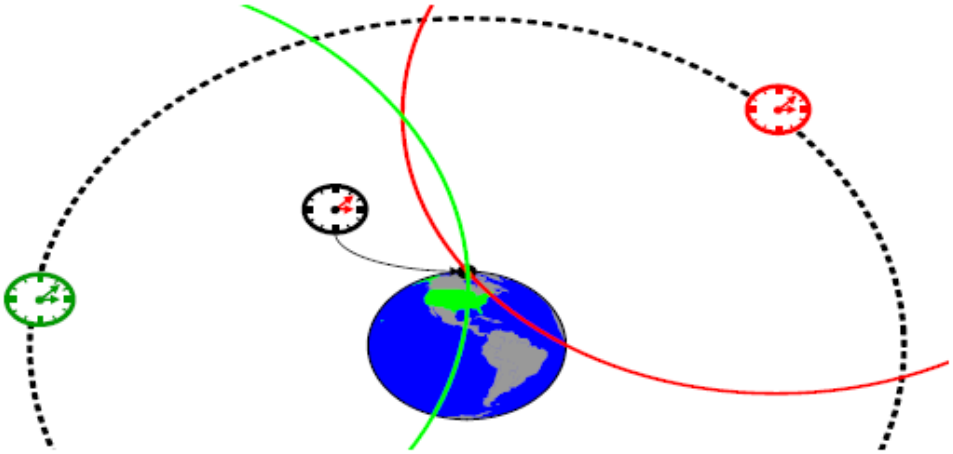

Fig. 2. 4: *Two satellites in view (red and green clock): circle formed by the intersection of two spheres.*

3). If the receiver picks up another satellite, another sphere is formed, and there are only two points where the three spheres intersect. Usually the receiver can discard one of the last two points because it is nowhere near the earth. So, we're left with one point which is the location of the GPS receiver. At this moment three of the initial unknowns are solved: X, Y, Z coordinates of the antenna. In practice, a fourth measurement is needed to correct for clock error, dt_R.

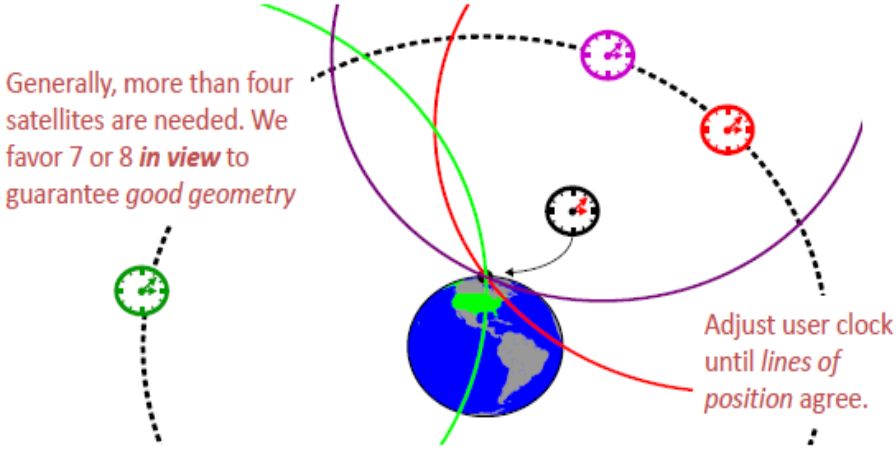

Fig. 2. 5: *Three satellites in view (red, green and purple clock): location of the GPS receiver is at the point of intersection of the three spheres.*

GPS positioning is based on trilateration, which is the method of determining position by measuring distances to points at known coordinates. At a minimum, trilateration requires 3 ranges to 3 know points. GPS point positioning, on the other hand, needs range measurement to 4 satellites.

2.1.3. GPS L1 C/A signal and the other available signals

GPS satellites continuously broadcast satellite position and timing data via radio signals on two frequencies, L1 and L2, and a third one is already under testing, L5.

The satellite signals require a direct line to GPS receivers and cannot penetrate water, soil, walls or other obstacles. For example, heavy forest canopy causes interference, making it difficult, if not impossible, to compute positions. In canyons (and "urban canyons" in cities) GPS signals are blocked by mountain ranges or buildings.

The GPS L1 C/A (Coarse Acquisition) signal is transmitted on the L1 band at a frequency of f = 1575.42 MHz. The signal is composed of three components:

- The carrier wave at f =1575.42 MHz and wavelength λ = 19 cm.
- C/A code modulated on top of the carrier wave; a sequence of 1023 chips with a chipping rate of 1.023 MHz giving a period of 1ms (a chip corresponds to a bit and its name emphasize that it does not hold any information - K. Borre, D. M. Akos, N. Bertelsen, P. Rinder, and S. H. Jensen, A Software-Defined GPS and Galileo Receiver A Single-Frequency Approach. Birkäuser, 2007.). The code is commonly known as PRN (Pseudo Random Noise) because it looks like random signals but in reality C/A code is carefully crafted using a mathematical algorithm.

- The navigation message containing information about all the satellites.

Each satellite is assigned a unique C/A code, which enables GPS receivers to identify which satellite is transmitting a particular code. C/A (Coarse Acquisition) code is available to civilian GPS users and provides Standard Positioning Service (SPS). Using the Standard Positioning Service one can achieve 15 meter horizontal accuracy 95% of the time. This means that 95% of the time, the coordinates you read from your GPS receiver display will be within 15 meters of your true position on the earth, this is less precise than P(Y) code solution.

The navigation message is used to send all the necessary information needed by the user in order to perform the positioning service. It includes the Ephemeris parameters, needed to compute the satellite coordinates with enough accuracy, the Time parameters and Clock Corrections, to compute satellite clock offsets and time conversions the Service Parameters with satellite health information (used to identify the navigation data set), Ionospheric parameters model needed for single frequency receivers, and the Almanacs.

The speed of this message is 50 bit/s and repeats every 12.5 minutes. The whole message contains 25 pages (or 'frames') of 30 seconds each, forming the master frame that takes 12,5 minutes to be transmitted. Every frame is subdivided into 5 sub-frames of 6 seconds each; in turn, every sub-frame consists of 10 words, with 30 bits per word. Every sub-frame always starts with the telemetry word (TLM), which is necessary for synchronism. Next, the transference word (HOW) appears. This word provides time information (seconds of the GPS week), allowing the receiver to acquire the week-long P(Y)-code segment.

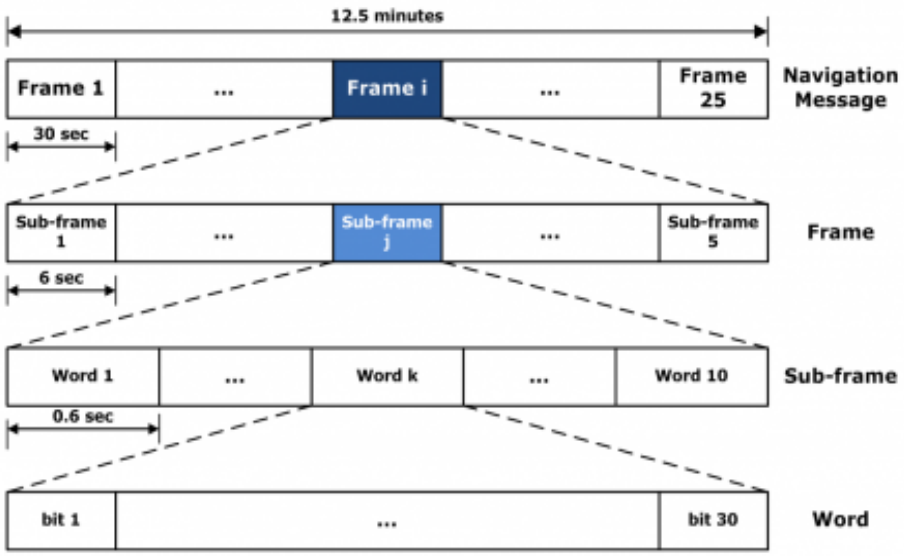

Fig. 2. 6: *Format of the navigation method.*

GPS satellites are capable of transmitting radio signals on the L2 band. The signal is composed of:

- The carrier wave at $f = 1227.60$ and wavelength $\lambda = 24$ cm.
- The precise P(Y) code. As in the case of C/A, P(Y) code consists of a stream of binary digits, zeros and ones, known as bits or chips. The modulation is called biphase modulation, it means the carrier phase is shifted by 180^0 when the code value change from zero to one or from one to zero (Wells, D.E, et al., 1987). The P-code is a very long sequence of binary digits that repeats itself after 266 days. It is 10 times faster than C/A and more precise. The code is divided in 38 segments; each one week long. Of these, 32 segments are assigned to the various GPS satellites; in other words, each satellite transmits a unique 1-week segment of the P-code. This code was designed for military purposes, and was encrypted by adding to it an unknown W-code. The resulting encrypted code is called the Y-code.
- L2C code is the newly civilian code modulated on top of the L2 carrier wave. This code was introduced with the help of the Block IIR satellites, lunched with beginning of 2003.
- The navigation message.

The availability of the two carrier frequencies allows for correcting a major GPS error, known as the ionospheric delays (see Chapter 3 and Chapter 4 for more details).

To satisfy aviation user requirements, a third civil signal called L5 was introduced with the help of first Block IIF satellites, launched in 2005. This third frequency will be robust and will have a higher power level. In addition, this new L5 signal has wide broadcast bandwidth (a minimum of 20 MHz) and a higher chipping rate (10.23 MHz), which provide higher accuracy under noisy and multipath conditions. L5 is composed of:

- The carrier wave at $f = 1176.45$ MHz and wavelength $\lambda = 26$ cm.
- A new military code called M-code, designed with the purpose of replacing the P(Y) code in the future. This code offers better jamming resistance than the P(Y) signal and more robust signal acquisition than is achieved today.
- The navigation message, which will contain more or less the same data as the L1 and L2 channels, has an entirely different, more efficient, structure.

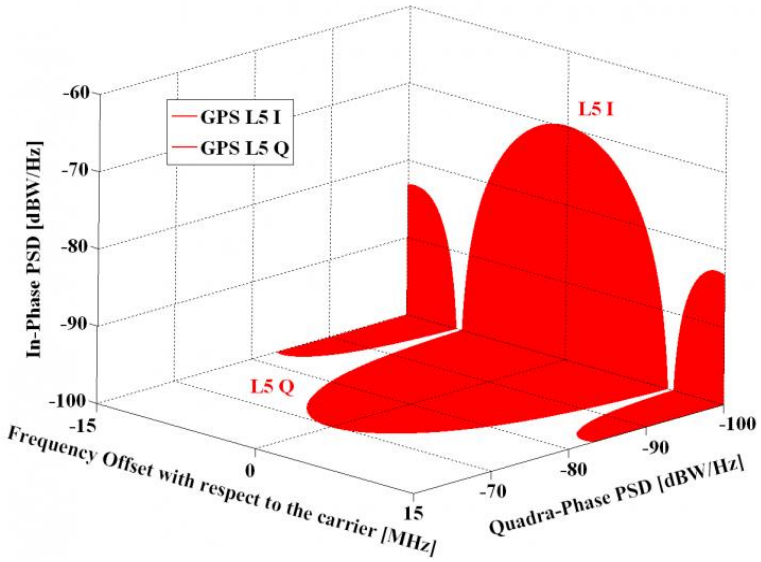

Fig. 2. 7: *Spectra of the GPS Signals in L5.*

For more details on L5, refer to (Kaplan, E. D., Hegarty, C., 2006).

2.2. Other global navigation systems

The increase in civilian use has led to the desire of autonomy by different nations who have in turn embarked on designing and developing their own systems. In this regard, the European nations are developing the Galileo system, the Russians are modernizing their GLONASS system, while China is improving BeiDou. Together with GPS, all these systems form GNSS with desirable positional capability suitable for navigation and positioning applications.

In the following part of this chapter the remaining GNSS are described: first, GLONASS will be introduced and Frequency Division Multiple Access (FDMA) will be explained, then a short look into BeiDou characteristics and last, Galileo system.

2.2.1. GLONASS

The purpose of the Global Navigation Satellite System GLONASS, operated by Russian Space Agency and Russian Ministry of Defense, is to provide unlimited number of air, marine, and any other type of users with three-dimensional positioning, velocity measuring and timing anywhere in the world or near-earth space.

GLONASS, as GPS, includes three components:

- Constellation of satellites (space segment),
- Ground-based control facilities (control segment),
- User equipment (user segment).

Completely deployed GLONASS constellation is composed of 24 satellites in three orbital planes whose ascending nodes are 120 apart. 8 satellites are equally spaced in each plane with argument of latitude displacement 45. The satellites operate in circular 19100-km orbits at an inclination 64.8, and each satellite completes the orbit in approximately11 hours 15 minutes. The spacing of the satellites allows providing continuous and global coverage of the terrestrial surface and the near-earth space.

The control segment includes the System Control Centre and the network of the Command and Tracking Stations that are located throughout the territory of Russia. The control segment provides monitoring of GLONASS constellation status, correction to the orbital parameters and navigation data uploading.

User equipment consists of receives and processors receiving and processing the GLONASS navigation signals, and allows user to calculate the coordinates, velocity and time.

Each GLONASS system Space Vehicle (SVs) "Glonass" and "Glonass-M" transmits navigational radio signals on fundamental frequencies in two frequency sub-bands (L1 ~ 1,6 GHz, L2 ~ 1,25 GHz). SVs, being in opposite points of an orbit plane (antipodal NKA), can transmit navigation radio signals on equal frequencies. In most GNSS systems, each satellite broadcasts ranging codes and navigation data using a method called Code Division Multiple Access (CDMA), i.e., each satellite uses different ranging codes that have low cross-correlation properties with respect to one another (Rodriguez, J-A., Hein, G.W., 2007). This is not the case of GLONASS, which uses a technique called Frequency Division Multiple Access or FDMA. The nominal values of L1 and L2 carrier frequencies are defined by the following expression (GLONASS Interface Control Document):

$$f_{K1} = f_{01} + K\Delta f_1 \quad 2.5$$

$$f_{K2} = f_{02} + K\Delta f_2 \quad 2.6$$

where K is a frequency number of the signals transmitted by GLONASS satellites in the L1 and L2 sub-bands correspondingly:

$$f_{01} = 1602\ MHz \text{ and } \Delta f_1 = 562.5\ kHz \quad 2.7$$

$$f_{02} = 1246\ MHz \text{ and } \Delta f_2 = 437.5\ kHz \quad 2.8$$

The nominal values of carrier frequencies for channel numbers K are given in Table 2.1.

No. of channel	Nominal value of frequency in L1 sub-band, in MHz	No. of channel	Nominal value of frequency in L2 sub-band, in MHz
06	1605.375	06	1248.625
05	1604.8125	05	1248.1875
04	1604.25	04	1247.75
03	1603.6875	03	1247.3125
02	1603.125	02	1246.875
01	1602.5625	01	1246.4375
00	1602.0	00	1246.0
-01	1601.4375	-01	1245.5625
-02	1600.8750	-02	1245.1250
-03	1600.3125	-03	1244.6875
-04	1599.7500	-04	1244.2500
-05	1599.1875	-05	1243.8125
-06	1598.6250	-06	1243.3750
-07	1598.0625	-07	1242.9375

Table 2. 1: *Nominal values of carrier frequencies for specific channel (after GLONASS ICD).*

The carrier of L1 sub-band and phases of bearing oscillations of sub-bands L1 and L2 is modulated by the Modulo-2 addition of the following binary signals: pseudo random (PR) ranging code, digital data of navigation message and auxiliary meander sequence. All above-mentioned components are generated using a single on-board time/frequency oscillator.

The GLONASS broadcast ephemeris describes a position of transmitting antenna phase centre of given satellite in the PZ-90.02 Earth-Centred Earth-Fixed reference frame defined as follows:

- The origin is located at the centre of the Earth's body;
- The Z-axis is directed to the Conventional Terrestrial Pole as recommended by the International Earth Rotation Service (IERS);
- The X-axis is directed to the point of intersection of the Earth's equatorial plane and the zero meridian established by BIH;
- The Y-axis completes the coordinate system to the right-handed one.

Geodetic coordinates of a point in the PZ-90.02 coordinate system refers to the ellipsoid which semi- major axis and flattening are given below:

Semi- major axis: a = 6 378 136 m

Flattening: f = 1/298,257 84

2.2.2. BeiDou

The BeiDou Navigation Satellite System (BDS), also known as BeiDou-2, is China's second – generation satellite navigation system that will be capable of providing positioning, navigation, and timing services to users on a continuous worldwide basis (BeiDou ICD). First, China implemented a regional system, BeiDou-1, and this evolved to a global solution and it is expected to provide global navigation services by 2020. As of December 2011, BeiDou system was able to provide Initial Operational Service with a constellation of 10 satellites (5 GEO satellites and 5 IGSO satellites). During 2012, 5 additional satellites (1 GEO satellites and 4 MEO satellites) were launched increasing to 14 the number of the constellation.

When fully deployed, the space constellation of BDS consists of five Geostationary Earth Orbit (GEO) satellites, twenty-seven Medium Earth Orbit (MEO) satellites and three Inclined Geosynchronous Satellite Orbit (IGSO) satellites. The GEO satellites are operating in orbit at an altitude of 35 786 kilometres and positioned at 58.75°E, 80°E, 110.5°E, 140°E and 160°E respectively. The MEO satellites are operating in orbit at an altitude of 21 528 kilometres and an inclination of 55° to the equatorial plane. The IGSO satellites are operating in orbit at an altitude of 35 786 kilometres and an inclination of 55° to the equatorial plane.

BeiDou adopts the China Geodetic Coordinate System 2000 (CGCS2000), and the definition is listed below:

- The origin is located at the mass centre of the Earth;
- The Z-axis is in the direction of the IERS (International Earth Rotation and Reference System Service) Reference Pole (IRP);
- The X-axis is directed to the intersection of IERS Reference Meridian (IRM) and the plane passing the origin and normal to the Z-axis;
- The Y - axis, together with Z-axis and X-axis, constitutes a right handed orthogonal coordinate system.

The origin of the CGCS2000 is also the geometric centre of the CGCS2000 ellipsoid, and the Z-axis is the rotation axis of the CGCS2000 ellipsoid. The parameters of the CGCS2000 ellipsoid are as follows:

Semi- major axis: a = 6378137.0 m

Flattening: f = 1/298.257222101

The carrier frequencies of B1I and B2I shall be coherently derived from a common reference frequency source on board of the satellite. The nominal frequency of B1I signal is 1561.098 MHz, and the nominal frequency of B2I signal is 1207.140 MHz.

2.2.3. Galileo

Galileo is Europe's contribution to the next generation Global Navigation Satellite System (GNSS). Unlike GPS, which is funded by the public sector and operated by the U.S. Air Force, Galileo will be a civil-controlled system that draws on both public and private sectors for funding. The basic service will be free, but a range of chargeable services with additional features will also be offered. These additional features would include improved reception, accuracy and availability.

The Galileo navigation signals are transmitted in four frequency bands. These bands are E5a, E5b, E6 and E1 bands. Galileo carrier frequencies are shown in Table 2.2. Their names are the same as the corresponding carrier frequencies (E5a and E5b are part of the E5 signal)

Signal	**Carrier frequency, in MHz**
E1	1575.420
E6	1278.750
E5	1191.795
E5a	1176.450
E5b	1207.140

Table 2. 2: *Carrier frequency for Galileo (after Galileo)*

The fully deployed Galileo system consists of 30 satellites (27 operational + 3 active spares), positioned in three circular Medium Earth Orbit (MEO) planes at 23 222 km altitude above the Earth, and at an inclination of the orbital planes of 56 degrees to the equator.

Once the Initial Operational Capability phase is reached, the Open Service, Search and Rescue and Public Regulated Service will be available with initial performances. Then as the

constellation is built-up beyond that, new services will be tested and made available to reach Full Operational Capability (FOC).

On 21 October 2011 came the first two of four operational satellites designed to validate the Galileo concept in both space and on Earth. Two more followed on 12 October 2012. This In-Orbit Validation (IOV) phase is now being followed by additional satellite launches to reach IOC around mid-decade.

On August 22, 2014 a Soyuz rocket was tasked to correctly orbit two Galileo satellites. However, this mission failed: though the satellites were in good health, they failed to reach the correct orbit because of a too early release from the rocket. To correctly place the satellites on the orbit a big amount of fuel is needed, which is not the case. Thus, the satellites are lost from a navigation and positioning point of view; luckily, they are not completely useless as the investigation can prevent situation like this for the future missions.

The latest launch took place on 27th of March from Korou, French Guiana when a Russian Soyuz rocket lifted Galileo FOC 3 and 4 into orbit.

As there were many details presented, it is worth mentioning on short the status of current GNSS systems:

System	Country	Coding	Orbital height and period	Number of satellites	Status
GPS	US	CDMA	20 200 km 12 h	>24 (around 30)	Operational
GLONASS	Russia	FDMA CDMA	19 100 km 11.3 h	29	Operational with restrictions
BeiDou	China	CDMA	21 150 km 12.6 h	35	In preparation
Galileo	EU	CDMA	23 222 km 14.1 h	30	In preparation

Table 2. 3: *Status of current GNSS system (after European GNSS Open Service SIS ICD).*

2.3. SBAS (Satellite Based Augmentation Systems)

SBAS is an augmentation technology for GPS, which calculates GPS integrity and correction data with RIMS (Ranging and Integrity Monitoring Stations) on the ground and uses geostationary satellites (GEOs) to broadcast GPS integrity and correction data to GPS users (Kaplan, E.D., Hegarty, C.J., 2006.). The correction data is transmitted on the GPS L1 frequency (1575.42 MHz), and therefore no additional receiver is required to make use of the

correction and integrity data. While the main goal of SBAS is to provide integrity assurance, it also increases the accuracy with position errors below 1 meter (1 sigma).

2.3.1. SBAS Principle

SBAS is designed to augment other GNSS system and not to perform stand-alone positioning. To improve position accuracy SBAS uses different types of correction data:

- Fast corrections for short-term disturbances in GPS signals (due to clock problems, etc).
- Long-term corrections for GPS clock problems, broadcast orbit errors etc.
- Ionosphere corrections for Ionosphere activity

Another benefit of SBAS is the use of GPS integrity information. In this way SBAS Control stations can 'disable' the use of GPS satellites within a 6 second alarm time in case of major GPS satellite problems. If integrity monitoring is enabled, u-blox GPS technology only uses satellites, for which integrity information is available.

As it can be seen in Figure 2.8 this system consists of a ground network of reference and integrity monitor data processing sites, a space segment, support segment and users.

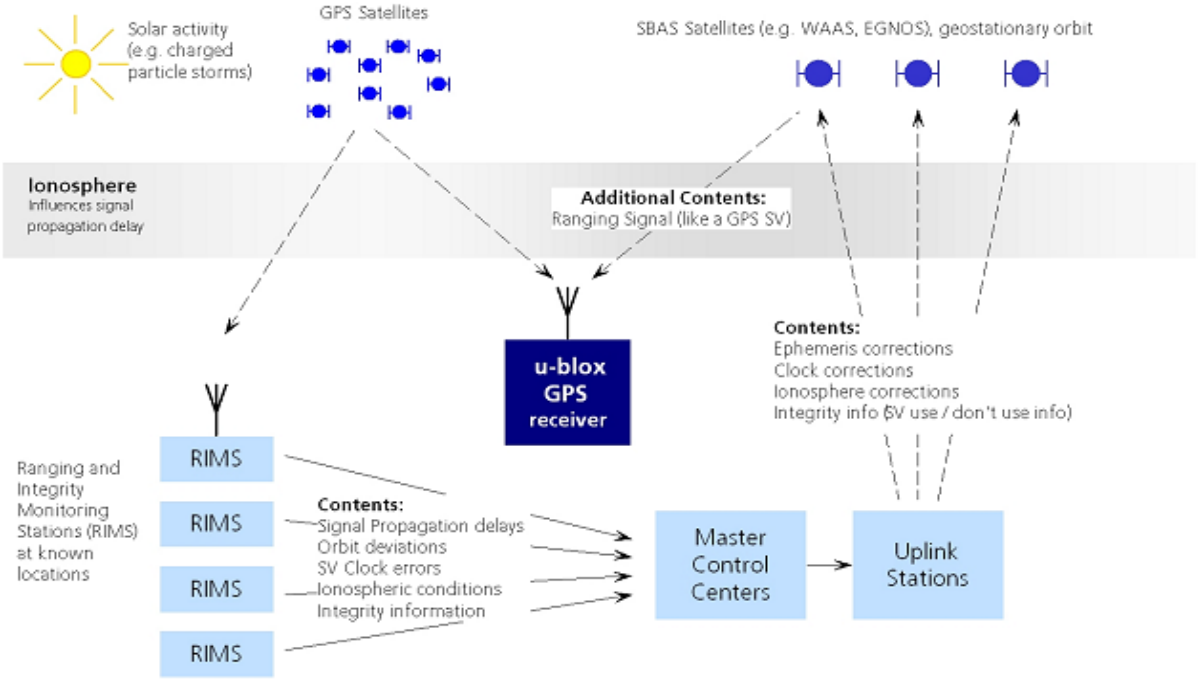

Fig. 2. 8: *SBAS principle.*

The space segment comprises geostationary satellites with navigation payloads capable of transmitting a GPS – like carrier signal with the SBAS information. Ideally, in any point of the

covered area the signal of at least two GEO satellites should be available to users (to assure continuity of the signal in case one of them would face transmission problems).

The ground segment is the heart of the system and it identifies with all the ground elements necessary for the provision of the SBAS data. The most important parts are the GNSS tracking stations, the processing centres, monitoring and control centres and the communication services. The input data for the SBAS system is collected by a network of GNSS receivers which have as main characteristics:

- dual frequency receivers,
- atomic frequency standards,
- excellent site conditions: no multipath, no interference,
- positioned in ITRF within 1 – 3 cm,
- 1 Hz data acquisition.

Support segment comprising all the elements need to support the correct operation and maintenance of the SBAS: configuration control, performance evaluation, maintenance and development, help desk, etc.

The SBAS Support Segment collects all the elements needed to support the development and operation of a SBAS system. These elements are not related with the provision of the SBAS service but they are needed as external support facilities.

User segment refers to the user equipment necessary to receive and use the SBAS information. In fact, this segment is not under control of the SBAS provider but is driven by the application market: different applications, different equipment. In general, the SBAS service operator provides different services aiming at different market sectors, namely an Open Service (OS), a Safety of Life Service (SoL) and even a Commercial Service (CS).

The OS targets low cost, general purpose GNSS equipment that uses the SBAS Signal In Space (SIS) to provide the user with an enhanced accuracy performance in comparison with the one provided by a standalone GPS device. Finally, some SBAS service providers (see http://www.navipedia.net/index.php/Category:EGNOS) include the provision of the information computed by the SBAS ground element (input raw data, corrections, integrity information) by dissemination means different to the SBAS GEO link (generally, using terrestrial telecommunication networks). This constitutes the Commercial Service. This market sector comprises professional users (land and geodesy applications, maritime or terrestrial

transport applications) that are not subject to the integrity and latency requirements needed in the SoL service.

The SoL, which provides the most stringent level of signal – in – space performance to all communities of Safety of Life users over Europe, was officially started on 2 March 2011. Civil aviation is the most important beneficiary of SoL and the certified equipment is in the highest rank with respect its cost. There exist a large number of certified receiver manufacturers worldwide both in the US (GARMIN, Honeywell, Rockwell Collins, General Avionics, etc) and in Europe.

The SoL signals allow and provide a positioning service along En-Route (during flight), Terminal, Non-Precision Approaches (NPA) and Approaches with Vertical guidance (APV).

2.3.2. Broadcast SBAS signals

Every SBAS provides ranging signals transmitted by GEO satellites, differential corrections on the wide area and additional parameters aimed to guarantee the integrity of the GNSS user:

- **GEO Ranging**: transmission of GPS-like L1 signals from GEO satellites to augment the number of navigation satellites available to the users.
- **Wide Area Differential (WAD)**: differential corrections to the existing GPS/GLONASS/GEO navigation services computed in a wide area to improve navigation services performance. This includes corrections to the satellite orbits and clocks, as well as information to estimate the delay suffered from the signal when it passes through the ionosphere.
- **GNSS/Ground Integrity Channel (GIC)**: integrity information to inform about the availability of GPS/GLONASS/GEO safe navigation service.

The specification of the SBAS message data format is contained in the ICAO SARPS Appendix B for the aspects related with the signal in space, as well as in the RTCA MOPS DO-229D for the minimum performance requirements applicable to the airborne SBAS receiver equipment.

The SBAS satellite shall transmit a GPS-like L1 (1574.42 MHz) signal, modulated with a Coarse/Acquisition Pseudo-Random Noise (PRN) code. The SBAS L1 radiofrequency characteristics are:

Parameter	Description
Modulation	Bi-phase shift key (BPSK) modulated by a bit train comprising the PRN code and the SBAS data (modulo-2 sum).

Bandwidth	L1 ±30.69 MHz. At least 95% of the broadcast power will be contained within the L1 ±12 MHz band.
Ranging codes	A PRN Code (Gold code) of 1 millisecond in length at a chipping rate of 1023 Kbps.
SBAS data	500 symbols per second, module-2 modulated (250 effective bits per second)
Power	Minimum power –131 dBm at 5 degrees elevation Maximum power –119,5 dBm

Table 2. 4: *Characteristics of SBAS signals.*

Signal data structure

The raw navigation message of the SBAS contains 500 bits. These raw data are ½ convolutional encoded with a Forward Error Correction (FEC) code, which means that 250 bits of information are available every second at user level. The following table and figure summaries the message format. Bit 0 is considered the most significant bit, i.e. the bit that is transmitted and received first.

Position in message	Name	Purpose
0-7	Preamble	Assure frame synchronisation
8-13	Message type identifier	Define the type of message
14-225	Data field	GIC/WAD information
226-249	Parity information	Redundancy & error checking

Table 2. 5: *SBAS message format.*

A brief explanation of the different data fields is presented hereafter:

- Preamble. It is a unique 24–bit field, distributed over three successive words. It is assured that the start of the preamble is synchronous with a 6-second GPS sub-frame. Thus, the preamble allows the receiver to achieve frame synchronization.
- Message Type Identifier. It is a 6-bit field, which permits up to 64 different messages (identifiers 0 to 63).
- Data Field. It contains different corrections and integrity information that depends on the type of message.

- Parity Information. The 24 bits of the end of the message (CRC parity bits) provide protection against burst and random error.

Messages are interrelated using the Issue of Data parameters (IOD), which are present in the message data. Also satellite messages are related with satellite navigation services ephemeris via the issues of data.

Message types

SBAS messages have a 6-bit message type identifier, which informs the receiver about the information the message holds. Due to the limited size of the type identifier (6 bits), 64 types of messages are possible. Nowadays, only 20 of these messages are defined. The following table summarizes the current message types and the contained information.

Type	Contents
0	Do not use for safety applications
1	PRN mask assignments, set up to 51 of 210 possible
2-5	Fast corrections
6	Integrity information
7	Fast correction degradation factor
9	Geo Navigation message (*X*, *Y*, *Z*, time, etc.)
10	Degradation parameters
12	SBAS Network time / UTC offset parameters
17	Geo satellite almanacs
18	Ionosphere grid points masks
24	Mixed fast corrections/long term satellite error corrections
25	Long term satellite error corrections
26	Ionosphere delay corrections
27	SBAS Service message
28	Clock Ephemeris Covariance Matrix message
62	Internal test message
63	Null message

Table 2. 6: *SBAS message explained*

(http://www.navipedia.net/index.php/The_EGNOS_SBAS_Message_Format_Explained).

2.3.3. Existing SBAS systems

Several countries have implemented their own satellite-based augmentation system (see Figure 2.9). Europe has the European Geostationary Navigation Overlay Service (EGNOS) which covers the EU and possibly beyond. The USA has its Wide Area Augmentation System (WAAS). Japan is covered by its Multi-functional Satellite Augmentation System (MSAS). India has launched its own SBAS program named GPS and GEO Augmented Navigation

(GAGAN) to cover the Indian subcontinent. Both Korea (2013) and China (2014) have announced plans to start their own SBAS implementation.

- EGNOS is a satellite based augmentation system developed by the European Space Agency and the European Commission. It supplements GPS, GLONASS and Galileo and leads to horizontal accuracy at the meter level. EGNOS consists of 4 GEO satellites and a network of ground stations.
- WAAS is an air navigation aid developed by the Federal Aviation Administration to augment GPS, with the goal of improving its accuracy, integrity, and availability. Essentially, WAAS is intended to enable aircraft to rely on GPS for all phases of flight, including precision approaches to any airport within its coverage area (Federal Aviation Administration [FAA]). When WAAS is used with GPS, an accuracy of 0.9 m (horizontal) and 1.3 m (vertical) is expected; this numbers are obtained excluding receiver errors.
- MSAS is a Japanese SBAS designed to supplement GPS system by improving the reliability and accuracy of those signals up to 1.5 – 2 meters in both the horizontal and vertical dimensions (http://www.unoosa.org/pdf/icg/2008/icg3/08-1.pdf).
- GAGAN has the same mission as the other augmentation systems, its GEO satellites will broadcast SBAS navigation data, on L1 and L5 signals, used for positioning with accuracy of about 3 m in the horizontal dimensions (Suryanarayana Rao, K.N., and Pal, S., June 2004).

Fig. 2. 9: *Existing SBAS (http://egnos-portal.eu/discover-egnos/about-egnos/what-sbas).*

SBAS support allows u-blox GPS technology to take full advantage of the augmentation systems that are currently available (WAAS, EGNOS, MSAS), as well as those being tested and planned (such as GAGAN).

With SBAS enabled the user benefits from additional satellites for ranging (navigation). u-blox GPS technology uses the available SBAS Satellites for navigation just like GPS satellites, if the SBAS satellites offer this service.

For more information on SBAS and associated services please refer to

• RTCA/DO-229D (MOPS). Available from www.rtca.org

• gps.faa.govfor information on WAAS.

• www.esa.intfor information on EGNOS.

• www.essp-sas.eufor information about European Satellite Services Provider (ESSP), the EGNOS operations manager.

Chapter 3. GNSS Receivers

In a short time GNSS receiver market improved greatly in offer and price. For instance, in the 1980, only one commercial GPS receiver was available on the market, at a price of several hundred thousand U.S. dollars (Langley, R.B., January 1991). This has changed considerably as more than 500 different GPS receivers were available in 2014. The current receiver price varies from about 100 $ to 15 000 - 20 000 $ for the sophisticated geodetic units.

This chapter treats GNSS receivers, both high cost, geodetic ones and low-cost sensors. A short introduction presents the GNSS receiver classes. Then, two geodetic receivers used as reference stations are discussed and in the last part, a more detailed image of u-blox receivers will be offered.

3.1. Types of GNSS receivers

A further classification can be done based on the receiving capabilities:

- single-frequency code receivers,
- single-frequency carrier-smoothed code receivers,
- single-frequency code and carrier receivers,
- dual-frequency receivers
- multi-frequency receivers (L1, L2 and L5). Leica GRX1200 and Leica GR10/25 generations are in this category.

At this moment the following classification of GNSS sensors can be done:

- Chipsets in smartphones. Generally, these units are single - frequency (L1 band) and capable of only code measurements, moreover only positions and no output data at user interface
- Evaluation kits. The main difference with the previous category consists in the possibility to store raw data. The classification of Evaluation kits can be taken one step further: they started as single-frequency receivers capable of providing only C/A code solution, then evolved to single frequency carrier-smoothed code receiver (phase observations are used to smooth the code, which will smooth the noise) and in the end improved by adding phase observations to the already available C/A code observations. The low-cost sensor tested, the u-blox NEO 7P, is falling in this last category.

- Geographic Information System (GIS)/cartographic handheld receivers. They are again L1 receivers but typically have better components (antenna). A GIS data collector is composed by a special graphic computer, GIS software and GPS module for real-time land use.
- Geodetic receivers. This type is the most complete one, it comes in pair with geodetic antenna, which are more resistant to interference and multipath.

Today, most of the geodetic sensors are dual - frequency receivers. Companies like Trimble, Leica, Topcon and Novatel are the most important GNSS solutions providers that compete on today's geospatial market.

3.2. Geodetic receivers

The geodetic receivers require the full range of code and phase measurements and the application of relative data processing technique to benefit the high accuracy phase measurements (accuracy between 1 and 5 cm, even better in optimal conditions). Among this category, one sub-category can be specified, which have the same accuracy requirements but it is designed as Continuously Operating Reference Station (CORS). They are practically internet servers, and transfer continuous observation data stream from a permanent station to different data and processing centres. Such type of receivers are Leica GRX1200 and Leica GR10, which are the author choice for reference sites, but more about them in the next two subsections.

3.2.1. Leica GRX1200

The Leica GRX1200 Series is designed specifically for use at reference stations. The measurement engine supports GPS, GLONASS, Galileo and BeiDou. Regarding data management, removable and robust CompactFlash cards up to 1 GB are used for logging data. According to Leica, 1 GB is sufficient for about 7 weeks of 1Hz L1+L2 GPS data. There is no need for power-consuming external memory storage, which typically cannot fulfil in the tough environment conditions to which reference stations are exposed. Files can be logged in raw data and/or RINEX format.

The measurement technology is called SmartTrack and consists in advanced GPS acquisition technique: after switching on the time needed to acquire all satellites is typically 30 seconds; after loss of lock re-acquisition starts typically within 1 second; very high sensitivity, it acquires more than 99% of all possible observations above 10 degrees elevation.

Among the main characteristics of this geodetic applications, it can be listed:

- acquisition within seconds,
- excellent signal strength,
- reliable tracking to low elevations,
- suppresses phase and code multipath,
- jamming resistant,
- measurements up to 20 Hz,
- low power consumption.

Fig. 3. 1: *Leica GRX1200 and AX1202 GG antenna.*

The performance of this sensor is directly influenced by the type of antenna connected. For standard applications, normal geodetic antenna (AX1202GG, see Figure 3.1) are suffice: they deliver high-quality observations for single stations and networks. Latest generation of geodetic antenna from Leica includes sub-millimetre phase centre accuracy, high quality measurements even from low elevation satellites and have built-in ground plane for multipath suppression.

For national and continental first – order networks, and for IGS stations, Leica suggests the use of geodetic choke – ring antenna. This antenna will suppress multipath, has excellent phase centre stability and, when used with the Leica GRX1200 or GR10/25 performs at its best.

Another important feature is the built-in File Transfer Protocol (FTP) server, allowing simple and quick manual download of data without the need for special software. Alternatively, FTP Push can be used, which automatically upload data from the receiver to a remote FTP server.

To control it, the administrator can simply open a web browser from any computer hooked up in the same network or via Internet. Moreover, the web browser can be used to pre-configure the receiver for connections with GPS Spider software.

To prove even more the completeness and complexity of these two sensors, Leica implemented the possibility to connect meteorology and tilt sensors to its receivers: the relevant data are logged and downloaded together with GPS data.

When it comes to protection, Leica GRX1200 Series is sheltered inside a strong magnesium housing and is designed to MIL-STD-810 (United States Military Standard) specifications to withstand the roughest use and the most severe environments. These receivers can operate through a wide temperature range, are fully waterproof, rain, sand and dustproof (see Table 3.1 for more details).

Leica GRX1200	**Nominal value of frequency in L1 sub-band, in MHz**
GNSS technology	SmartTrack+
Measurement precision - **carrier phase** - **code**	 L1: rms = 0.2 mm; L2: rms = 0.2 mm L1: rms = 20 mm; L2: rms = 20 mm
Web & FTP services	yes
Optional control software	Leica GPS Spider software
Weight	1.2 kg
Temperature range	-40^0C to $+65^0$C
Waterproof	MIL-STD-810F Temporary submersion to 1 m
Shock/drop on hard surface	Withstand 1.0 m drop
Supply voltage	Nominal 12V DC
Raw data logging	MDB (Leica proprietary format) and RINEX
Data streaming	RTCM v2.1/2.2/2.3/3.0 NMEA 0183 Leica LB2 raw data
NTRIP	Integrated NTRIP server

Table 3. 1: *Technical data for GRX1200 (courtesy Leica Geosystems).*

3.2.2. Leica GR10

This new receiver has a lot in common with the old Leica GRX1200, Leica GR10 is designed for straightforward installation and offers various mounting options including IT rack, wall mount, cabinet and tripod. But some improvements have been made: the control of the receiver had been improved: plug and play setup using a unique receiver hostname means no pre-configuration of IP address is needed. A simple connection to the Local Area Network (LAN) or the USB port on the user PC and start working. Last but not least, a comprehensive online help, tool tips and multiple languages make the receiver easy to manage. In case assistance is required, the support tool will collect all the necessary system information and send it directly to Leica GNSS support team.

The measurement technology is the same, SmartTrack+, but more satellites can be simultaneously observed (up to 60). Contrary to GRX1200, where only one logging session could be enabled, GR10 creates up to 12 parallel logging sessions, using MDB, RINEX and Hatanaka and data rates up to 50 Hz. Data coming from these sessions can be stored on a removable SD card with storage capacity up to 32 GB or can be pushed to multiple locations.

A new addition is the Smart Clean-up feature. Prioritized clean-up of data allows full usage of the available storage space and ensures the most important data is preserved in case capacity is reached.

Regarding streaming, the number was increase to 20 parallel data streams, each supporting multiple user connections. Streaming rates up to 50 Hz can be configured and a wide range of RTK and raw data formats are supported.

Leica GR10	**Nominal value of frequency in L1 sub-band, in MHz**
GNSS technology	SmartTrack+
GNSS signals	GPS L1 C/A, L2P, L2C, L5 GLONASS: L1 C/A, L2P, L2C Galileo: E1, E5a, E5b, AltBOC BeiDou: B1, B2, B3 QZSS: L1, L2C, L5 SBAS: WAAS, EGNOS, GAGAN, MSAS
Measurement precision - **carrier phase**	L1: rms = 0.2 mm; L2: rms = 0.2 mm

- **code**	L1: rms = 20 mm; L2: rms = 20 mm
Web & FTP services	yes
Optional control software	Leica GPS Spider software
Weight	1.67 kg
Temperature range	-40^0C to $+65^0$C
Waterproof	MIL-STD-810F; Temporary submersion to 1 m
Shock/drop on hard surface	Withstand 1.0 m drop
Supply voltage	Nominal 12V DC
Raw data logging	MDB (Leica proprietary format) and RINEX
Data streaming	RTCM v2.1/2.2/2.3/3.0 NMEA 0183 Leica LB2 raw data
NTRIP	Integrated NTRIP server

Table 3. 2: *Technical Specifications of GR10 (courtesy Leica Geosystems).*

One of the most important features of this receiver is the dynamic channel assignment: for example, assume GPS and GLONASS are enabled in the tracking configuration but just a small number of GLONASS satellites are visible at the monitoring site (smaller than the number of channels assigned to GLONASS satellites), the free channels are automatically reassign to GPS constellation, in this way raw data for greater number of satellites is logged; thus, a better and more accurate solution is obtained.

3.3. u-blox EVK NEO – 7P receiver

The Evaluation Kit with Precision Timing output was developed by u-blox, a Swiss-based company and a leading provider of wireless and positioning sensors and modules for the automotive, industrial and consumer markets. EVK 7P is a consumer-grade GNSS receiver equipped with the u-blox next generation GPS platform NEO-7P and a high performance active GPS antenna.

The NEO-7P module combines the high performance of the u-blox 7 multi-GNSS engine with Precise Point Positioning (PPP) technology for GPS. u-blox' industry-proven PPP algorithm, in combination with SBAS, provides exceptional precision in clear-sky applications. For world-wide application, the NEO-7P supports Differential GPS (DGPS) operation as an alternative to SBAS and PPP, using RTCM correction messages from a local reference station or aiding network.

Highlights:

- High precision GPS < 1m (SBAS + PPP)
- Differential GPS by SBAS or RTCM
- Raw measurement data (GPS)
- 56 channel: GPS L1 C/A; GLONASS L1 FDMA, QZSS L1 C/A; SBAS
- GNSS receiver: GPS, GLONASS, QZSS and Galileo

Figure 3.2 presents the evaluation kit 7P including the antenna and the USB cable. The size of the receiver is 10.5x6.4x2.6 cm.

Fig. 3. 2: *u-blox EVK – 7P and antenna.*

u-blox develops and markets leading GPS technology, GPS chip sets, miniaturized GPS modules and smart antennas. The package includes the software u-center permitting to configure the transmitted data format and messages as well as to visualise in real time the data received via the configured interface. The most important feature of the software is the option to configure the interface. Here the sensor is connected via USB cable and the software redirects the computer USB automatically to a serial port. Moreover, the user can chose the output format, NMEA (National Marine Electronics Association) or ubx as well as the content of the format. Usually ubx binary format is chosen since raw measurements are available only in this case.

3.3.1. Potential of u-blox receivers

As already revealed the position accuracy can be better than 1 m (according to u-blox EVK - 7P technical sheet), in case SBAS and PPP options are enabled. This is possible since u-blox 7P sensor uses the carrier phase L1 and the C/A code for real time positioning. Not only this but also the data can be stored on a computer in a binary proprietary format, which can be then converted into RINEX file processed by geodetic approaches. Moreover, this receiver supports the output format NMEA, the standard for navigation applications and the Radio Technical

Commission for Maritime Services (RTCM) 2.3 standard. This last protocol is a unidirectional protocol (input to the receiver) that is used to supply the GPS receiver with real-time differential correction data (DGPS). The RTCM protocol specification is available from http://www.rtcm.org.

4 messages are supported: type 1, 2, 3 and 9; if either message 1 or 9 is received, then the receiver will use the corrections delivered to provide a position estimate using the available satellites for which corrections are available.

Message type	Description
1	Differential GPS corrections
2	Delta Differential GPS corrections
3	GPS Reference Station Parameters
9	GPS Partial Corrections Set

Table 3. 3: *Supported RTCM 2.3 messages types.*

The DGPS feature does not need any configuration to work properly. When an RTCM stream is input on any of the communication interfaces, the data will be parsed and applied if possible, which will put the receiver into DGPS mode.

The following restrictions apply to DGPS mode:

• The DGPS solution will only include measurements from satellites for which DGPS corrections were provided. This is because the navigation algorithms cannot mix corrected with uncorrected measurements.

• SBAS corrections will not be applied when using RTCM correction data.

• Precise Point Positioning will be deactivated when using RTCM correction data.

• RTCM correction data cannot be applied when using Assist Now Offline or Assist Now Autonomous.

3.3.2. u-blox challenges

Based on GPS Interface Control Document (ARINC, 2000), the minimum C/A code strength for a user on the earth surface is -160 dBW, value reached in case of no attenuation due to the propagation medium and environment of the user. Because of this attenuation the strength of the signal decreases and in many cases a geodetic receiver is not able to track signals with low dBm values. If low cost single frequency receivers are concerned, most of them acquire signal below -180dBW. They are called high-sensitivity receivers. Further information may be found e.g. in Wieser & Hartinger (2006).

As high sensitivity type, this receivers are capable of tracking signals close to -160 dBm which means that even the attenuated and reflected signals (multipath) are used and proper mitigation techniques become critical. In addition, being a single frequency receiver u-blox performance can be greatly influenced by ionosphere delays.

3.3.2.1. Multipath

Nowadays great effort is put in multipath analysis, which produces errors that cannot be removed by differential operation. In the following, the nature of multipath will be defined and some mitigation methods will be presented. As already mentioned in the beginning of the chapter, all GNSS receivers compute their position using the pseudorange from their antennas to the antennas of at least four satellites. These four distances determine the point in space where the receiver is located. As long as each satellite's signal travels along a direct path to the antenna, the receiver is able to compute the pseudorange with a very good accuracy, provided that atmospheric corrections, clock offsets and so on were applied. Unfortunately, this is not always the case: the ground and other objects can reflect the satellite's signal resulting in one or more secondary paths, always longer than the direct one, as shown in Figure 3.3.

In other words, multipath describes the effect of satellites signals arriving at the receiver by more than one path. This means that the direct line of sight signal overlays with one or more indirect signals, non-line-of-sight (Tawk, Y., 2013).

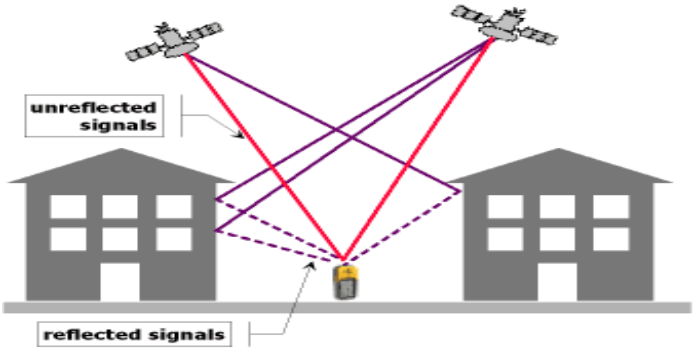

Fig. 3. 3: *Multipath.*

Due to longer propagation path of indirect signals, there is a phase offset (shift in code and carrier) between multipath signals. The phase offset is a function of the geometric conditions but also of time. Multipath propagation can be divided into static and dynamics. For automotive applications in urban environment, the multipath conditions will change continuously, and therefore it is one of the most disturbing problems of GNSS-based navigation systems (Twak, Y., 2013). For the purposes of this research only the static one is dangerous for the final results since the acquisition method is static as well. In this case the propagation geometry changes

slowly, making the multipath parameters constants for several minutes. Mostly static applications, such as surveying, are the main drivers for error reduction. Usually, in these situations the users experience one dominant and stable secondary path.

In less expensive receivers that use only C/A-code ranging, these secondary-path signals lead to errors that can be tens of meters or even more, especially in urban canyons (Dodson, A.H., Meng, X., Roberts, G.W., 2001).

For this research u-blox 7P platform was used. This cannot track at the same time two or more satellite systems. Therefore multipath errors will be more significant than in the case of concurrent GPS and GLONASS acquisition. However, the latest model from u-blox, the eight generation positioning platform 8M, allow the user to enable in the tracking configuration 2 satellite systems: GPS and GLONASS or BeiDou or GLONASS and BeiDou. Although having more satellites in view is of great help in the processing mode, concurrent tracking of more systems is not enough.

For example, u-blox carried a test in Tokyo to analysis the performance of the receiver when GPS and GLONASS are used together. The values of PDOP did not change much by using GPS and GLONASS together than the case with GPS alone. However, GLONASS significantly benefits from combining it with GPS (see Figure 3.4).

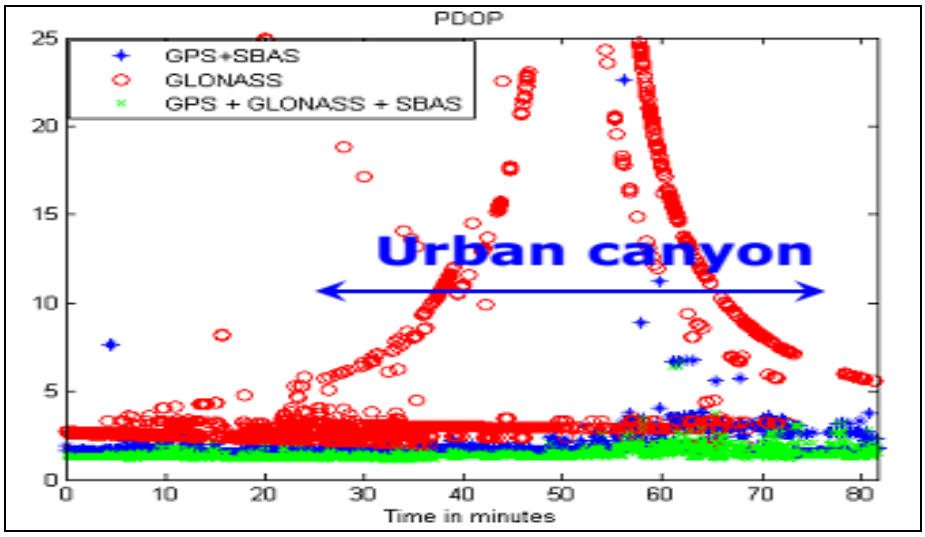

Fig. 3. 4: *Values of PDOP for different tracking configurations (courtesy u-blox).*

Regarding multipath, in this specific test, big values were recorded: GPS multipath appears up to 150 meters and GLONASS multipath appears up to 300 meters (according to u-blox GLONASS considerations, Product Marketing brochure, July 2011). Obviously this is a particular case but still is enough to prove how critical is to reduce the multipath errors.

There are few methods that can be applied in the field for reducing the influence of multipath on the data. Some of this spatial mitigation techniques required the use of a special antennas (such as the choke-ring type), multi-antennas arrays, antenna location strategy and ground plane. More details can be found in the work of Radovanovic, R. (2000) or Peres, T. (2008).

Sometimes these spatial mitigation techniques are combined with receiver processing methods to further decrease the multipath errors. By far the most promising methods for reducing multipath effects use real-time signal processing within the receiver.

For the experiments carried on during the research, to reduce the influence of the reflecting surfaces located near the antenna on the satellite signal, carefully selected location, cut off angle and SNR masks were used.

3.3.2.2. Ionosphere delays

The ionosphere is the zone of the terrestrial atmosphere that extends itself from about 60 km until more than 2.000 km in high. As it name says, it contains a partially ionized medium, as result of the X and UV rays of Solar Radiation and the incidence of charged particles.

The propagation speed of the GNSS electromagnetic signals in the ionosphere depends on its electron density, which is typically driven by two main processes: during the day, sun radiation causes ionization of neutral atoms producing free electrons and ions. During the night, the recombination process prevails, where free electrons are recombined with ions to produce neutral particles, which leads to a reduction in the electron density. As it can be seen in Figure 3.5 the signal is both refracted and retarded as it travels through the Earth's atmosphere, causing the signal to arrive at a GPS receiver later than it would have had if travelled through vacuum.

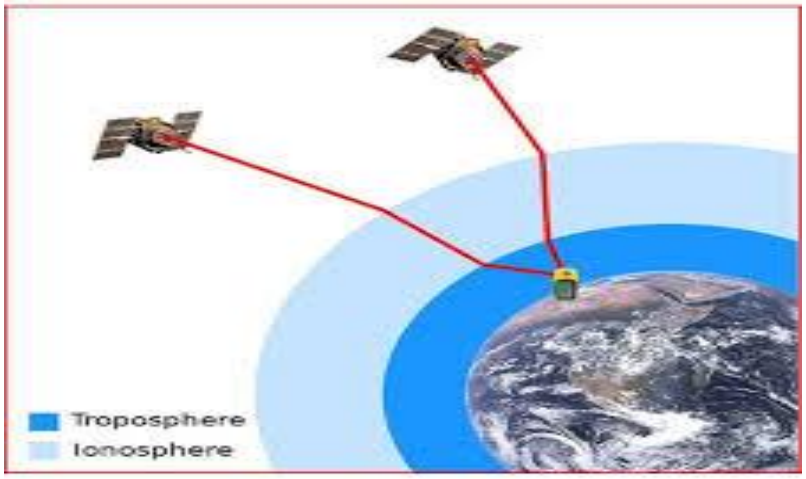

Fig. 3. 5: *Tropospheric and ionospheric delays (source: http://www.brighthub.com/electronics/gps/articles/111933.aspx).*

In a good approximation the ionospheric range error is related to the total electron content by

$$I = \frac{40.3}{f^2} * TEC \quad 3.1$$

with

I: ionospheric range error at frequency f [m]

TEC: the number of electrons per unit area along the path of propagation

Because the ionospheric error is not equal on L1 and L2 the following relation holds true:

$$I2 = \frac{f_1^2}{f_2^2} I1 \quad 3.2$$

Moreover, L1 and L2 carrier phases can be combined together that will reduce the ionospheric delay to zero. A new equation L3 is obtained:

$$L3(t) = \frac{f_1^2}{f_2^2 - f_2^2} L1(t) - \frac{f_2^2}{f_1^2 - f_2^2} L2(t) \quad 3.3$$

Substituting L1 and L2 with the observation equation for carrier phase and rearranging the terms in the end the ionospheric delay vanishes:

$$\frac{f_1^2}{f_2^2 - f_2^2} I1(t) - \frac{f_2^2}{f_1^2 - f_2^2} \frac{f_1^2}{f_2^2} I1(t) = 0 \quad 3.4$$

A significant number of GNSS applications uses single-frequency GNSS receivers. Therefore the precise estimation of ionospheric range error from single-frequency GNSS data is and remains to be an important issue (Mayer et al., 2006).

One option to correct the ionospheric range error in single-frequency applications is the use of models such as the Klobuchar (Klobuchar, 1987) model for GPS (GPS Interface Control Document [ICD] 200C). Another option is to take advantage of an additional augmentation service such as EGNOS in Europe (or WAAS in US). Finally, there is the option to derive the ionospheric correction term from code and carrier phases provided by single - frequency receivers (Mayer et al., 2006).

u-blox receivers, as all the other low cost devices, are single frequency and only L1 raw measurements are available hence the iono-free combination of L1 and L2 carrier is not possible. However, as aforesaid there are options for reducing the influence of the ionosphere: most processing software have ionospheric models implemented, Klobuchar is the most popular one by far, or they read and apply in processing IONEX grids from the International GPS Service for Geodynamics (IGS) or products from the Center for Orbit Determination in

Europe (CODE) that illustrates the geographic variation of TEC. Both IGS and CODE offer to user ionosphere maps on daily basis and free of cost (see Figure 3.6).

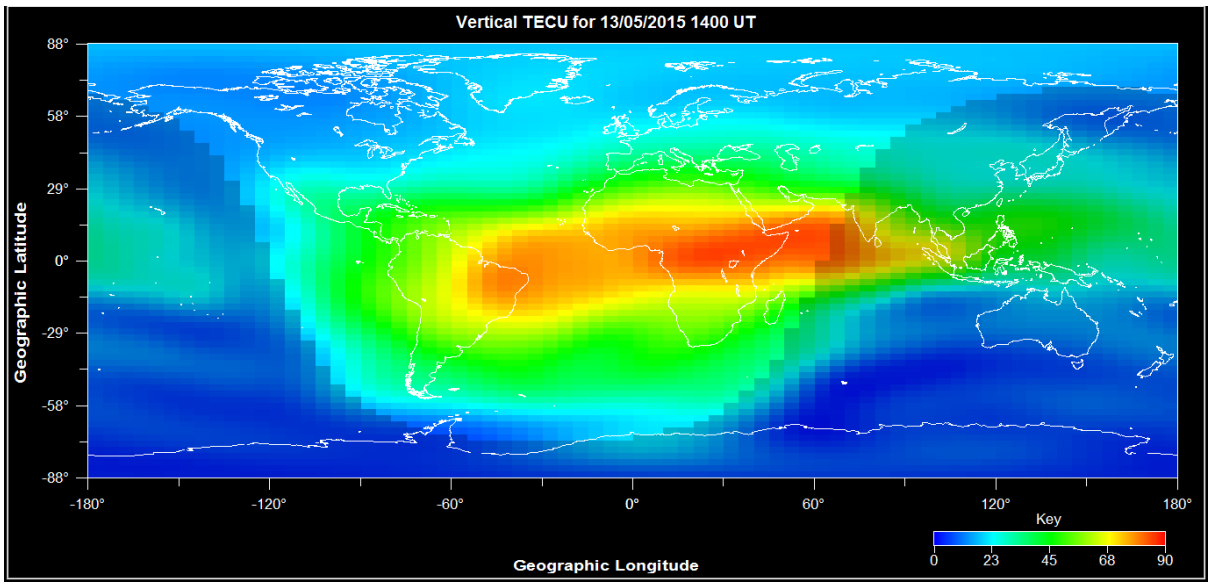

Fig. 3. 6: *Global Ionosphere map for May 13, 2015, at 02:00 UTC. Map generated by Leica Spider QC.*

Although this is a good alternative for Iono-free combination another problem arises: these precise products are not available in due time, it takes around 11 days to generate final ionospheric TEC grid and less than 24 hours for rapid ones. It is quite obvious that latency of this magnitude cannot simply be accepted in monitoring applications where near real time results are needed. As an administrator of a monitoring network composed by low cost receivers one might be tempted to simply use in processing mode the ionospheric corrections stored in the Navigation RINEX files. However, u-blox EVK-7P offers another way of modelling more accurate the ionosphere: this receiver is capable of tracking 3 SBAS satellites and therefore can take advantage of the ionospheric corrections sent by this augmentation system.

3.3.2.3. Antenna calibration

For precise positioning the accurate electronic antenna phase centre with respect to the geometric centre, the antenna offset, has to be known. This has been shown by Schwieger & Wanninger (2006) in their investigations about accurate positioning using low-cost GPS receivers.

Antenna calibration is the act of determining the point of reception of the GNSS carrier phase signals. Antenna hardware such as the antenna elements and pre-amplifiers create signal phase advance and delay before the signal is transmitted to the receiver. The phase advance/delay

changes the range measurement and introduces error to position solutions. The point of reception is not a physically measureable location on the antenna, and the point of reception varies depending upon the direction of the satellite signal being received.

In practice there are two methods of calibration, absolute and relative. For this research, a relative calibration of u-blox antenna can be performed on a short baseline with well-known end points. However, this experiment did not take place because of lack of time, therefore is not a part of the present thesis. What has been done till this moment is a PCF file in Bernese GPS software that contains all the necessary programs to perform and extract the Phase Centre Variation (PCV). In the near future the author has the intention to continue its work on this topic and perform the relative calibration of the u-blox antenna.

The concepts of average Phase Centre Offset (PCO) and Phase Centre Variation (PCV) are introduced to describe entirely the characteristics of antenna phase response. The average phase centre of an antenna is defined as the mean location of the antenna phase centre over a certain range of directions. The Antenna Reference Point (ARP) is defined as the geometric centre of the antenna, therefore the computed GPS station position. The difference between the average phase centre and the ARP is the phase centre offset (PCO), typically a vector up to 15 cm, given in north-east-up components and frequency dependent. The offset between the phase centre in a particular direction and the average phase centre is known as phase centre variation (PCV) in that direction, therefore azimuth and elevation dependent. PCV is not a point in a mathematical sense and are up to 2 cm.

In the end phase centre corrections (PCC) are determined by the calibration and divided in 2 parts: PCO and PCV. The mathematical representation of the antenna phase centre variation (PCV) correction is the following:

$$\Delta\phi(\alpha, z) = \Delta\phi'(\alpha, z) + \Delta r * e, \qquad 3.5$$

where

$\Delta\phi(\alpha, z)$: is the total phase centre correction in direction α, z,

α, z: is the azimuth and the zenith angle of the satellite line of sight,

Δr: defines the position of the mean antenna phase centre with respect to the mechanically defined ARP,

e: denotes the unit vector in the direction from the receiver antenna to the satellite,

$\Delta\phi'(\alpha, z)$: is the function modelling the phase centre variations. Usually two different model functions may be used: piece – wise linear function in elevation (and

optionally in the azimuth) and spherical harmonic function of maximum degree n and maximum order m < n.

Figure 3.7 presents in a simple manner all the above technical concepts.

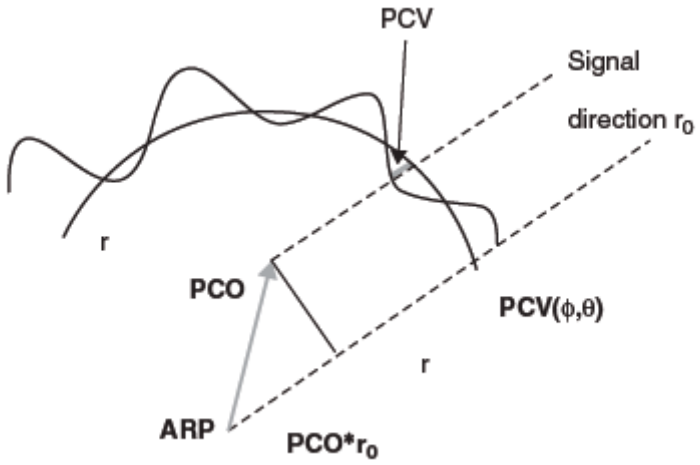

Fig. 3. 7: *Illustration of ARP, PCO and PCV.*

The results of the calibration, relative or absolute, are stored in an ATX file (Antenna Exchange Format) that may be included into commercial software such as Bernese GPS software, Leica Geo Office as well as into free and open source software (RTK Lib and goGPS).

The offsets as well as the elevation and azimuth dependent corrections are crucial for short baselines: most of the systematic GPS errors are eliminated in double difference processing, only the antenna phase centre variations (PCV) are neither available nor considered for low-cost antenna.

Based on what is written above it can be stated that there is a gap to be bridged between geodetic receivers and evolution kits. Efforts have been made in this direction and u-blox sensors are an example of low-cost GNSS platforms that improved greatly in the last years (multi-GNSS units capable of connecting to RTCM and NMEA streams). However, more improvements are needed. The challenges that u-blox 7P receiver has to overcome (as well as any other GNSS receiver) it can be stated that PCV and multipath are the most important station dependent errors. They can induce errors of cm level which may lead to wrong interpretation of landslide monitoring results and therefore, false critical situations may be alarmed.

Chapter 4. Carrier Phase and its Measurement

Each GPS satellite transmits unique navigational positioning and identification information centred on two L – band frequencies L1 (1575.42 MHz) and L2 (1227.6 MHz) and some satellites transmit also on L5 frequency (1176.45MHz). From now own only L1 carrier will be mentioned since it is the only one implemented into the u-blox receiver used for the experiments.

In the following sections, carrier phase will be described, modelled and analysed in terms of performing relative positioning. The discussion will begin with a description of carrier phase and the measurement of carrier phase. Then a model of the raw measurement will be presented. Some practical least – squares considerations will be included. At the end, an extended introduction into Bernese processing algorithm will be given. In addition, some of the features of the RTKLIB and goGPS free and open source software will be highlighted.

4.1. The carrier phase measurement and the carried information

Simply put, the carrier phase measurement is a measure of the range between satellite and receiver expressed in units of cycles of the carrier frequency (Cillian O'Driscoll, July/August 2010). The range can be measured with very high precision (of the order of millimetres), but the whole number of cycles between satellite and receiver is not known.

All current GNSS satellites transmit signals in the L-band. When discussing the phase of a signal it is important to realize that phase is fundamentally a property of sinusoids. Every sinusoid has an amplitude A and a phase Θ expressed in radians (at $t = 0$). Figure 4.1 depicts the received carrier signal with its cycles (in this case just 10 cycles).

L1 carrier is modulated with C/A (Coarse Acquisition) code, a precise code, P and the navigation message (see Chapter 2). In this situation the radio frequency (RF) carrier is no longer a sinusoid but can be expressed as a linear combination of sinusoids, therefore one must find the phase of the sum to two sinusoids. For GNSS analysis, the signal phase (carrier modulated with PRN code and navigation message) is the phase of the L1 carrier signal after all modulated information was wiped off.

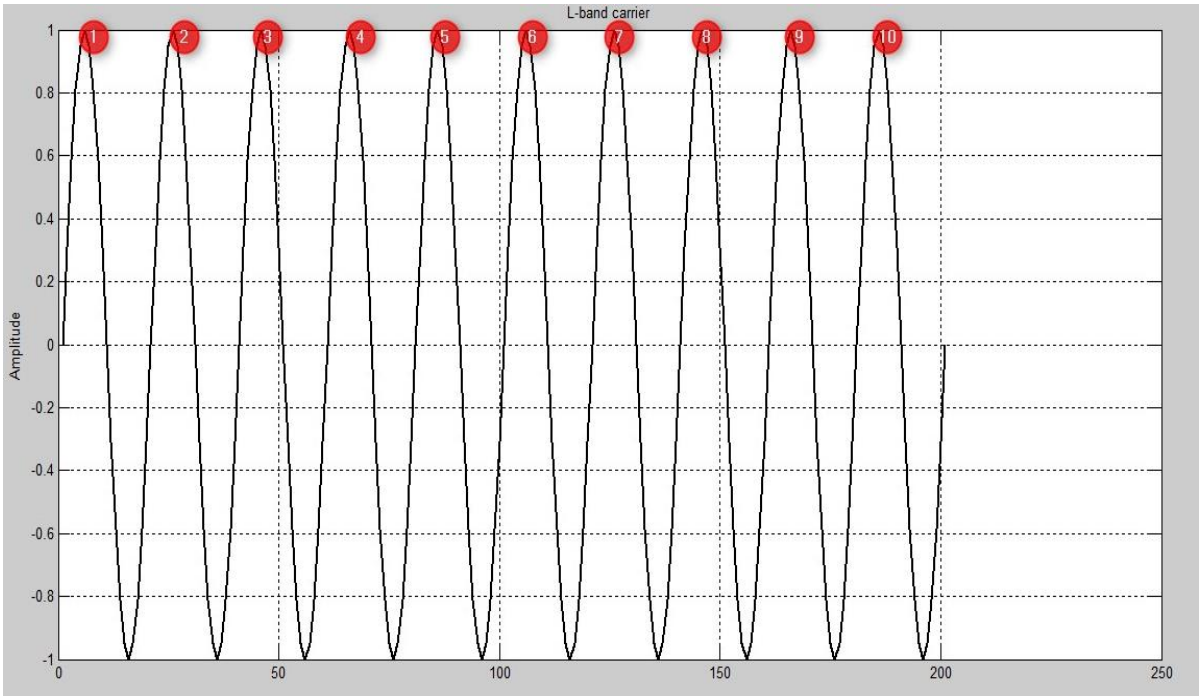

Fig. 4. 1: *Received L-band carrier signal (in red, number of cycles).*

Before deriving the phase observation model an introduction into waves must be provided.

Phase is simply angle of rotation, which is conventionally in units of cycles for GPS analysis. Consider a point moving anti-clockwise around the edge of a circle, and draw a line from the centre of the circle to the point. As illustrated in Figure 4.2, the phase ϕ(t) at any given time t can be defined as the angle through which this line has rotated.

Phase is closely connected with the concept of time, which is always based on some form of periodic motion, such as the rotation of the Earth, the orbit of the Earth around the Sun ("dynamic time"), or the oscillation of a quartz crystal in a wristwatch ("atomic time"). Angles of rotation give us our measure of time. In this way, phase can be thought of as a measure of time (after conversion into appropriate units).

$$T(t) = k(\varphi(t) - \varphi_0) \qquad 4.1$$

where T(t) is the time according to our clock at time t (whatever the clock may be), $\varphi_0 = \varphi(0)$ is so that the clock reads zero when t = 0, and k is a calibration constant, converting the units of cycles into units of seconds. Indeed, we can take the above equation as the definition.

The frequency expressed in units of cycles per second, is the number of times the line completes a full 360 degrees rotation in one second (which of course, is generally a fractional number). One can better define frequency instantaneously as the first derivative of phase with respect to time; that is, the angular speed (Blewitt, G., 1997).

$$f = \frac{d\varphi(t)}{dt} \quad 4.2$$

Constant frequency is the basis of an ideal clock. If the frequency can be written as a constant, f_0, then we can write the phase of an ideal clock as:

$$\varphi_{ideal} = f_0 t + \varphi_0 \quad 4.3$$

Therefore

$$t_{ideal} = k f_0 t \quad 4.4$$

An appropriate choice for the calibration constant is k = $1/f_0$, where f_0 is the nominal frequency of the oscillator. The clock time can be written now as:

$$t_R(t) = \frac{\varphi(t) - \varphi_o}{f_o} \quad 4.5$$

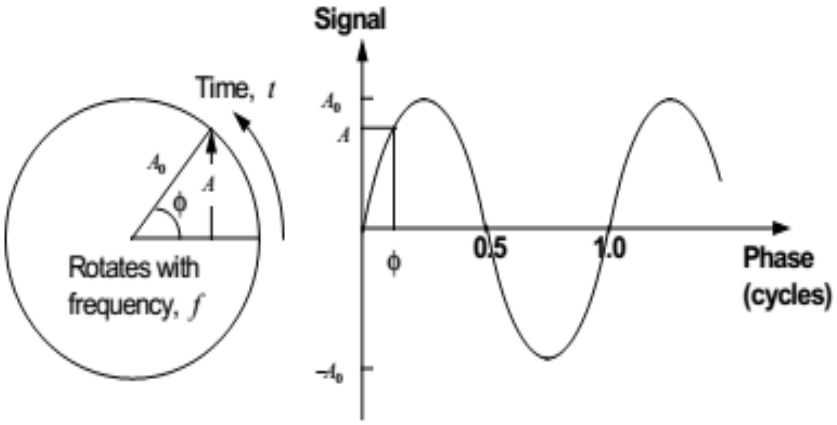

Fig. 4. 2: *The meaning of phase.*

At time t, the height of point A(t) above the centre of the circle in figure 4.2 is given by:

$$A(t) = A_0 \sin[2\pi\tau\varphi(t)] \quad 4.6$$

Where A_0 is the radius of the circle. Here we treat a periodic signal thus we can call A(t) the 'signal' and A_0 the 'amplitude of the signal'. For example, in the case of radio waves, A(t) would be the strength of the electric field, which oscillates in time as the wave passes by. Inverting the above formula, we can therefore determine the phase $\varphi(t)$ if we measure the signal A(t) (and similarly, we could infer the clock time).

In the case of an ideal clock, the signal would be a pure sinusoidal function of time:

$$A_{ideal} = A_0 sin 2\pi\varphi_{ideal}$$

$$= A_0 \sin(2\pi f_0 t + 2\pi\varphi_0)$$

$$= A_0 \sin(2\pi f_0 t + 2\pi\varphi_0)$$

$$= (A_0 \cos 2\pi\varphi_0)\sin 2\pi f_0 t + (A_0 \sin 2\pi\varphi_0)\cos 2\pi f_0 t$$

$$= A_0^S \sin(\omega_0 T) + A_0^C \cos(\omega_0 T) \qquad 4.7$$

Where $\omega_0 = 2\pi f_0$ is the 'angular frequency' and is measured in radians per second. For a real clock, the signal would be the same sinusoidal function of its own 'clock time'

$$A(T) = A_0^S \sin(\omega_0 T) + A_0^C \cos(\omega_0 T) \qquad 4.8$$

As already explained the above form of the nominal GNSS signal is not entirely completed because of the modulation by 'chips', formed by multiplying the amplitudes A_0^S (for C/A code) and A_0^C (for P code) by a pseudorandom sequence of +1 or -1. The base sinusoidal signal is called the *carrier signal*. It is the phase of the carrier signal that gives us precise access to the satellite clock time; therefore we can use this phase for precise positioning.

The range between satellite and receiver is expressed in units of cycles of the carrier frequency but in the model an integer number of cycles N is missing. To deal with this, the following assumption holds true. Suppose we only record the fractional phase of the first measurement. There is no way of knowing which integer N has to be added to this recorded phase so that it really provides the difference in phase between the replica signal and the GPS signal. This is fundamentally because we have no direct measure of the total phase of the incoming GPS signal. We can express this as follows:

$$\phi + N = \varphi_R - \varphi_G \qquad 4.9$$

Where ϕ represents the phase value actually recorded by the receiver. Provided the receiver does keep track of how many complete signal periods there have occurred since the first measurement, it can attach this number of cycles to the integer portion of the recorded phase. However, there will still be an overall unknown constant ambiguity N that applies to all measurements.

$$\text{N} = (\text{integer portion of } \varphi_R - \varphi_G) - (\text{integer portion of } \phi) \qquad 4.10$$

The second term is completely arbitrary, and depends on the receiver firmware. For example, some receivers set this value to zero for the first measurement. Let us assume this is true, and drop this term. We can interpret N as equal to the number of carrier wavelengths between the receiver (at the time it makes the first observation), and the satellite (at the time it transmitted the signal).

If the receiver loses count of the oscillations (e.g., because the signal is obstructed), then a new integer parameter must be introduced to the model, starting at that time. This integer discontinuity in phase data is called a *cycle slip*.

4.2. Carrier phase observation model

The satellite carrier signal is mixed with reference signal generated by receiver's clock. The result, after high pass filtering, is a 'beating' signal. The phase of this beating signal equals the reference phase minus the incoming GPS carrier phase from a satellite; however, it is ambiguous by an integer number of cycles. By ''carrier beat phase'' it is simply meant the ''carrier phase'' but not the phase of the incoming signal. Observation of satellite S produces the carrier phase observable:

$$\phi^S(t) = \varphi(t) - \varphi^S(t) - N^S \qquad 4.11$$

Where φ is the replica phase generated by the receiver clock, and φ^S is the incoming signal phase received from GPS satellite S. The measurement is made when the receiver clock time is t.

Now take the point of view that the phase of the incoming signal received at receiver clock time t is identical to the phase that was transmitted from the satellite at satellite clock time t^S

$$\varphi^S(x, y, z, t) = \varphi^S_{transmit}(x^s, y^s, z^s, t^s_{transmit}) \qquad 4.12$$

Of course, if we adopt this point of view, then we shall eventually have to consider the model of how long it takes a wave front of constant phase to propagate from the satellite to the receiver, so that we may model the appropriate satellite clock time at the time of signal transmission, t^S. We return to that later.

We can write clock time as a function of phase and nominal frequency:

$$t(t) = \frac{\varphi(t) - \varphi_0}{f_0} \qquad 4.13$$

We can therefore substitute all the phase terms with clock times:

$$\varphi(t) = f_0 t + \varphi_0 + f_0 \Delta t \qquad 4.14$$

$$\varphi^S_{transmit} = f_0\, t^s_{transmit} + \varphi^S_0 + f_0\, \Delta t^s_{transmit} \qquad 4.15$$

Therefore, the carrier phase observable becomes:

$$\phi^S(t) = f_0\,(t_R - t^S) + \varphi_0 - \varphi^S_0 - N^S \qquad 4.16$$

Where we implicitly understand that the clock times refer to different events (reception and transmission, respectively).

It is convenient to convert the carrier phase model into units of range. This simplifies concepts, models, and software. In the range formulation, we multiply the carrier phase equation by the nominal wavelength.

$$L_R^S(t) = \lambda_0 \phi_R^S(t)$$
$$= \lambda_0 f_0(t_R - t^S) + \lambda_0(\varphi_{0R} - \varphi_o^S - N_R^S)$$
$$= c(t_R - t^S) + \lambda_0(\varphi_{0R} - \varphi_o^S - N_R^S)$$
$$= c(t_R - t^S) + B_R^S \quad 4.17$$

Where we still retain the name *carrier phase* for $L_R^S(t)$, which is in units of meters. We see immediately that this equation is identical to that for the pseudorange, with the exception of the carrier phase bias, B.

We note that the first term in the carrier phase model is simply the pseudorange, and the second term is constant. We have already developed a simplified model for pseudorange, so we can therefore write a model for carrier phase as follows:

$$L_R^S(t) = c(t_R - t^S) + B_R^S$$
$$= \rho_R^S(t_R, t^S) + c(dt_R(t) - dt^S(t)) + T_R^S - I_R^S + B_R^S \quad 4.18$$

In the above expression, we have explicitly included the delay on the signal due to the troposphere T_R^S and the ionosphere $-I_R^S$ (the minus sign indicating that the phase velocity actually increases).

The model for pseudorange, derived in Chapter 2, can be similarly improved, with the small difference that the ionospheric delay has a positive sign.

$$P_R^S(t) = \rho_R^S(t_R, t^S) + c(dt_R(t) - dt^S(t)) + T_R^S + I_R^S \quad 4.19$$

This is because, from the physics theory, any information, such as the +1 and -1 chips which are modulated onto the carrier wave, must travel with the group velocity rather than phase velocity: groups are delayed while phases are advanced.

We typically do not know the true time of signal reception t_R which we need to calculate the satellite – receiver range term $\rho_R^S(t_R, t^S)$ precisely. As it has been already written at the beginning of this chapter the true time of reception can be written:

$$t_R = t + dt_R \quad 4.20$$

Where the epoch t_R is known exactly, as it is the receiver clock time written into the data file with the observation (and hence called the ‘’time-tag’’). However, the receiver clock bias dt_R

is not known initially, but could be as large as milliseconds. The problem is that, due to satellite motion and Earth rotation, the range will change by several meters over the period of a few milliseconds, so specific numerical techniques are applied to model this in data processing.

The key point to note is that the received carrier phase gives information regarding the range between satellite and receiver. Ideally, we want to obtain a measure of the range expressed in units of cycles.

The number of unknowns reduces to three since the receiver can estimate the received phase. These are:

- the receiver time t_R
- the initial satellite phase offset and the initial receiver phase offset
- the integer number of cycles between satellite and receiver N

A way of accounting for the effects of the first two is differencing the observations as it will be explained in the next lines.

4.3. Differencing techniques

Differences of the original observations allow to eliminate or reduce some biases. Differencing between satellites removes errors in the receiver time component, while differencing between receivers removes errors in the satellite phase offset.

GNSS can also provide relative position information. For example, positioning one receiver relative to a known static receiver. In DGPS algorithms, if the base station coordinates are known in an absolute coordinate frame, the position of the other receiver is also absolute only because it is computed relative to a receiver with an absolute position (Petovello, M., May/June 2011).

The standard DGNSS technique consists of the determination of the GNSS position from an accurately-surveyed position known as reference station. As prerequisites, a reference station in the vicinity of the rover and concurrent continuous tracking at both sites are needed. In the neighbourhood of a clean – sky location, the main errors are constant or present slow variation with time and user position. Consequently, they cancel out when differential processing is performed. Starting from the reference station, the system computes and broadcasts either corrections to the GNSS position or to the pseudorange measurements to the DGNSS users. Other uncorrelated errors (e.g. multipath, receiver noise) cannot be corrected by this method and specific techniques have to be applied to mitigate them.

4.3.1. Single difference

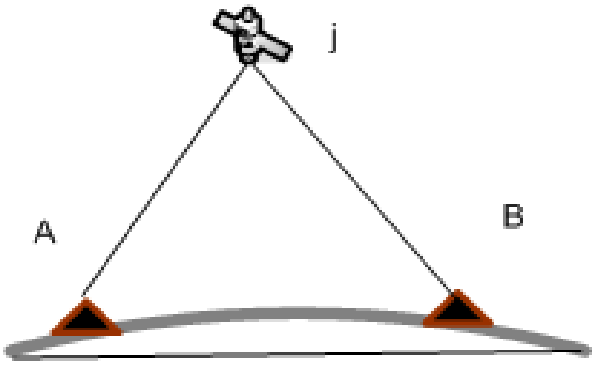

Fig. 4. 3: *Single difference geometry.*

The purpose of single differencing is to eliminate satellite clock offsets and initial phase. Consider the observation equations for two receivers, A and B observing same satellite j:

$$L_A^j = \rho_A^j + c(dt_A - dt^j) + T_A^j - I_A^j + B_A^j \quad 4.21$$

$$L_B^j = \rho_B^j + c(dt_B - dt^j) + T_B^j - I_B^j + B_B^j \quad 4.22$$

The single difference phase is defined as the difference between these two:

$$\Delta L_{AB}^j = L_A^j - L_B^j = (\rho_A^j + c(dt_A - dt^j) + T_A^j - I_A^j + B_A^j) - (\rho_B^j + c(dt_B - dt^j) + T_B^j - I_B^j + B_B^j)$$

$$= \Delta\rho_{AB}^j + c\Delta t_{AB} + \Delta T_{AB}^j - \Delta I_{AB}^j + \Delta B_{AB}^j) \quad 4.23$$

An assumption has been made, that the satellite clock bias is effectively identical at the slightly different times that the signal was transmitted to A and B. Another point worth mentioning, is that the coordinates of the satellite at transmission time can easily be significantly different for receivers A and B, and this should be modelled when computing $\Delta\rho_{AB}^j$.

The atmospheric delay terms are now considerably reduced, and vanish in the limit that the receivers are standing side by side. The differential troposphere can usually be ignored for baselines less than approximately 15 km, however differences in height should be modelled (Basics of the GPS technique). The differential ionosphere can usually be ignored for separations of 1 to 10 km, depending on ionospheric conditions. Due to ionopsheric uncertainty, it is wise to calibrate for the ionosphere using dual-frequency receivers for distances greater than 10 km.

Although the single difference has the advantage that many error sources are eliminated or reduced, the disadvantage is that only relative position can be estimated (unless the network is

global-scale). Moreover, the receiver clock bias is still unknown, and very unpredictable. This takes us to double differencing.

4.3.2. Double differencing

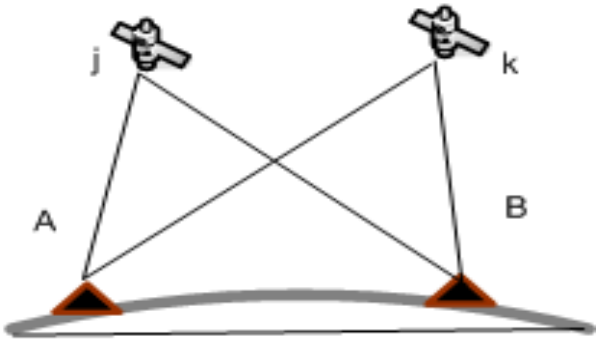

Fig. 4. 4: *Double differencing geometry.*

The purpose of double differencing is to eliminate receiver clock bias. Consider the single differenced observation equations for two receivers A and B observing satellites i and j:

$$\Delta L^{i}_{AB} = \Delta\rho^{i}_{AB} + c\Delta t_{AB} + \Delta T^{i}_{AB} - \Delta I^{i}_{AB} + \Delta B^{i}_{AB}) \quad 4.24$$

$$\Delta L^{j}_{AB} = (\Delta\rho^{j}_{AB} + c\Delta t_{AB} + \Delta T^{j}_{AB} - \Delta I^{j}_{AB} + \Delta B^{j}_{AB}) \quad 4.25$$

The double difference phase is defined as the difference between these two:

$$\Delta L^{ij}_{AB} = (\Delta\rho^{i}_{AB} + c\Delta t_{AB} + \Delta T^{i}_{AB} - \Delta I^{i}_{AB} + \Delta B^{i}_{AB}) - (\Delta\rho^{j}_{AB} + c\Delta t_{AB} + \Delta T^{j}_{AB} - \Delta I^{j}_{AB} + \Delta B^{j}_{AB})$$
$$= (\Delta\rho^{ij}_{AB} + \Delta T^{ij}_{AB} - \Delta I^{ij}_{AB} + \Delta B^{ij}_{AB}) \quad 4.26$$

Where we use the double-superscript to denote quantities identified with two satellites, and the upside – down triangular symbol as a mnemonic device, to emphasise that the difference is made between two points in the sky. Figure 4.4 illustrates the geometry of double differencing.

Any systematic effects due to not modelled atmospheric errors are generally increased slightly by approximately 40 % by double differencing as compared to single differencing. Similarly, random errors due to measurement noise and multipath are increased. Overall, random errors are effectively doubled as compared with the undifferenced observation equation. On the other hand, the motivation for double differencing is to remove clock bias which would create much larger errors.

The double difference combination has an additional advantage, in that the ambiguity is an integer:

$$\Delta B_{AB}^{ji} = \Delta B_{AB}^{j} - \Delta B_{AB}^{i}$$

$$= \left(B_A^j - B_B^j\right) - \left(B_A^i - B_B^i\right)$$

$$= \lambda_0\left(\varphi_{0A} - \varphi_o^j - N_A^j\right) - \lambda_0\left(\varphi_{0B} - \varphi_o^j - N_B^j\right) - \lambda_0\left(\varphi_{0A} - \varphi_o^i - N_A^i\right) + \lambda_0\left(\varphi_{0B} - \varphi_o^i - N_B^i\right)$$

$$= -\lambda_0\left(N_A^j - N_B^j - N_A^i + N_B^i\right)$$

$$= -\lambda_0 \Delta N_{AB}^{ji} \qquad 4.27$$

Hence we can write the double differenced phase observation equation:

$$\Delta L_{AB}^{ji} = \Delta \rho_{AB}^{ji} + c\Delta\tau_{AB} + \Delta T_{AB}^{ji} - \Delta I_{AB}^{ji} - \lambda_0 \Delta N_{AB}^{ji} \qquad 4.28$$

4.4. Double differencing in GPS software

In the next lines a step by step introduction to data processing in commercial, academic and FOSS software is given. The author picked Bernese GPS software, Leica Geo Office, RTKLIB and goGPS for this research.

4.4.1. Bernese processing

In this last part of the chapter a detailed description on how double differences are processed by Bernese software is provided. Before starting any routine the input data must be organised and download: RINEX files and IGS products, i.e. Earth Rotation Parameters and Orbits. Once all this step is finished the next ones can be carried out.

First, a pre-processing part is needed in order to scan the data for possible problems and to convert it to Bernese format. In this part final results are not produced but data is prepared for the main estimation program (GPSEST).

Some standard preparatory steps must be performed (see Figure 4.5). Orbit and earth orientation files downloaded from IGS are converted to Bernese formats.

Program POLUPD: The IERS formatted pole file (IEP) provided, e.g., by the IGS, is converted to Bernese format (ERP).

Program PRETAB: The precise orbit file (PRE), e.g., from the IGS, is converted to a Bernese tabular orbit file (TAB). In addition, the satellite clock corrections are extracted from the precise file and stored in a Bernese satellite clock file (using a polynomial representation).

Program ORBGEN: Starting from the tabular orbit file, a standard orbit file is created by means of numerically integrating the equations of motion.

After this, the RINEX files are converted to Bernese format. A summary of all available observation data is created. Program RXOBV_P is responsible for converting RINEX files to Bernese observation files.

Program CODSPP – used to synchronize the receiver clocks to GPS time. Only code observations are used for this step.

Program SNGDIF – forms baselines from zero-difference observation files. The output are single-difference observation files. The program may create single-differences for both, phase and code measurements. Usually, only the phase single-differences are used for further computations. For this research, STAR algorithm was selected. Using this strategy the baselines are built by connecting one reference station with all remaining stations.

Program MAUPRP – pre-processes the files formed by SNGDIF: finds and solves cycle slips, removes outliers, and adds multiple ambiguities for the phase observation files. In current project it will work with baseline observation files (single-difference mode).

Regarding ambiguity resolution, first a float solution characterized by real valued ambiguities is computed, then with the help of an ambiguity resolution strategy these float values are resolved to their integer numbers.

In the last step an ambiguity fixed solution is computed and normal equation information is stored. The estimated parameters are: coordinates, zenith path delays and horizontal tropospheric gradients.

Program RESRMS – screens the post-fit residuals produced in a GPSEST run to identify outliers.

Typically the normal way to process phase observations as double-differences is to perform the receiver clock synchronization (program CODSPP), form baselines from phase observation files (program SNGDIF) and clean the single – difference phase observation files (program MAUPRP).

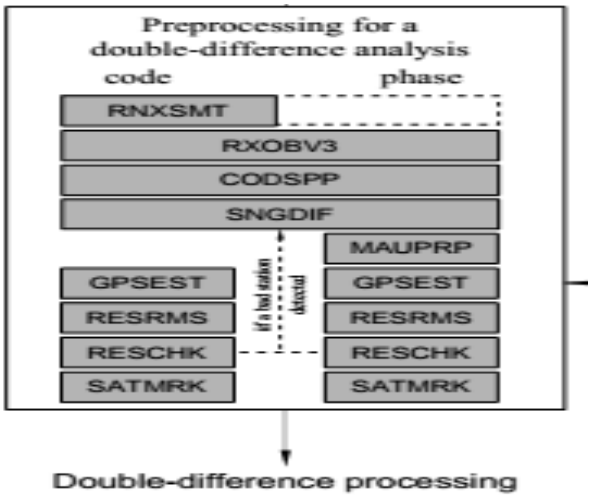

Fig. 4. 5: *Functional flow diagram for pre-processing for a double-difference analysis.*

The final processing is based on Least Squares Estimation. In the Bernese GPS Software two main programs are used for the adjustment of model parameters:

Program GPSEST – processes the observations, sets up the observation equations and solves the normal equation. To be able to successfully run this program all observation must be available in files (runs in batch mode).

Program ADDNEQ2 – manipulates and combines solutions on the normal equation level

Before going deeper into GPSEST program and explaining how it works, a short introduction to Least Squares theory must be given:

Basic Theory of Least-Squares Estimation

Observations of the same quantity (noted here with u) that have been performed at the highest possible accuracy provide different values. This leads to the conclusion that high precision observations are not a deterministic phenomenon but are characterized by several, unpredictable errors. Therefore, high precision observations can be seen as following a normal distribution.

The fundamental principle of least squares can be shortly defined as the most probable value for a quantity obtained from repeated observations is the value that is giving the sum of the squares of the residuals a minimum.

$$v'v = min,$$

where v is the difference between estimated and real observation.

The linearized observation equations in the Gauss-Markoff Model of full rank are given, e.g., by (Koch, 1988):

$$E(y) = A\,x \qquad 4.29$$

$$C(y) = \sigma^2 P^{-1} \qquad 4.30$$

with

n, u: number of observations, number of unknowns,

$A_{n\,x\,u}$: matrix of given coefficients with full rank A =u, is called design matrix,

x: u x 1 vector of unknowns,

y: n x 1 vector of observations,

P: n x n positive definite weight matrix,

E (.): operator of expectation,

C (.): covariance matrix,

σ^2: variance of unit weight (variance factor).

The observation equations may be written in this form. For n > u, the equation system $Ax = y$ is not consistent. With the addition of the residual vector v to the observation vector y, one obtains a consistent but ambiguous system of equations, also called system of observation equations:

$$y + v = A\,x \quad with \quad E(v) = 0 \quad and \quad C(v) = C(y) = \sigma^2 P^{-1} \qquad 4.31$$

Equations (4.30) and (4.31) are formally identical. $E(v) = 0$, because $E(y) = Ax$, and $C(v) = C(y)$ follows from the law of error propagation.

There are two components involved in Least – Squares Adjustment: a stochastic model, the covariance matrix (introduces information about the precision of observations) and the deterministic model, which is basically a set of equations that defines an adjustment condition. As it can be seen in (4.30), the deterministic model expresses mathematically the relations between observations y and unknown parameters x.

The method of least-squares asks for restrictions for the observation equations (4.30) and (4.31). The introduction of the restrictions assumes a minimum is necessary to lead us from the ambiguous observation equations (4.30) and (4.31) to an unambiguous normal equation system (called NEQ system in Bernese) for the determination of p.

Just to summarize the Least-Squares Estimation:

Normal equations: $(A^tPA)x^{est} = A^tPy \quad or \quad Nx^{est} = b \qquad 4.32$

Estimates:

the vector of unknowns: $x^{est} = (A^tPA)^{-1}A^tPy$ 4.33

the (variance) covariance matrix: $C(x^{est}) = \sigma^{2est}(A^tPA)^{-1}$ 4.34

the observations: $y^{est} = Ax^{est}$ 4.35

the residuals: $v^{est} = y^{est} - y$ 4.36

Degree of freedom, redundancy:

$$f = n - u \quad 4.37$$

All these formula are used by the program GPSEST for parameter estimation. The current version of GPSEST supports GNSS phase observations, GNSS code observations and Satellite Laser Ranging (SLR) observations. The first two are the interesting ones for the purpose of this research and they will be processed together at a first step while for the final solution only phase observations will be take into account.

For reaching the aims of this research the phase observations should be processed as double differences. These are obtained GPSEST from the input single-difference (baseline) observation files.

Regarding the other processing parameters:

First frequency L1. Usually a user would chose to use both frequencies available in most of the most the geodetic receivers on the market. However, in this case the author had to limit to L1 frequency since u-blox receivers are single-frequency sensors and no L2 observations are available. In addition, to account for the disadvantage of not having L2 observations and therefore no iono-free combination local or global ionosphere models can be used.

The modelling of the observables includes tropospheric and ionospheric refraction, phase centre variations for receiving and sending antennas (Bernese GPS Software User Manual, January 2007).

If double – differenced observations are processed, mathematical correlations between the differenced observations have to be considered because the same original observations may occur in several observation differences (Bernese GPS Software User Manual, January 2007).

With the difference operator D defined in the following way

$$\Delta L = D\,y \quad 4.38$$

where y represents the vector of undifferenced observations and y'' is the vector containing the double-differenced observations, the covariance matrix is:

$$D(\Delta L) = CD(\Delta L)C^t \qquad 4.39$$

For the moment, Least-Squares Estimation may be put aside and focus more on the GPSEST program. The core of the program is the loop over all epochs in which the observations are read, the partials are computed and the normal equation is accumulated the inversion of the normal equation and computation of the solution (see Figure 4.6).

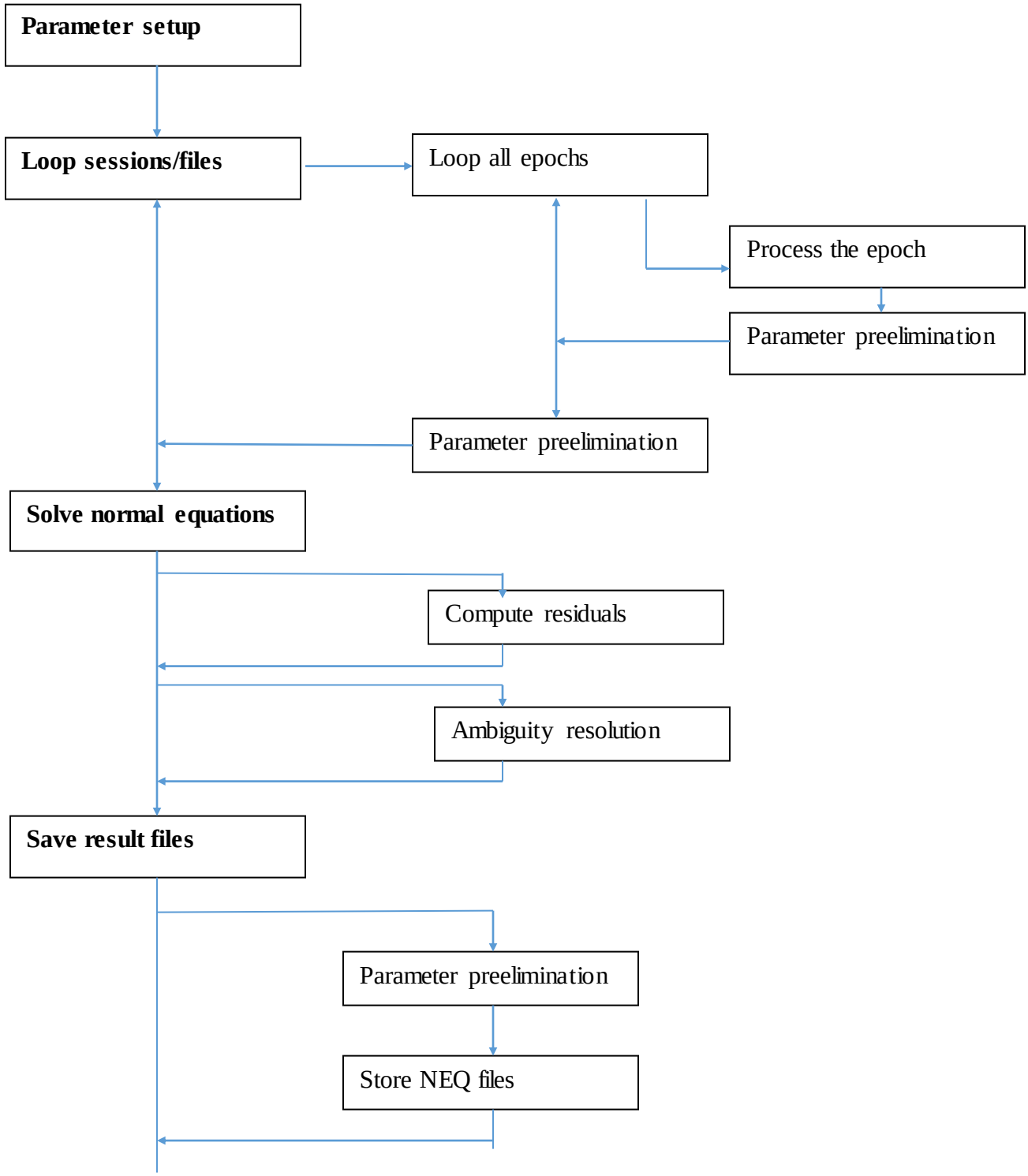

Fig. 4. 6: *Flow diagram of GPSEST.*

By forming the double differencing the clock corrections, hardware delays for receiver and satellite as well as the initial phase shift term have cancelled out. However, the integer number of cycles between satellite and receiver are still ambiguous. At this moment, two steps are performed in Bernese GPS software (1) the initial phase ambiguity parameters have to be estimated as real-valued parameters in a first step (the so called float solution is obtained) and (2) the ambiguities are resolved by assigning integer values to the float solution. The main advantage by fixing ambiguities is the reduction in the number of parameters and the stability of the solution. Actually, most of the unknown parameters are the ambiguities themselves.

In Bernese GPS software there are 4 methods implemented to resolve ambiguities. Although one is more appropriate than the other in different occasions, all consist in the two steps notified above:

Step 1: Real numbers are given for ambiguities.

Step 2: Results of step 1 become integer numbers based on some statistical tests performed.

In the Bernese GPS software ambiguities may be resolved only if double-difference observations are processed. (Bernese GPS Software User Manual, January 2007).

As stated before there are 4 ambiguity resolution strategies implemented in the current version of the Bernese GPS software: ROUND, SIGMA, SEARCH and QIF (selection takes place in panel ‘’GPSEST 3.2: General Options 2’’). The user has the possibility to deactivate the ambiguity resolution by selection ‘’NONE” but this is not recommended.

In few words the 4 strategies will be described emphasising their strong and weak points.

ROUND algorithm is the simplest and only rounds the real numbers to the nearest integers without using any statistical tests. Typically, this is option is not selected since SIGMA strategy can do the same. For long baselines, longer than few kilometres, this preference should not be take into account.

SEARCH algorithm is related to FARA (Fast Ambiguity Resolution Approach) algorithm (see [Frei and Beutler, 1990], [Frei, 1991]). Here, the variance factor and the corresponding cofactor matrix are used for the standard deviation for the ambiguity parameter. Next, a confidence level alfa and a statistic distribution (most probably Student’s distribution) the upper and lower range width for the integer valued is computed. It is almost mandatory to use SEARCH strategy in

rapid static mode. When both L1 and L2 phase observations are available in few minutes the fixed solution can be obtained with an accuracy of a centimetre. For the case when only L1 data are used, a longer session should be processed, of about 30 minutes. The main problem introduced by this ambiguity resolution strategy is the fact, that either all the ambiguities are fixed or none (not acceptable for long baselines, see Bernese User Manual, Chapter 8, section 8.3.2 for more details).

SIGMA algorithm works as the previous two, after the real-valued numbers are obtained, the integer values are introduced for the resolved ambiguities. The process is terminated if all ambiguities have been resolved, or if in the last step no ambiguity could be resolved.

The sigma-dependent strategy makes use of the full variance-covariance information and is useful for linear combinations like L1, L2, L3, L5 and L1&L2. This strategy is recommended when only single-frequency measurements are processed (but long sessions), the baseline should be less than 20 km. The developers of the Bernese GPS software recommend it also for code measurements of high quality on both frequencies.

QIF (Quasi Ionosphere-Free) Algorithm. In the newly double-difference equation the troposphere bias is neglected. Iono-free combination is used. This strategy is good for very long baselines (1000-2000km) and long sessions.

Based on the characteristics of the u-blox sensors used in experiments, based on the length of the sessions and the baselines SIGMA algorithm was the preference of the author for post-processing data.

To summarize, to be able to process double-differences in the Bernese GPS software the following files are required to execute the routine:

- Station name abbreviation file
- Coordinate file
- List of reference sites in the coordinate file
- Velocity file

4.4.2. Leica GeoOffice

Leica Geo Office Software (LGO) is a single software package that supports all sensors and surveying techniques. LGO allows handling GNSS, Terrestrial Positioning System (TPS) and levelling data either individually or in an integrated way.

In LGO the user can select between Manual and Automatic processing modes. In the first case, he can configure how the data is processed: baseline processing is allowed. In this case, all processing parameters will be computed automatically.

No matter the mode there is a complete list of processing parameters. For low elevation satellites, that many times proved to be problematic, the user can set an appropriate cut-off angle (default is 15 degrees). Broadcast and precise ephemeris are supported, however only NOAA/NGS SP3 format is supported currently. As solution type, LGO supports Automatic, Phase: all fix, Phase: GPS fix, GLONASS float, Code and Float mode.

- Automatic mode supposed to use code and phase observations for the computation and to resolve the ambiguities. When only code or phase measurements are available the system automatically switches to use the appropriate observations.
- Phase: all fix, no difference from automatic mode, the results should be more or less the same.
- Phase: GPS fix, GLONASS float will only attempt to resolve ambiguities for GPS satellites and keep GLONASS ambiguities at their float values.
- Code mode offers only code solution and it is less accurate than the Phase options but much faster.
- Float type means the ambiguities are not solved.

Like in Bernese the user can define the processing strategy. LGO offers the following choices:

Automatic, L1/E1, L2, L1/E1 + L2, Iono free (L3). The software selects the best frequency or combination of frequencies for the final solution. For dealing with ionosphere delays, a linear combination of L1 and L2 carriers is offered (L3 solution). In addition, tropospheric models and ionospheric models are implemented as well to help when only single-frequency receivers are used. Two options have to be described here: for ionospheric model, Computed option results in an ionospheric model computed based on an observation session of at least 45 minutes of static dual-frequency data when they are available. This is advantageous, as the model computed is in accordance with the conditions prevalent at the time and position of observation (Leica Geo Office Online Help). The other option is Klobuchar model, which has its parameters broadcast by satellites and stored in the header of navigation RINEX files; this is daily updated (Leica Geo Office Online Help).

The continuous ambiguity check algorithm SmartCheck increases the reliability, in the way the ambiguity is permanently and independently determined, approximately every ten seconds, and checked for consistency during the whole kinematic processing. In addition to that, the processing kernel also includes backwards processing, which ensures and unprecedented reliability of the results provided (Bilban, G., et al., December 2007).

Post-processing results are provided in XML/HTML reports with an extensive amount of information: point information, baseline information, antenna, initial coordinates, computed iono model, used observations and rejected observations, ambiguity statistics (the total number of ambiguities, the number of fixed ambiguities), cycle slips statistics and final coordinates.

4.4.3. RTKLIB

RTKLIB is an open source program for standard and precise positioning with GNSS. All current satellite systems are supported within the positioning algorithms. Data coming from these systems can be processed in various positioning modes for both real-time and post-processing: Single, DGPS/DGNSS, Kinematic, Static, Moving-Baseline, Fixed, PPP-Kinematic, PPP-Static, PPP-Fixed. For the current research only Static and Kinematic mode present interest.

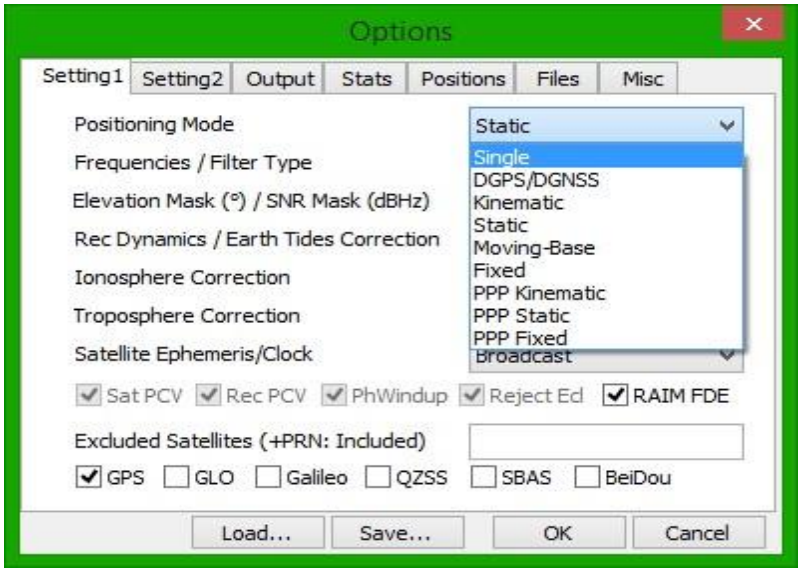

Fig. 4. 7: *Positioning Mode in RTKLIB.*

Regarding the algorithms for processing of GPS data, RTK employs extended Kalman filter to obtain the final solution in DGPS/DGNSS, Kinematic, Static and Moving-Baseline. From obvious reasons phase observations model, the single and double difference equations will not be repeated here. Suffice to say that Kalman filter and LAMBDA (Teunissen, 1993) – Least-Squares AMBiguity Decorrelation Adjustment strategy for ambiguity resolution are the

differences with Bernese GPS software (next Bernese update will contain also LAMBDA strategy but at the moment of writing this thesis the option was not available). The same principles are implemented in goGPS as well and because of this reason they will be presented in next section.

4.4.4. goGPS

goGPS is a software package published for the first time in August 2009 and designed to improve the positioning accuracy of low-cost (single-frequency) GPS devices by RTK technique and with the aid of a DTM. Currently it requires raw data (observations) at 1 Hz in input (http://www.gogps-project.org/about/).

goGPS development started in 2007 at the Geomatics Laboratory of Politecnico di Milano, Como campus (Italy), under the supervision of Dr. Mirko Reguzzoni, as a Master thesis project (Dominioni, Teruzzi). It was then continued during two other Master theses (Colla; Palmulli, Tettamanti) and one Ph.D. thesis (Realini).

As already noted Bernese GPS software is the most sophisticated one and a special attention had to be given. On the other hand, in goGPS and RTKLIB algorithms based on Kalman filtering and LAMBDA (Teunissen, 1993) strategy are implemented. In the next lines, these two subjects are presented more completely.

- **LAMBDA method**

The main features are: sequential conditional least squares estimation and decorrelation of the ambiguities.

The implementation of integer least-squares estimation is a search in the hyper-ellipsoid defined by the variance-covariance matrix of the ambiguities. In the search, the integer vector nearest to the float solution has to be found. Note however, that nearest must be measured in the metric of the variance covariance matrix of the float ambiguities, in order to take into account their correlation and precision (Teunissen, 1993).

With GNSS, the ambiguity search ellipsoid is extremely elongated; the search is very time consuming. By a multi-channel re-parameterization of the ambiguities, the outstretched ellipsoid is transformed to an almost spheroid. The number of candidates is preserved, but they can be found much more efficiently. Decorrelating the ambiguities has the following effect on the search ellipsoid: the number of candidates is preserved but a much more efficient search

takes place. Once the integer candidate closest to the float solution is found, a back-transformation can be carried out to obtain the integer solution.

LAMBDA was first implemented in Fortran-77, which is Version 1.0 of LAMBDA software. The current version 3.0 (Matlab implementation) can be downloaded at http://saegnss2.curtin.edu.au/~gnssweb/index.php?request=getlambda .

- **Kalman Filter**

This filter is an algorithm used to optimally predict (i.e. infers parameters of interests from indirect, inaccurate and uncertain observations) trajectory of a moving body, updating the estimate at the previous epoch by using the new observations as they arrive (it is a recursive estimator) and the dynamics of the system.

The optimality of the filter is deduced from the minimisation of the mean square error of the estimated parameters if all noise is Gaussian. Moreover, if this hypothesis does not hold, given only the mean and the standard deviation of the noise, the Kalman filter is the best linear estimator.

Some of the reasons that make Kalman filter very popular in practice are:

- good results due to optimality and structure,
- convenient form for real time processing.

The dynamic model, a discrete one, has the following shape:

$$\begin{cases} X_{t+1} = T_{t+1} * X_t + \varepsilon_{t+1} \\ X_0 = \bar{X}_0 + \varepsilon_0 \end{cases} \quad 4.40$$

where X_{t+1} is the state of the system at epoch $t+1$, T_{t+1} is the transition matrix, ε is the model error and X_0 is the initial state. X_{t+1} is a vector and in our case is formed by X, Y, Z and ambiguities N.

The model error ε can be stochastically described as:

$$\begin{cases} E\{\varepsilon_t \varepsilon_t^t = \delta_{tt'} * C_t^\varepsilon \\ E\{\varepsilon_t\} = 0 \end{cases} \quad 4.41$$

where C_t^ε is the covariance matrix of the model error.

The observation equations can be modelled as:

$$Y_t = H_t * X_t + \nu_t \quad 4.42$$

where Y_t is the observation, H_t is the design matrix and ν_t is the measurement noise.

Stochastic description of the measurement noise ν can be described as:

$$\begin{cases} E\{v_t v_t^t\} = \delta_{tt'} * C_t^v \\ E\{v_t\} = 0 \end{cases} \quad 4.43$$

where C_t^v is the covariance matrix of the observation noise and

A first remark has to be made: the observation process is not related to the evolution of the system; therefore, the two error types can be considered independent, i.e. $E\{\varepsilon_t v_t^t\} = 0$

At time t+1 there is another information available: the estimation of the system state at the previous time t:

$$X_{t|t} = X_t + e_t \quad 4.44$$

where the term on the left side is the estimate of the state at time t, using the information up to time t and e_t is the estimation error.

Stochastic description of the estimation error:

$$\begin{cases} E\{e_t e_t^t\} = C_{tt}^e \\ E\{e_t\} = 0 \end{cases} \quad 4.45$$

Moreover, both the model error ε_{t+1} and the observation noise ν_{t+1} are stochastically independent from the estimation error e_t at previous time t.

$$\begin{cases} E\{e_t v_t^t\} = 0 \\ E\{e_t \varepsilon_t^t\} = 0 \end{cases} \quad 4.46$$

The problem to solve, after some simplifications, can be written as:

$$\begin{cases} X_{t+1} = T_{t+1} * X_{t|t} + \xi_{t+1} \\ Y_{t+1} = H_{t+1} * X_{t+1} + \nu_{t+1} \end{cases} \quad 4.47$$

The term $T_{t+1} * X_{t|t}$ estimates the state at time t+1 using information up to time t. The estimation error, using the same reasoning, is:

$$\xi_{t+1} = X_{t+1} - X_{t+1|t} \quad 4.48$$

$$\begin{cases} E\{\xi_{t+1}\xi_{t+1}^t\} = C_{t+1}^{\xi} + T_{t+1} * C_t^e * T_{t+1}^t = K_{t+1} \\ E\{\xi_{t+1}\} = 0 \end{cases} \quad 4.49$$

Once the estimated states obtained update, the float carrier-phase ambiguities can be resolved into integer values in order to improve accuracy and convergence time. At first, the estimated states and the covariance matrix are transformed to DD forms to eliminate receiver initial phase terms and to obtain the float solution for N. Furthermore, the most appropriate integer vector

N for the integer ambiguities is obtained by solving and integer least square problem written as:

$$N^{est} = argmin((N - N^{real})' Q_N^{-1} (N - N^{real})) \quad 4.50$$

where

N^{est}: is the integer value for the ambiguity resolution,

Q_N: is the covariance matrix.

To solve this least square problem, LAMBDA (Teunissen, 1993) search strategy are employed. Based on this a combination of linear transformation to shrink the integer vector search space is offered. The search is validated by a ratio-test: the ratio factor R, defined as the ration of the weighted sum of the squared residuals by the second best solution N^2 to one by the best N^{est}, is used to check the reliability of the solution. In the next step, the fixed solution of the rover antenna position and velocity is obtained.

To sum up, the carrier phase measurement is a highly precise measure of the pseudorange between satellite and receiver, the generation of useable carrier phase measurements in a receiver requires a phase locked loop, ant the receiver designer must take care to ensure that 1) the integer ambiguity term is constant, and 2) the initial phase is chose so as to ensure a common phase bias in all tracking channels (Cillian O'Driscoll, July/August 2010).

Given that the position of the reference station is accurately known, the deviation of the measured position to the actual position and more importantly the corrections to the measured pseudoranges to each of the individual satellites can be calculated. These corrections can thereby be used for the correction of the measured positions of other GNSS user receivers. Usually, the accuracy of DGPS are influenced by the length of the baseline and the observation session. Table 4.1 highlights this dependency and it can be easily noticed the improvement in the accuracy with the increase of observation time and decrease of baseline length.

Baseline/ Time	**1 km**	**10 km**	**50 km**	**1000 km**
Kinematic	2.5 cm	4.0 cm	-	-
10 minutes	1.5 cm	2.5 cm	5 cm	-
1 hour	1.0 cm	1.5 cm	2 cm	-
24 hours	0.3 cm	0.5 cm	< 1 cm	1.5 cm
1 week	0.1 cm	0.1 cm	0.3 cm	< 1 cm

Table 4. 1: *Typical final accuracies in baseline estimates.*

Chapter 5. Research Approach

To assess the feasibility of low-cost GPS receivers for monitoring applications, the achievable accuracy and limitations of the GPS need to be identified. This study extensively investigates the performance of the low-cost single-frequency GPS for two experiments under perfect static assumption and for one experiment characterized by induced displacements after a fix time interval.

Static GPS survey procedures allow various systematic errors to be resolved when high-accuracy positioning is required. The field procedure of relative static survey is performed by placing a receiver on a known point and placing the second receiver on the unknown point, and collecting simultaneously data from at least four satellites (Magged, K.M.A., 2014).

Two static tests, one in Milano and one in Como, were carried out to assess the variation in the static measurements over time and the possibility of using the DGPS concept with low-cost single-frequency for applications with cm level accuracy. Additionally, these tests provide information about site specific limitations like multipath errors.

The chapter will start with a brief description of the instrumentation set-up used during the experiments, especially for tests in Como. In the next section, tracking configuration, data acquisition and its storing are disclosed. The final part of the chapter gives a detailed explanation of all the tests performed and analysed during the present research.

5.1. Experiment set – up

The field experiments were conducted in several locations in Como and Milano, inside Politecnico di Milano**.** In total, three experiments were performed: two under static conditions (one held in Milano in 2014 and a second one in Como, in 2015) and one described by controlled displacement of 5 mm for each 3 hours (in Como). In the following pages a very detailed description of this trials is provided.

5.1.1. Instrumentation

The main instrumentation employed in the experiments includes:

- 2 u-blox modules of different generation (LEA-4T for Milano Prova and NEO-7P for Como tests) and their default antennas,

- 2 geodetic Leica receivers (see Chapter 3),
- 2 geodetic antennas (Leica AT504 choke-ring antenna and Leica AX1202GG),
- a Leica tripod for centring and levelling u-blox antenna,
- a PC with u-center software,
- an external power supply,
- two internal plug-in batteries,
- an USB cable,
- a special electrical cabinet to keep safe the whole instrumentation.

In this section, only the set – up of the instrumentation used for the experiments performed in Como is going to be described thoroughly since the logistic set-up in Milano was not the work of the author but somebody else's. However, regarding the instrumentation used in Milano, it can be mention that in this case a much older u-blox, namely LEA-4T was placed at one of the end points of the estimated baseline. At the other end, a Topcon geodetic receiver took the role as a permanent station.

The u-blox receiver was placed in a protective impermeable plastic box and connected to a PC via a 30 m long USB cable to ensure power supply and communication; its antenna was fixed and centred with a tripod on the roof top (upper left corner of the image). A geodetic receiver, Leica GR10, from now on known as Como Test was already installed and permanently acquiring raw data at the moment of the test and is located in the Geoinformatic laboratory, in Valleggio building, Politecnico di Milano and its antenna on the roof of the same building. However, it was decided to install a second geodetic receiver in proximity to check if u-blox NEO-7P experiences the same multipath effect, atmospheric delays and loss of visibility to satellites as does the geodetic receiver.

The choice for this second site is a Leica GRX1200 GNSS unit (see Chapter 3). Power supply is ensured by an external source and 2 fully charged internal plug-in batteries, as back-up for the unfortunate events of power supply shortage (bottom right corner). This point, called Como Geodetic, was established on the roof of the same building from via Castelnuovo, at a very small distance from u-blox site, called Como u-blox. Thus, a very short baseline, approximately 3 m was established having as end points the Como Geodetic and u-blox NEO-7P.

At a last step, the PC, which acts as the main power source and server for u-blox receiver, was placed and locked inside the rack to protect it against the elements and other unpleasant situations (see Figure 5.1).

From now on the sites will be named in the following way:

- Como Test, is the site where Leica GR10 was installed,
- Como Geodetic, is the site where Leica GRX1200 was installed (in the vicinity of u-blox site),
- Como u-blox, the site where u-blox NEO-7P is installed.

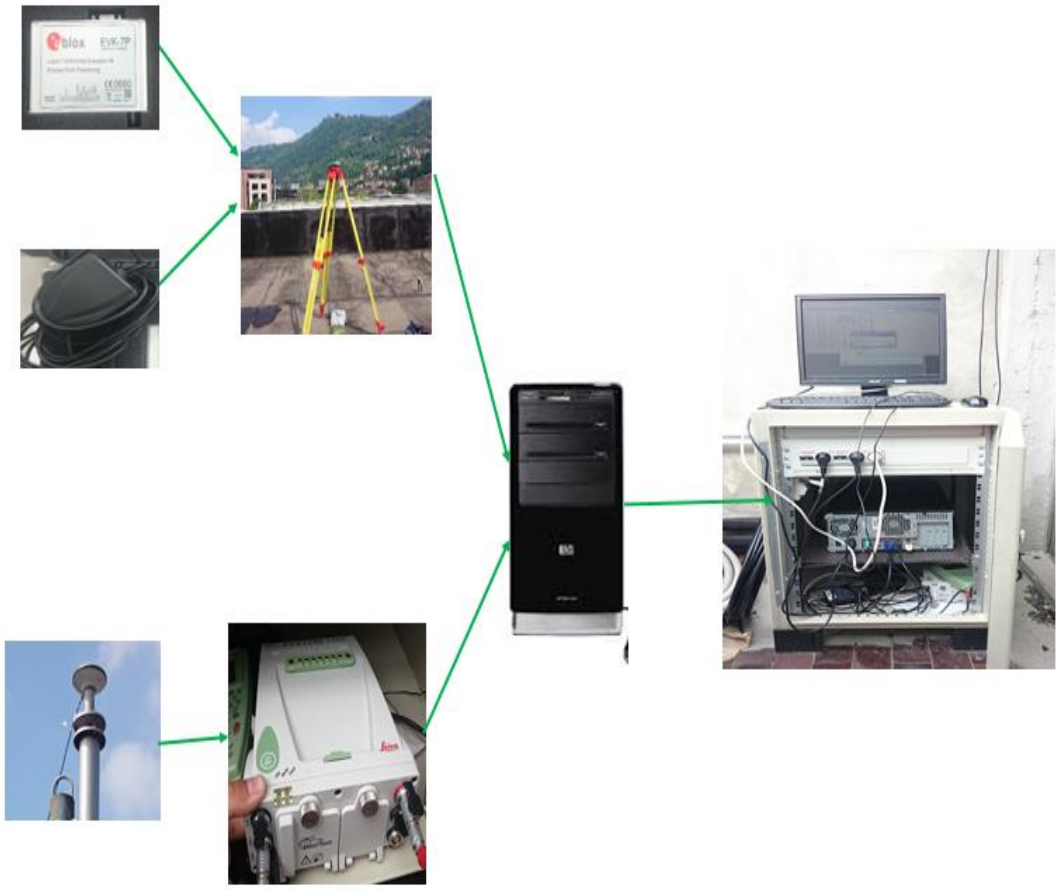

Fig. 5. 1*: Logical scheme of instrumentation set-up: the u-blox receiver and its antenna (upper left corner), Leica GRX1200 (bottom right corner), the PC server and the special cage that protects the server.*

The GNSS receivers are dual-frequency with the sampling rate of up to 10 Hz respectively 50 Hz. Both of them are capable of tracking in the same time more than one satellite constellations, provided an appropriate licence is installed.

Both receivers (see Figure 5.2) are capable of acting as reference stations: they can send corrections to users using the well-known standards RTCM and NMEA (for real time positioning) or their raw data can be used in post-processing for baselines estimation. For short baselines an accuracy of few millimetres can be obtained with these GNSS sensors (Leica GRX1200 and Leica GR10 Technical Data).

Fig. 5. 2: *Leica GRX1200 (left) and Leica GR10 (right) dual-frequencies GNSS receivers.*

For the experiments performed in Como Leica GR10 receiver, mounted on the roof of Valleggio building, was always used as reference station for both tests carried out in Como. On the contrary, Leica GRX1200 was used both as rover and as permanent station during the experimental studies.

About antenna option, a choke-ring antenna and a geodetic antenna were used to reduce multipath error, which is one of the main error sources for the GNSS stations. More specifically, an AT504 choke-ring antenna was used on the permanent reference station, from now on known as Como Test (together with Leica GR10 receiver) and the AX1202GG was used for Como Geodetic station.

Therefore, 3 GNSS sensors were available for the tests in Como. They simulate a local geodetic network formed by 3 sites: ComoTest, Como Geodetic and Como u-blox UBX, which serves for testing the reliability of u-blox in monitoring applications.

5.1.2. Data acquisition

As already reported in the introduction of this chapter two type of acquisition were performed: static and dynamic (constant displacements after regular time intervals). Both experiments are used to estimate accuracies provided by different GPS units by recording data over an extended period of time.

The geodetic receivers are placed on stable pillars on the roof of two different buildings during all the experiments. Regarding u-blox, its antenna was fixed, centred and levelled with the help of a tripod on the roof of Castelnuovo building (see Figure 5.3).

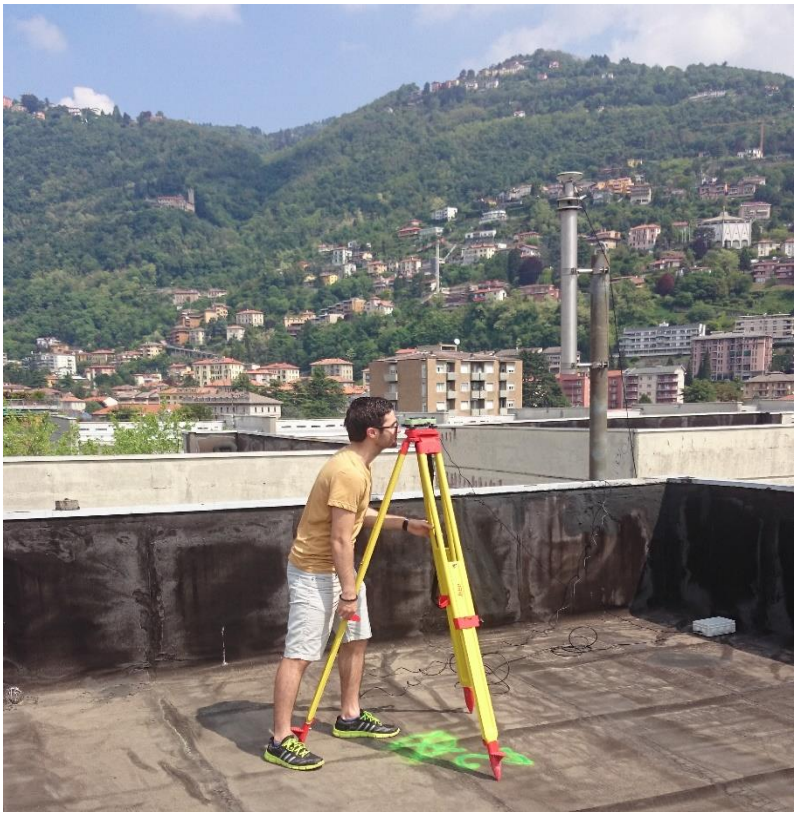

Fig. 5. 3: *Centring and levelling procedure.*

For the tests performed on the roof the stations location have been carefully selected to ensure open sky and no sources of multipath. Even though there were several small steel structures, the roof provided a quite open field environment, free from other buildings that may obstruct the view of low elevation satellites. However, low elevation satellites may be blocked by the mountains surrounding Como but this issue will be investigated in more detail with Leica Spider QC software and presented in the next chapter.

After solving also the problem related to site location, the tracking configuration for each receiver had to be decided. Parameters like mask elevation, SNR masks, enabling of augmentation systems or not and antenna height must be defined. These will be listed in the experiments description in the next section of this chapter.

Next step is to decide data handling, this is the most important part of the preliminary phase of the research. Each logging session acquired by Como Test is pushed on an FTP server and consists in compressed or uncompressed RINEX files, both observations and navigation, available to users as soon as they were created. The other geodetic receiver is storing data in Leica proprietary format on its memory card, with size of 1GB, and can be converted to RINEX with Leica Geo Office only at the end of the surveying campaign.

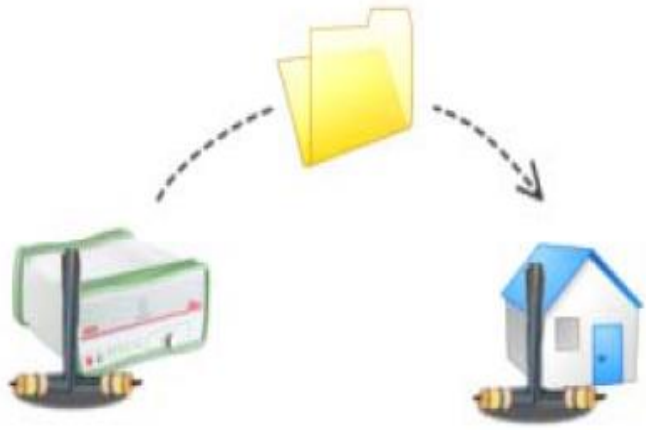

Fig. 5. 4: *FTP protocol components: data source (GR10), data packets and data server (courtesy Leica Geosystems).*

Figure 5.5 presents the connection scheme for power supply and data storing used in the case of u-blox unit. The low-cost platform is connected to a PC via a standard USB 2.0 cable which ensures the power supply and allows users to access the sensor and configure it. Once the connection is functional with the help of u-center software the desired settings can be imposed, together with the output messages required based on the purpose of the survey (real-time positions or raw data stored in a file). For reaching the objectives of the thesis, the author is interested only in the raw data and not the real-time positions. EVK-7 evaluation kits include a GPS / GLONASS antenna with a 3.0 m cable that sends the raw data to the receiver. From here, the GPS data, in u-blox .ubx binary format, are recorded in a file by u-center software and stored on a PC. As in the case of Como Rover, these data has to be transformed to RINEX before going into the processing stage.

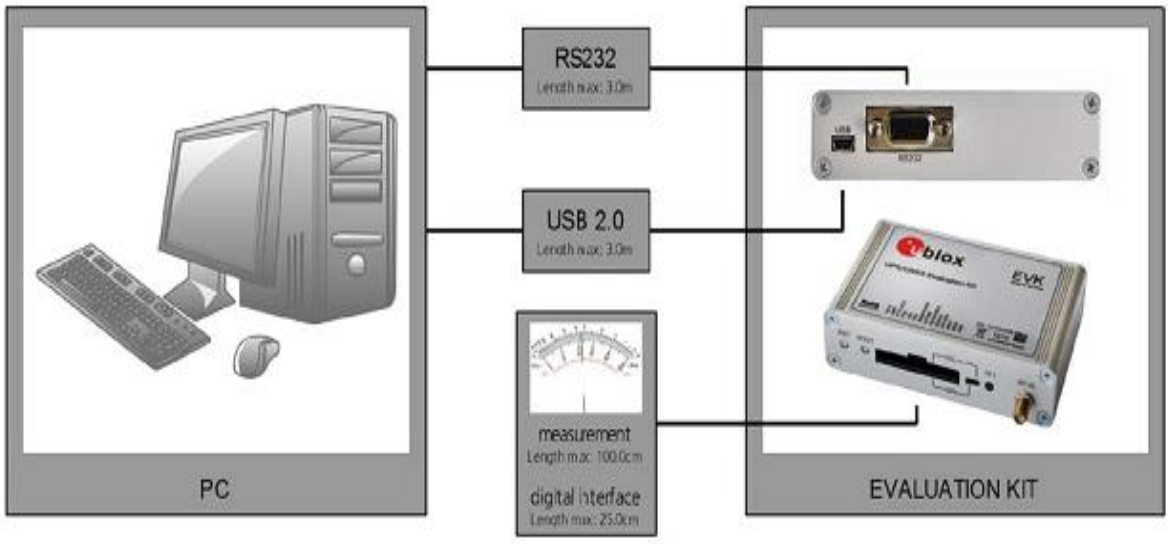

Fig. 5. 5: *u-blox set-up.*

Experiment 1: Milano Prova

First, the test carried out in Milano, from now on referred to as Milano Prova, took place in 2014, between GPS day 073 and 079 on the roof of Department of Architecture building (Politecnico di Milano), in via Edoardo Bonardi, 9.

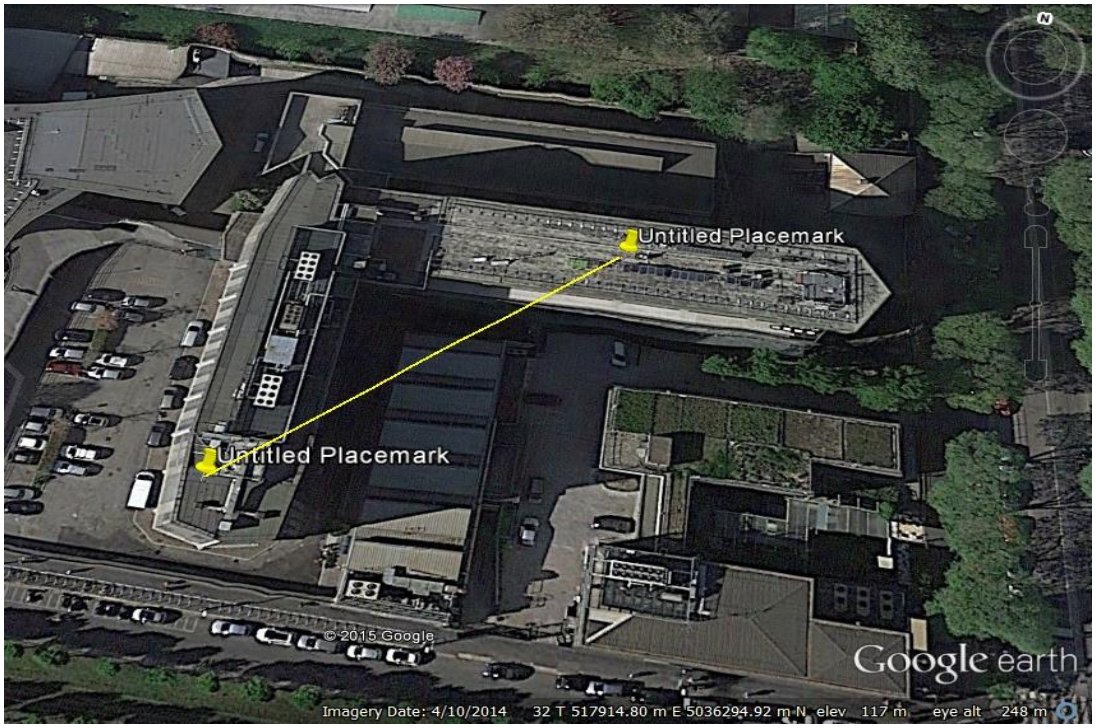

Fig. 5. 6: *Estimated baseline (in yellow).*

A short baseline, approximately 63 m in length, formed by Milano Permanent Station and u-blox LEA-4T was surveyed for one week, from March 14 – 20, 2014 with the following observational operating parameters:

- static mode,
- only GPS satellites,
- elevation mask 10^0,
- no SNR mask
- sampling rate of 1 Hz (1 observation for each second).

The 3-D coordinates of the Milano Permanent Station are listed in Table 5. 1 as they appear in the header of the RINEX files.

X [m]	Y [m]	Z [m]
4421892.5980	718469.9400	4525016.3566

Table 5. 1: *Reference coordinates in ITRF2008-WGS84 for Milano PS.*

At the end, the raw output of the observation campaign was downloaded and transformed to RINEX format using RTKLIB FOSS software. The processing of the RINEX files was conducted by the author with the help of three software (see Chapter 6).

As it can be seen in Figure 5.6 the location of the end points of the baselines are in suitable places as they are on the most dominant building, free of obstructions at 10º angle view above the horizon and at least 4 satellites were tracked continuously. The selected observation points are in open sky to decrease the errors due to multipath though some errors were still present, especially in the case of the u-blox antenna which has a lower protection against multipath.

Experiment 2: Castelnuovo Test

This second test, performed in Como, comprises one week of measurements, between May 8 and 15, 2015 (GPS Day 128 and 135) and was planned to assess the accuracy of the u-blox NEO-7P for displacements monitoring.

In this case, all 3 available receivers were used simultaneously. On u-blox side the following tracking configuration was adopted:

- static mode,
- GPS satellites and available EGNOS,
- elevation mask 0^0,
- no SNR mask,
- sampling rate of 1 Hz.

The geodetic receivers follow the same plan but with a slightly different tracking configuration, namely all available signals and satellite constellations were enabled. However, in the processing part only L1 code and phase GPS data will be used in order to obtain a more realistic comparison with u-blox, which is a single – frequency receiver.

This last arrangement, with a geodetic unit in the vicinity was adopted for having a reference in the preliminary evaluation of the low-cost platform. In other words, a very small baseline composed by a geodetic and a low-cost sensor makes sense when one wants to compare the performance of this two different type of units. By performance comparison the author meant to confront the number of observations on L1 carrier (with and without a mask), cycle slips, SNR and multipath recorded by the u-blox NEO-7P with those registered by Leica GRX1200.

The aim is to get a first idea of how much better is a geodetic receiver with respect to a mass market one when both are used in the same filed condition. The findings of this investigation are presented in detail in Chapter 6 under the pre-processing part.

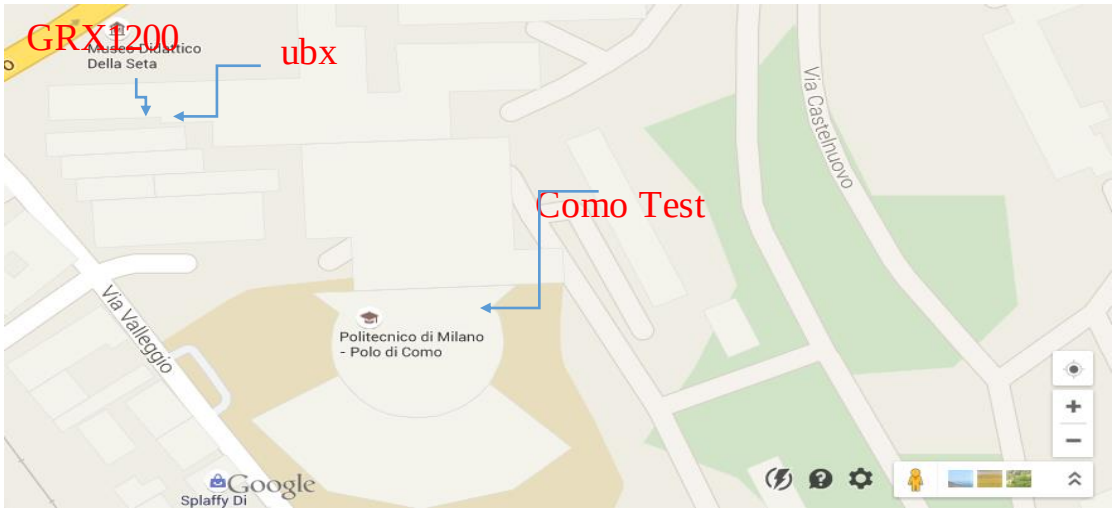

Fig. 5. 7: *Location of the testing site.*

The configuration deployed for this first Como experiment can be seen as a very small geodetic network where two receivers of different category (and accuracy) were placed in the monitored area (roof of Castelnuovo building) and a permanent station outside the monitored area of about 100 m (Valleggio building), on a stable pillar with location known at 1 mm level. In total, there are 3 baselines to be processed in the following sequence: with respect to Como Test, Como Geodetic and Como u-blox will be estimated first; after this, the position of Como Geodetic can be fixed and assumed as known with millimetre level accuracy. Therefore, Como u-blox can be now estimated with respect to this new site reference site, Como Geodetic. At the end, for u-blox position two sets of coordinates for each session will be available for interpretation. More about this in Chapter 6.

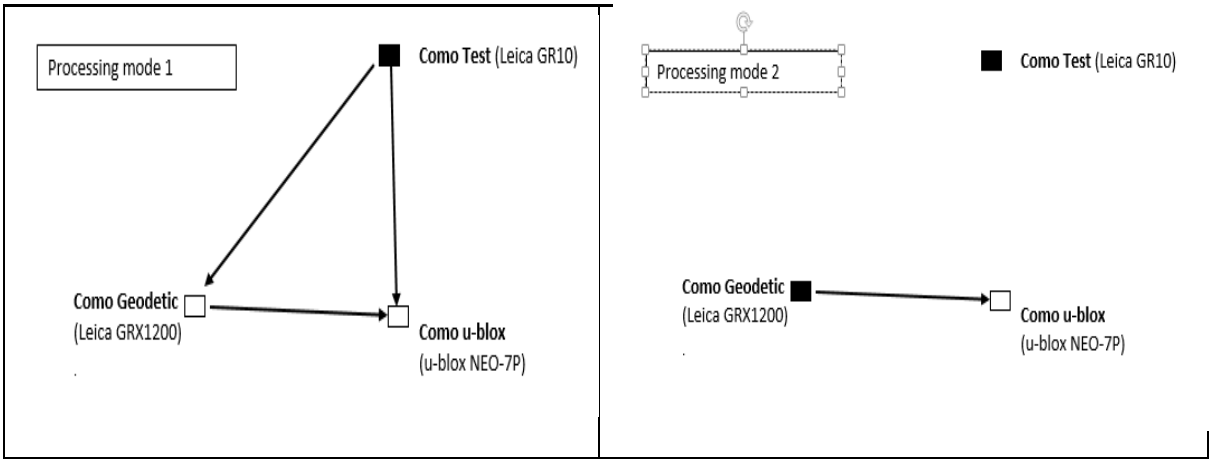

Fig. 5. 8: *Baselines to be estimated: ComoTest-GRX1200 and Como Test-ubx (left) and GRX1200-ubx (right).*

The 3-D coordinates of the Permanent Station (PS) are well known and there was no need to estimate them. In Table 5.2 are listed the coordinates of Como PS:

X [m]	Y [m]	Z [m]	E [m]	N [m]	h [m]
4398303.9154	704155.7363	4550156.9034	507436.777	5072073.8715	292.9078

Table 5. 2: *ITRF2008-WGS84 and UTM32N Como PS coordinates.*

Figure 5.8 illustrates better ideas presented above. Processing Mode 1 means to estimate the position of u-blox and GRX1200 with respect to Como Test and Processing Mode 2 supposes to estimate the position of u-blox with respect to GRX1200, which will be fixed by now. Thus, the second set of coordinates for the u-blox site is earned.

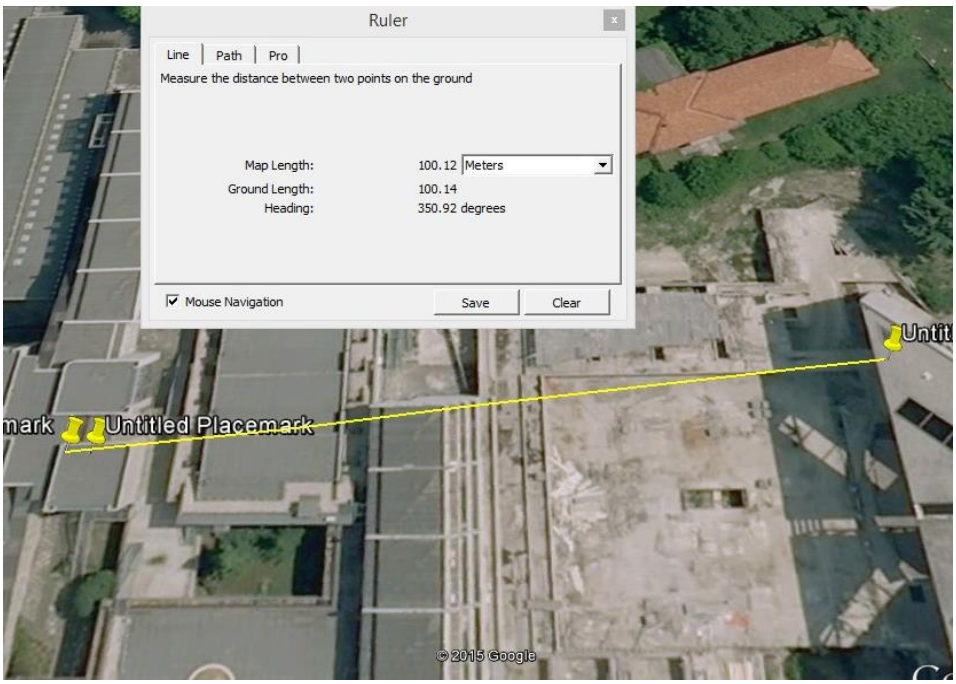

Fig. 5. 9: *Baseline Como Test – Como Geodetic (detail).*

Experiment 3: SIMU-SLIDE

The author completed one experiment to assess the precision and the accuracy of low-cost GPS for monitoring the dynamic displacement of structures and landslides. In this case, with an accuracy of 5 mm.

The assumption the author starts from is that in a local area there are few sites a priori known to be stable (known coordinates and not affected by displacements) and a site that suffers induced known displacements (the low-cost sensor location). If the sensitivity of the u-blox

EVK 7P is not sufficient to detect the displacements under the hypothesis just mentioned, the system will fail when the magnitude of the induced movements are not known a priori.

The actual capability of low-cost GPS sensors to detect local displacements has to be assessed. It seems reasonable to see the difference between the detected and the true deformations caused by local phenomena. To this aim, an experiment was planned and carried out on the roof of Castelnuovo building (Politecnico di Milano, Como Campus), in via Castelnuovo, 7, in the same location where Experiment 2: Castelnuovo Test took place. This last work, from now on referred to as SIMU-SLIDE project, started on GPS day 152 (1st of June, 2015) with two days of static acquisition to compute the reference start position of the antenna. Starting with GPS day 154 (3rd of June, 2015) antenna was shifted horizontally 5 mm for each session (for each of the day 3 sessions were planned, therefore a movement of 1.5 cm). The induced drifts continued till GPS day 162 (11th of June, 2015) with a break on GPS days 157 and 158. Before concluding the work, two more days of static acquisition were planned for computing the reference end position. The following tracking configuration:

- static mode,
- GPS satellites and available EGNOS,
- elevation mask 0^0,
- no SNR mask,
- sampling rate of 1 Hz.

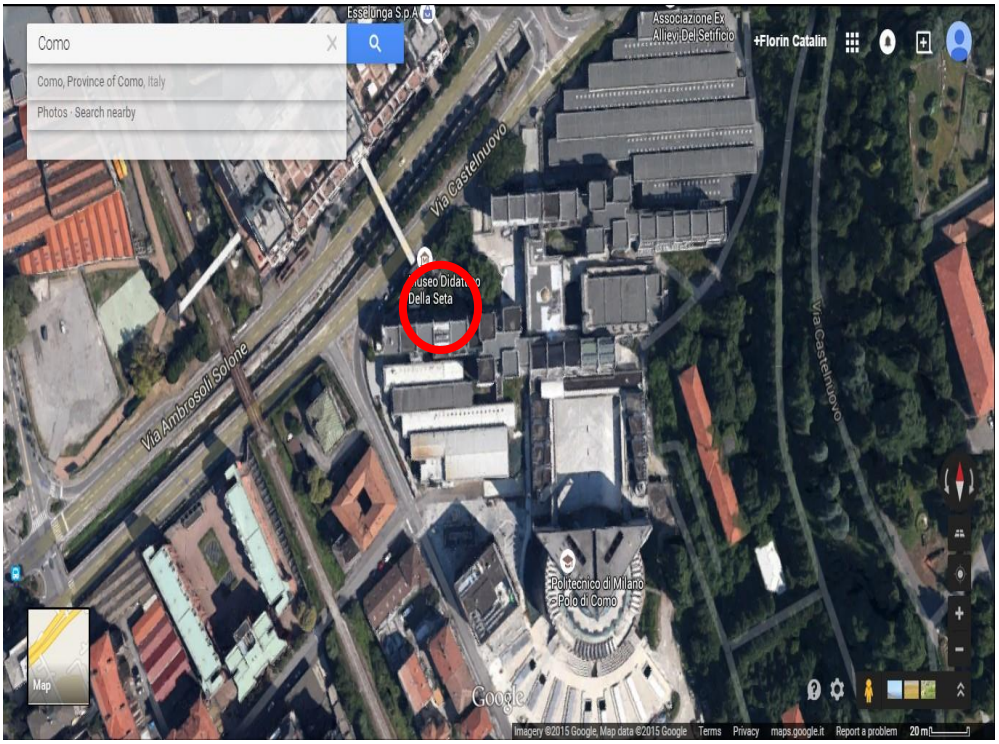

Fig. 5. 10: *Testing site (red circle).*

Here, three sites occupied by three receivers, two of which are geodetic, form a local network – same frame as in Experiment 2 (see Figure 5.12). The local network comprises the following observing sites: Como Test, Como Geodetic and Como u-blox.

In Table 5.3 are the coordinates of Como Test and Como Geodetic as they appear in the header of the RINEX files.

X [m]	Y [m]	Z [m]
4398303.9154	704155.7363	4550156.9034
4398269.5162	704071.9437	4550193.1069

Table 5. 3: *ITRF2008-WGS84 coordinates Como Test and Como Geodetic.*

The baselines of the network range between 5 and 100 m (see Table 5.1); two geodetic receivers, Leica GRX1200 and Leica GR10, and a low-cost sensor, u-blox EVK 7P were used in the experiment. u – blox site has been chosen in order to assure that the direction of the imposed displacements (5 mm for each session) in horizontal plan is along the baseline Como Test – Como u-blox and almost perpendicular to the baseline Como Geodetic – Como u-blox. However the orientation of the sliding device is not perfectly perpendicular on the above mentioned baseline: there is a bias of approximately 4 degrees– see Table 5.4 column 3, rows 1 and 2. Because of this, corrections are needed – see Chapter 6 for details.

Baseline	**Approximate Length [m]**	**Orientation**
u-blox – Como Test	97.1348	34.023615
u-blox – Como Geodetic	5.8402	137.795998
Como Test – Como Geodetic	97. 5027	-

Table 5. 4: *Baseline lengths.*

The differences with respect to the first experiment executed on the roof of this building are:

- no more static assumption but simulation of controlled displacements. On a tripod, a scaled device consisting in a 30 cm metal rod was fixed. The gradation of the rod is from 0 to 10 cm with 5mm intervals. On this rod the u-blox antenna is fixed and moved horizontally in such way to have three static hourly session in each position. By position, here is meant to move the antenna by 5 mm, after every 3 hours (see Figure 5.11).

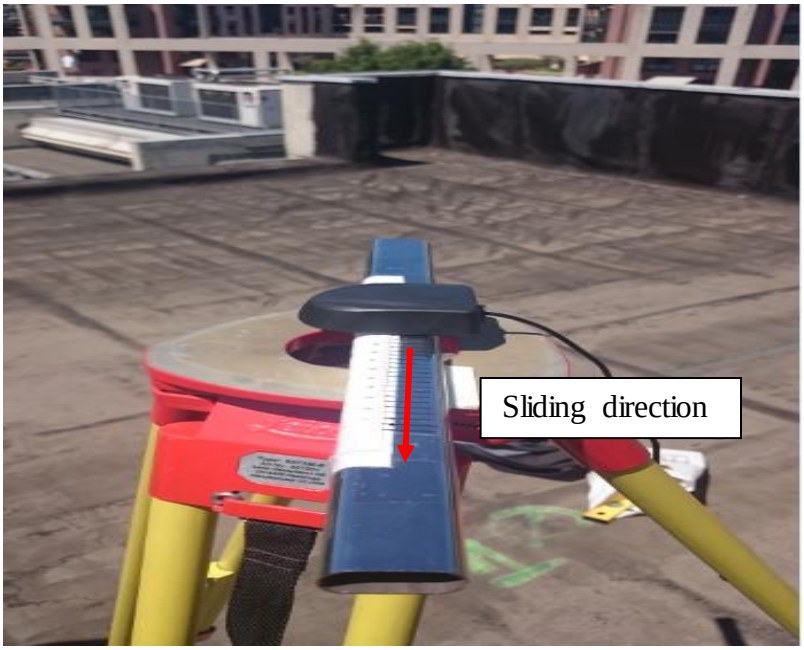

Fig. 5. 11: *Sliding device and direction of sliding (here, along the baseline Como Test - u-blox).*

- the almost right triangle having as end points the three receivers. The reason for doing this is to test two extreme situations: sliding the antenna along the baseline Como Test – Como u-blox (optimal condition) and in the same time sliding horizontally the antenna perpendicular to the baseline Como Geodetic – Como u-blox (worst situation).

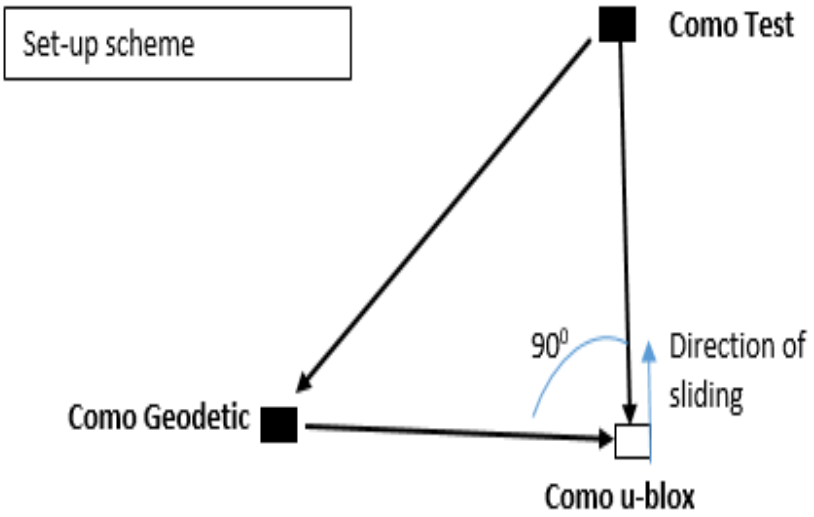

Fig. 5. 12: *Set-up scheme.*

The 5 mm sliding of the antenna is at least one order of magnitude better than the displacements one should expect in applications like landslides monitoring. Starting from the hypothesis that only the site SIMU-SLIDE suffers displacements with respect to the other sites of the network, the length of the baseline Como Test – Como u-blox should change as it is noted in Table 5.5.

Session	Known Displacement [mm]
0	0
1	5
2	10
3	15
4	20
5	25
6	30
7	35
8	40
9	45
10	50
11	55
12	60
13	65
14	70
15	75
16	80
17	85
18	90
19	95
20	100

Table 5. 5: *SIMU – SLIDE induced displacements.*

It must be mentioned that in the above table by session is meant a 3 hours observation window. In other words, the campaign was organized into 20 observing session of 3 hours each. Unfortunately during the experiment some instrumental problems happened and the test was stopped after 12 sessions. In the near future the author is planning to repeat this experiment with 20 sessions and using a better sliding device.

In the processing part this will be explained better, now it is suffice to say that each session gives a set of 3-D coordinates for every hour. Thus, at the end of the post – processing phase of raw data of each session the user will have 3 sets of 3 coordinates.

5.4. Software

Most commercial and scientific GPS evaluation software packages can deal with, besides proprietary formats, the receiver independent exchange format (RINEX) (Schwieger, V., 2009). As described in Chapter 2, the u-blox receiver records the code and phase data in a binary format: the ubx format. This has to be transformed into the RINEX format. For this task

the software RTK LIB may be used. It is available on the internet without the need of a license. For the follow-up processing of the code and phase data is realized by using a wide variety of software: commercial (Leica Geo Office, SpiderQC), academic (Bernese) and free and open source software (RTKLIB and goGPS).

RTKLIB and goGPS, have the possibility to convert ubx format to RINEX and performing double differencing on phase observations. The observation time, the reference station, coordinates, antenna types, elevation cut-off angles as well as excluded satellites may be entered interactively. As an additional tool, in Bernese and RTK LIB it is possible to divide a long observation period into multiple short observation windows and to automatically process the new generated files.

5.4.1. Bernese GNSS software

The Bernese GNSS software is a scientific, high-precision, multi-GNSS data processing software developed at the Astronomical Institute of the University of Bern (AIUB). It is used by Center for Orbit Determination in Europe (CODE) for its international (IGS) and European (EUREF/EPN) activities. This software is in a permanent process of development and improvement (http://www.bernese.unibe.ch/). The Bernese GPS software is a sophisticated tool meeting highest quality standards for geodetic and further applications using GNSS (Bernese GPS Software user manual, 2007).

5.4.2. Leica Geo Office features

LGO imports and combines data from all instruments (GNSS instruments, TPS instruments and levels) to produce the final results. Another advantage of LGO is the possibility to manage a project in an integrated way without the need to transfer data between the various modules.

Among the general components, Raw Data Import and ASCII Import & Export are of particular interest for the research. One can import raw data from GNSS receivers or import coordinate lists as user-defined ASCII files using the import wizard. The final results can be export as ASCII files.

For GNSS data processing, automatic or manual selection of baselines and definition of processing sequence is available: Single baseline or multi-baseline batch processing, wide range of processing parameters, cycle-slip fixing and outlier detection, option to process GPS L1 single frequency data or GPS dual frequency data and GLONASS data processing.

5.4.3. Leica Spider QC

Spider QC is a stand-alone software that can perform automatic quality checking and reporting of the logged RINEX data or derived data such as SINEX, IONEX and NMEA (http://www.leica-geosystems.com/en/Leica-SpiderQC_83496.htm).

This is a multi-purpose GNSS data analysis tool that can be used for:

- Site Assessment and Quality Control
- Network RTK Performance Monitoring
- Reference Station Integrity Monitoring
- RINEX data management (concatenation, decimation)

In this present thesis, Spider QC is used only for quality control of RINEX data of u-blox low-cost sensors. It is used to evaluate code and phase multipath, check for RF interference and signal attenuation, measure data quality and completeness and much more.

5.4.4. RTKLIB

RTKLIB is an open source program for standard and precise positioning with GNSS. All current satellite systems are supported within the positioning algorithms. Data coming from these systems can be processed in various positioning modes for both real-time and post-processing: Single, DGPS/DGNSS, Kinematic, Static, Moving-Baseline, Fixed, PPP-Kinematic, PPP-Static, PPP-Fixed.

5.4.5. goGPS

goGPS is a software package published for the first time in August 2009 and designed to improve the positioning accuracy of low-cost (single-frequency) GPS devices by RTK technique and with the aid of a DTM. Currently it requires raw data (observations) at 1 Hz in input (http://www.gogps-project.org/about/).

goGPS development started in 2007 at the Geomatics Laboratory of Politecnico di Milano, Como campus (Italy), under the supervision of Dr. Mirko Reguzzoni, as a Master thesis project (Dominioni, Teruzzi). It was then continued during two other Master theses (Colla; Palmulli, Tettamanti) and one Ph.D. thesis (Realini).

Chapter 6. Data Processing and Results Discussion

The chapter is subdivided into three sections, one for each experiment carried out. First, the results of Milano test will be presented, together with the pre-processing and processing phase. Next, the static test performed on the roof of Castelnuovo building (Como) will be discussed. And finally, the experiment simulating consecutive 5 mm displacements in one direction will be dealt with.

6.1. Milano Prova

First, the test carried out in Milano, took place in 2014, between GPS day 073 and 079 on the roof of Department of Architecture building (Politecnico di Milano). A short baseline, approximately 63 m in length, formed by a geodetic receiver and u-blox 4T was surveyed for one week, from March 14 – 20, 2014 with a sampling rate of 1 Hz (for more details see Chapter 5, Section 5.2.).

The flowchart in Figure 6.1 summarizes the overall procedure to identify the differences of each individual, hourly solution with respect to the reference position.

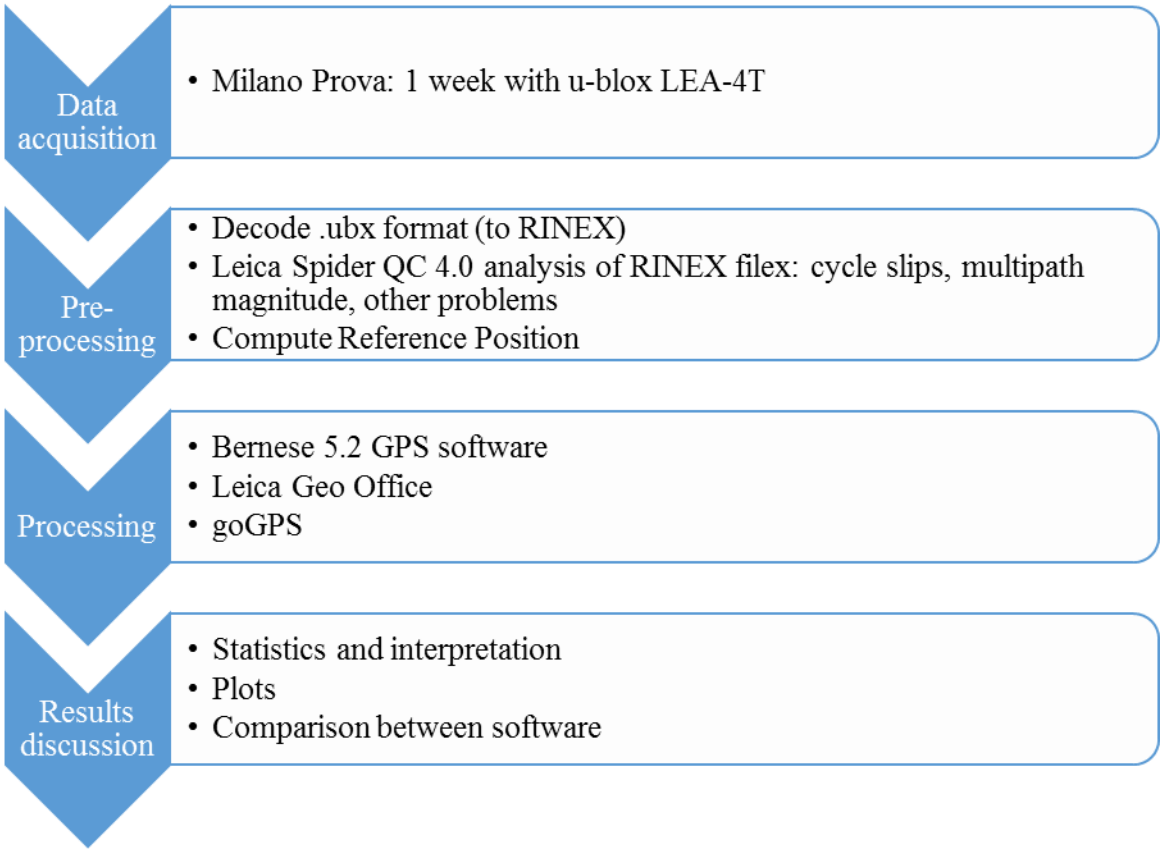

Fig. 6. 1: *Flowchart of the procedure adopted for Milano Prova.*

6.1.1. Pre-processing stage

The objective of this preliminary evaluation is to identify the problems occurred during the measurement campaigns and to understand how to remove or diminish their negative impact (for example, a satellite with a high number of cycle slips can be disabled in the processing phase and so on).

The whole dataset consisted in one week of data recorded with an elevation mask of 10^o at a sampling rate of 1 Hz, in u-blox .ubx binary format.

Once the acquisition was finished and data downloaded, first step was to convert to RINEX the on board logged u-blox message. To do this, several options are available but the author stopped at RTKLIB and goGPS (for cross checking of resulting files).

Once this stage was finished, with the help of Leica Spider QC software preliminary data evaluation could start. At the end of the quality check a report will be created summarizing the most important indicators for GPS data (see Appendix A for full size reports). In this step, the author was mostly interested in the following parameters:

- GPS Data completeness above 10^o (adopted cut off angle) and threshold of 95 %
- Number of complete GPS observations above 10^o, out of the maximum possible
- Epochs with Data
- Data gaps
- SNR values
- Multipath Analysis on L1 (threshold = 0.5 m)
- Cycle slips
- PDOP and GDOP

Data completeness: the percentage of complete observations to satellites above the elevation mask compared to a pre-defined limit. It can be computed in the following way:

$$Data_{completeness} = \frac{no.obs.(above\ 10^0) - no.obs.to\ unhealthy\ SV}{no.of\ possible\ obs.(above\ 10^0)} x\ 100\ \ [\%] \qquad 6.1$$

where the numerator of the ratio is the number of complete observations above a mask and the denominator of the ratio is the total number of theoretically possible observations to satellites above mask assuming no obstructions and perfect tracking; these values can be read from column 1 of Table 6.1.

Number of complete GPS observations: is the difference between the number of observations above a cut off angle and the number of observations to unhealthy space vehicles (SV); is the total number of observations to GPS satellites contained in the file and written here in column 1 of Table 6.1 (is the same with the numerator from equation 6.1).

Epochs with data: the number of epochs where all satellites above the mask were tracked and where all the required observation types were complete.

Data gaps: the total time of epochs missing from the file. The difference between the expected number of epochs (based on the session length, here 86 400 epochs for one day) and the number of epochs in the file:

$$Data_{gaps} = \frac{86\,400 - no.epochs\ in\ the\ file}{60} \quad [min] \qquad 6.2$$

SNR: Signal to Noise Ratio, is the average signal to noise ratio per satellite for L1 frequency, in dB.

Multipath: The average multipath estimates for each satellite and then averaged, in meters.

Cycle slips: The estimated number of cycle slips (for L1 frequency) on satellites above the elevation mask based on the cycle slip detection settings of the software.

PDOP and GDOP: The average Position Dilution of Precision and Geometric Dilution of Precision calculated from a single point position at each epoch.

GPS obs >10^0 (out of theoretic)	GPS Data Completeness	Cycle Slips	SNR [dB]	Data gaps [min]	Multipath [m]	PDOP	GDOP
702417/739687	95 %	1137	45.5	0	4.03	3.3	3.9
708324/747320	94.8 %	1869	45.3	0	4.10	3.3	3.9
708881/747570	94.8 %	2004	45.2	0	3.73	3	3.8
708646/744494	95.2 %	1968	45.5	0	4.15	3.3	3.9
708704/752889	94.1 %	2130	45.5	0	4.33	3.3	3.9
708844/747953	94.8 %	2086	45.4	0	3.97	3.3	3.9
708593/753260	94.1 %	1895	45.5	0	3.87	3.3	3.9

Table 6. 1: *Daily quality indicators for Milano Prova data.*

Table 6.2 contains the average statistics for the whole campaign giving a better idea of the setbacks and strong points of the data, which will be processed in the next step.

GPS obs $>10^0$ (out of theoretic)	GPS Data Completeness	Cycle Slips	SNR [dB]	Data gaps [min]	Multipath [m]	PDOP	GDOP
707773/747596	94.7 %	1870	45.5	0	3.95	3.3	3.9

***Table 6. 2**: Final Statistics for Milano Prova – 10^o cut-off.*

Looking at Table 6.1 is quite obvious that the main problems encountered by u-blox LEA-4T are multipath and cycle slips. The maximum value for multipath is 9.63 m (GPS Day 077, project day 5) and the minimum is 1.00 m (same day). These magnitudes are consistent throughout the whole week, no matter the time, satellite elevation and azimuth. One interpretation can be the u-blox receiver, being a high-sensitivity device recorded most of the secondary signals reflected by the near environment. Consequently, it can be assumed that in the vicinity of the site there are reflecting surfaces spread over all directions.

With reference to the number of cycle slips, they are well above the default threshold computed by Leica Spider QC for 24 hour files, almost double than this. A number of 2000 cycle slips for daily sessions is far from the expected values: however, most of the ambiguities induce by each cycle slip should be fixed if appropriate ambiguity resolution strategies are used.

On the bright side, the data completeness indicator for every single day was close to 95 %. The total number of observation to satellites above the elevation mask reached satisfying figures for a low-cost GPS sensor. Furthermore, the SNR values are comparable with those of geodetic receivers, with an average of 45 dB for the whole week. Finally, PDOP and GDOP values are optimal and nothing to be worried about.

The last step of pre-processing was to prepare the 3-D reference coordinates by post-processing the raw data in LGO. A solution was estimated for every day of the campaign, in total 7, and then averaged in a final set of 3-D coordinates (Table 6.3).

X [m]	Y [m]	Z [m]	E [m]	N [m]	h [m]
4421892.5980	718469.9400	4525016.3566	517880.331	5036253.7534	193.3798

***Table 6. 3:** Reference coordinates in ITRF2008-WGS84 and UTM 32N.*

To summarize, up to this point RINEX files were created and checked for problems, statistics about quality indicators have been organized in tables and reference coordinates were computed.

6.1.2. Processing

The data were processed with different software, three to be more precise (Bernese GPS software, Leica Geo Office, goGPS), to investigate inter software biases. Here the daily RINEX files were decimated into hourly files and the 3-D coordinates of the rover were computed for each of these hourly sessions, in total 168 results have been obtained. Then, the time series of the apparent displacements relative to the reference value of each coordinate were computed.

The GPS processing technique for this research is relative static positioning. Relative positioning exploits data from two or more GPS receivers, simultaneously tracking the same satellites. The principle of this technique is based on determining the vector, called baseline, between the reference site and the rover. Static relative positioning by double differencing the carrier phase observations is the most frequently used as it can reach accuracies at sub-centimetre level, according to literature 0.3 – 1cm.

In present research only single-frequency data is available for processing, therefore a slightly decrease in accuracy is expected. Moreover, the notion of outlier must be defined. Generally, it is called outlier a data point that is distinctly separate from the rest of the data; usually statistic tests are performed to identify and confirm an outlier. For this thesis the author assumed by default a threshold of 5 cm for outlier elimination based on expected accuracy of low-cost GNSS sensors, on accuracy required by landslide monitoring and lack of antenna calibration procedure.

6.1.2.1. Bernese Processing and Results

The use of commercial software, which is provided by the equipment manufacturer for processing raw data, limits the ability to modify the processing parameters. Consequently, this limits the possibilities of using advanced error models and at the end, limits the ability to improve the accuracy of the final results. For advanced and precise data processing it is endorsed to use software which facilitates unending selection of the processing parameters and error models. Therefore, Bernese GPS Software ver. 5.2 was one of the software used.

As basic essentials, the precise IGS final satellites orbits and clocks, Earth orientation parameters as well as ephemeris, sub daily pole model – IERS2000 and nutation model – IAU200 were vital. However, in real landslide monitoring (real-time results) it is not possible to use precise products but in this case it was decided to relate on them to produce a set of reference results.

As clearly described in Chapter 4, Bernese GPS software will first perform a pre-processing part to scan data for possible problems and to convert it to Bernese format. The output of this step is used by the main estimation program (GPSEST).

Typically the normal way to process phase observations as double-differences is to perform the receiver clock synchronization (program CODSPP), form baselines from phase observation files (program SNGDIF) and clean the single – difference phase observation files (program MAUPRP).

For clock synchronization L1 frequency was used, Saastamoinen troposphere model and 10 degrees at minimum elevation. Single – frequency observations are usually used for processing the baselines not longer than 10 – 15 km, where the ionosphereic delays cancel out during differencing of the observations. For a low cost GNSS sensor this is the only option since these platforms are all single-frequency.

At a next instance, the baseline was processed with the following parameters:

- measurement type: phase,
- observing session length: 1 hour.

The actual processing routine is based on Least Squares Estimation. In the BSW 5.2 GPSEST program is responsible for processing the observations, setting up the observation equations and solves the normal equation. The calculations were executed using the following options:

- observables: L1 phase observations,
- differencing level: double,
- ambiguity resolution: SIGMA (see Chapter 4),
- troposphere: Dry Neill a priori model with estimation residual dry delay (90% of the total tropospheric delay is due to the dry component),
- elevation cut-off: 10 degrees.

Milano PS was fixed as control point and u-blox relative coordinates were estimated for each hourly sessions. In total, 168 results have been obtained.

5 blunders are present, probably caused by problems in solving of cycle slips: sessions 22, 24, 30, 40 and 142. By averaging the hourly solutions, except those affected by blunders, BSW 5.2 gives as final solution the exact reference coordinates. In Table 6.4 are presented the residuals of blundered solution and their influence on the 3-D position of the u-blox site.

Session	dE [cm]	dN [cm]	dh [cm]	dS [cm]
22	7.55	-1.08	-22.4	23.66
24	12.62	39.7	-15.43	44.42
30	1.68	1.98	-9.1	9.45
40	17.48	4.75	-5.9	19.06
142	-25.52	10.1	-15.57	31.5

Table 6. 4: *Outliers identified for Milano Prova – Bernese processing.*

163 hourly sessions out of 168 were not affected by outliers, in any of the 3 components (East, North and Height); in percentage this is 97 %. With few exceptions the horizontal displacements present a smaller variations around the mean than the vertical displacements. To compute these variations the following relation was adopted:

$$\overline{\delta r} = \bar{X}_i - \bar{X}_{Ref} \qquad 6.3$$

where

$\overline{\delta r}$: is the vector of the residuals

$\bar{X}_i$: 3-D position (E, N and h) for each session

$\bar{X}_{Ref}$: the reference 3-D position of u-blox antenna

Figure 6.2 reports the number of the initial ambiguities and the unfixed ambiguities for each session. It can be easily seen that the data experiences a daily periodicity. Figures 6.3 – 6.5 depicts the time series of the residuals observed for the clean sessions, separately for each of the 3-D coordinates. Float solutions are graphically compared with the fix ones. From doing so, it can be easily seen the impact of ambiguities on the final results.

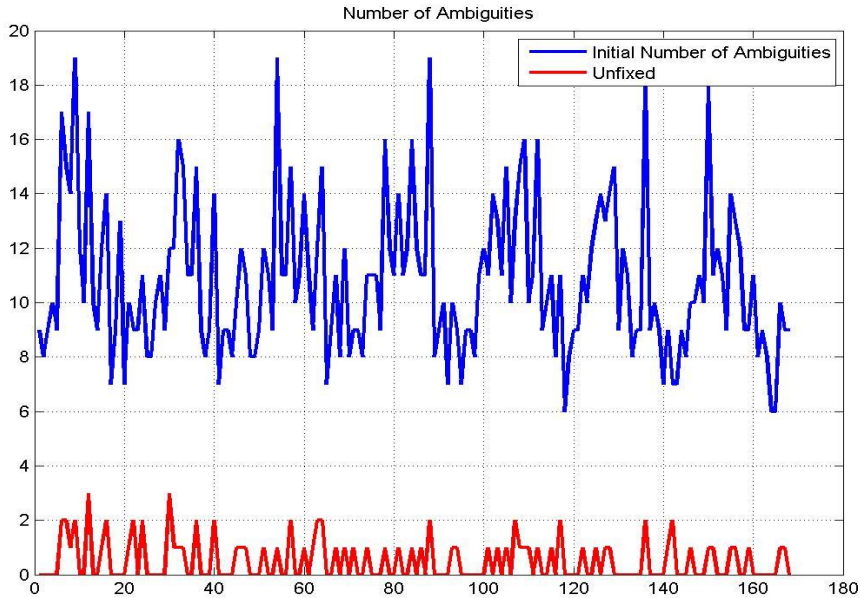

Fig. 6. 2*: Initial number of ambiguities – clean sessions (Float, in blue) and unfixed ambiguities (Fixed, in red).*

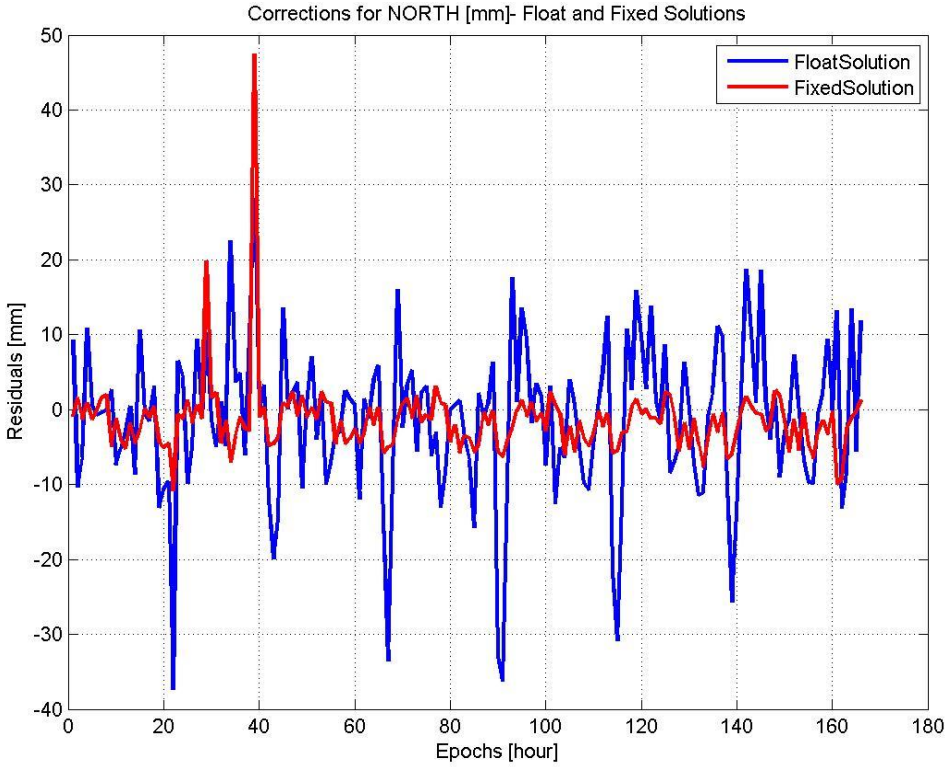

Fig. 6. 3: *Clean sessions - Time series of North residuals, static method, 1 hour sessions (Float solution, in blue and Fixed solution, in red).*

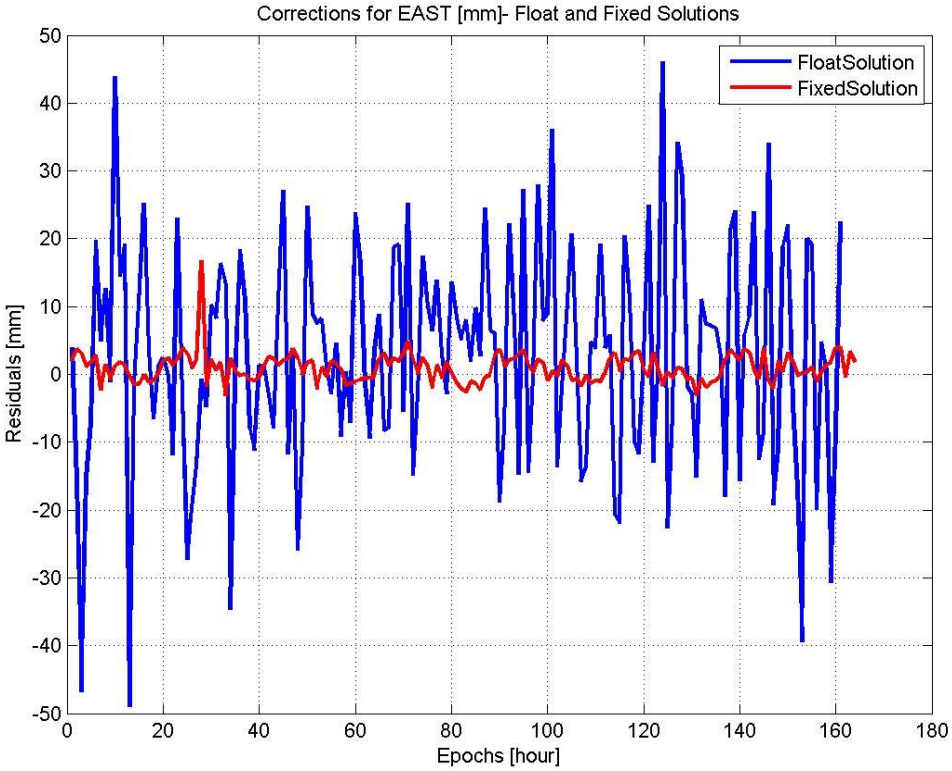

Fig. 6. 4: *Clean sessions - Time series of East residuals, static method, 1 hour sessions (Float solution, in blue and Fixed solution, in red).*

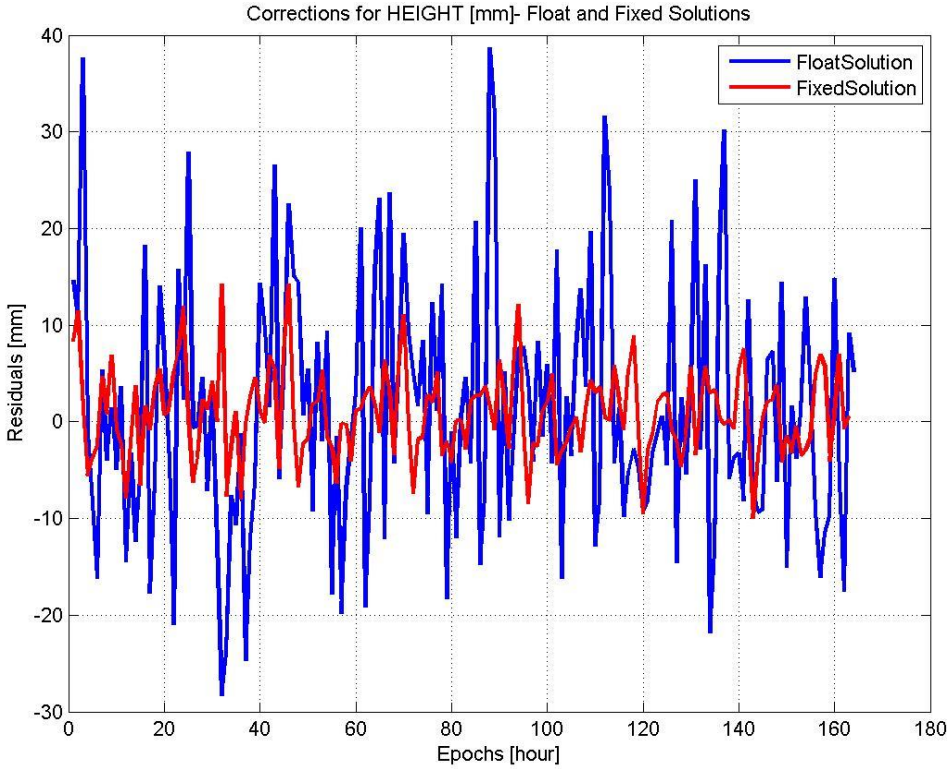

Fig. 6. 5: *Clean sessions - Time series of height residuals, static method, 1 hour sessions (Float solution, in blue and Fixed solution, in red).*

After ambiguity fixing step, the residuals shrunk from cm level to mm level in good sessions (see Figures 6.3 – 6.5, blue – float solution and red line – fixed solution). On the contrary, for problematic sessions, fixing had a double impact: for some of them the results become worst for others, better. However, there was no significant change in the magnitude of the residuals: it worsens the solution by increasing the residuals for sessions 20 (h component), session 24 (all components), session 30 (East and North components), session 40 (North and height component), session 142 (North component) and it improves the solution for session 20 (East and North components), session 30 (height component), session 40 (East component) and session 142 (East and height components). These problems are presented in Table 6.5.

Session	**dE [cm]**		**dN [cm]**		**dh [cm]**	
	Float	**Fixed**	**Float**	**Fixed**	**Float**	**Fixed**
22	9.34	7.55	-3.73	-1.08	-18.1	-22.4
24	10.6	12.62	37.7	39.7	-15.0	-15.43
30	-0.7	1.68	1.03	1.98	-14.9	-9.1
40	21.2	17.48	2.8	4.75	-2.47	-5.9
142	-27.7	-25.52	9.58	10.1	-19.68	-15.57

Table 6. 5: *Problematic sessions, evolution of residuals - before and after fixing the ambiguities.*

Table 6.6 shows the situation of the basic statistics that were computed on the results of the not blundered sessions.

Statistics	E [mm]	N [mm]	h [mm]
Min	-3.1	-10.8	-10
Max	16.8	47.5	14.3
Mean	1.0	-1.5	0.8
RMS	2.1	4.9	4.5

Table 6. 6: *Basic statistics of hourly residuals.*

6.1.2.2. LGO Processing and Results

Leica Geo Office it is able to handle all different processing scenarios: static, rapid static, stop-and-go, kinematic etc. (Bilban, G., et al., December 2007).

For this work the following processing parameters have been adopted:

Frequency: *L1*
Fix Ambiguities up to: *yes*
Cut-off: *10 degrees*
Ionospheric model: *Klobuchar*
Tropospheric model: *Saastamoinen*
Ephemerides: *broadcast*

Table 6. 7: *Processing parameters adopted in LGO.*

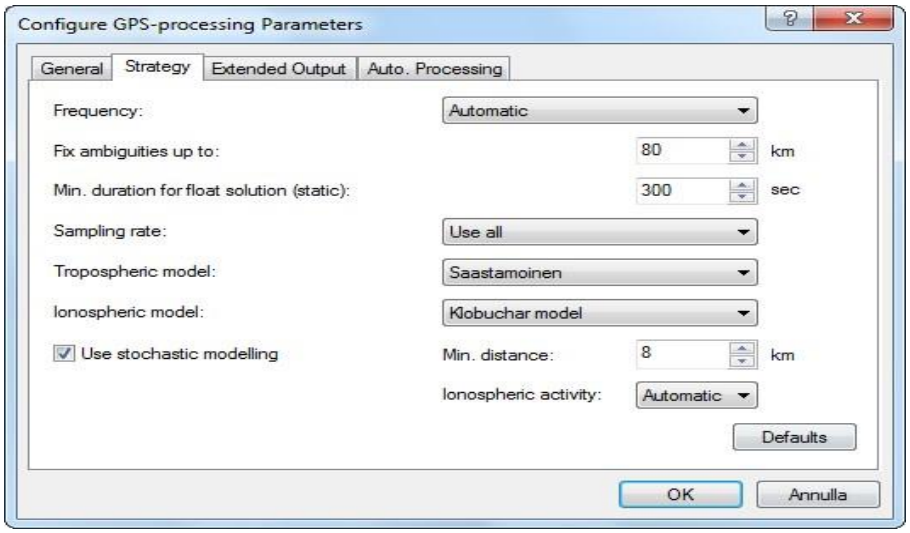

Fig. 6. 6: *Configure GPS - processing parameters in LGO.*

Then, u-blox data have been processed in LGO by hourly static sessions to assess their accuracy. Milano PS was fixed as control point and u-blox relative coordinates were estimated.

In total, 168 results have been obtained. First of all, during the processing 4 blunders, whose results differ more than 5 cm from reference solution, were identified for the whole session. For these solutions, ambiguities have not been resolved and errors' magnitude is of about 20 cm, the maximum reaching 1 m for East component.

Session	dS [cm]
34	37.1
58	12.3
106	129.9
160	38.9

Table 6. 8: *Outliers influence in the final 3-D position.*

In Table 6.9 are the basic statistics of the sessions without blunders:

Statistics	E [mm]	N [mm]	h [mm]
Min	-4	-36.30	-10.2
Max	4.1	3.3	14.5
Mean	0.2	-1.3	1.9
RMS	1.8	3.7	4.4

Table 6. 9: *Basic statistics of hourly residuals.*

Below, the graphical representation of residuals is provided with and without blunders to help visual interpretation of results. They prove that u-blox receivers are suitable for applications with cm-level accuracy when paired with an appropriate processing software: for the 2D position the errors are well below 1 cm in most of the cases (right side of Figures 6.7 – 6.9). However, for height, as expected, the residuals are slightly higher but still without moving away from the cm-level accuracy (around 1.5 cm the maximum residual).

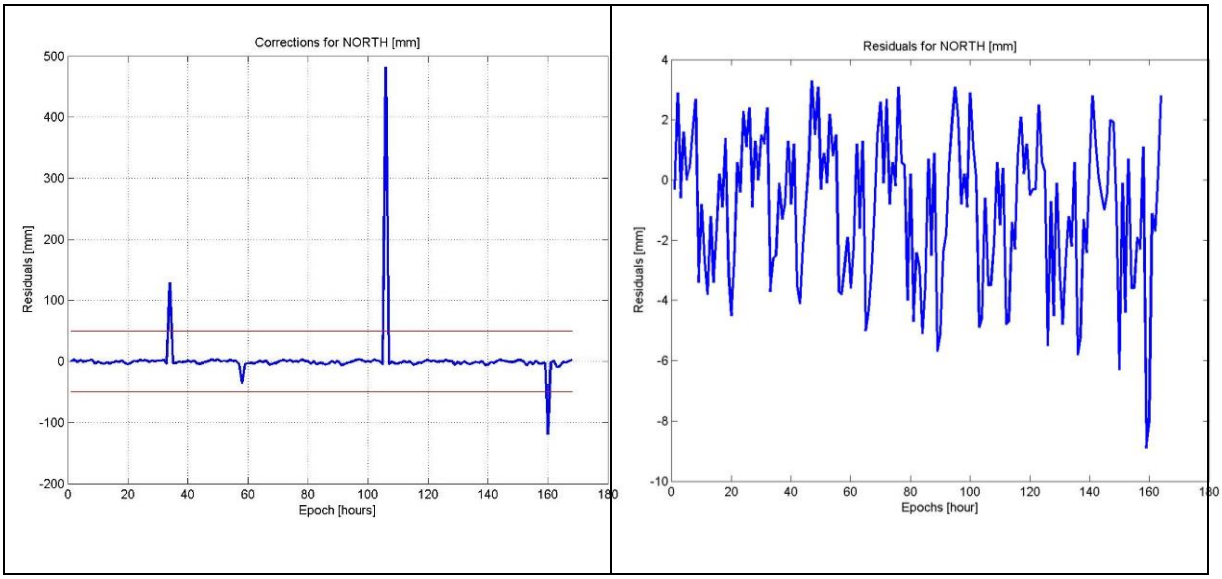

Fig. 6. 7: *Time series of North residuals, static method, 1 hour sessions: results with outliers (left side) and without outliers (right side).*

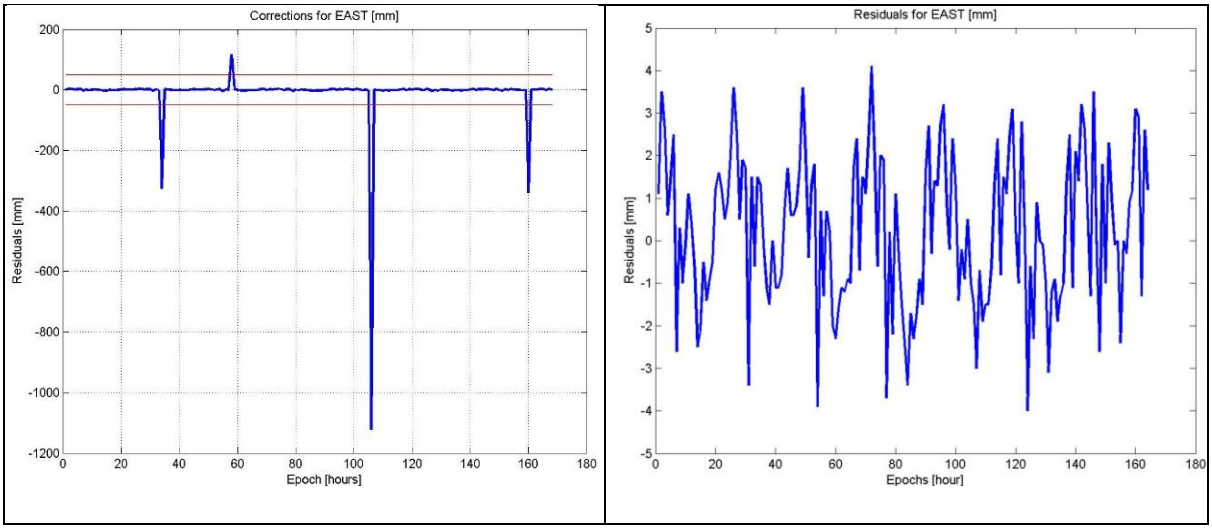

Fig. 6. 8: *Time series of East residuals, static method, 1 hour sessions: results with outliers (left side) and without outliers (right side).*

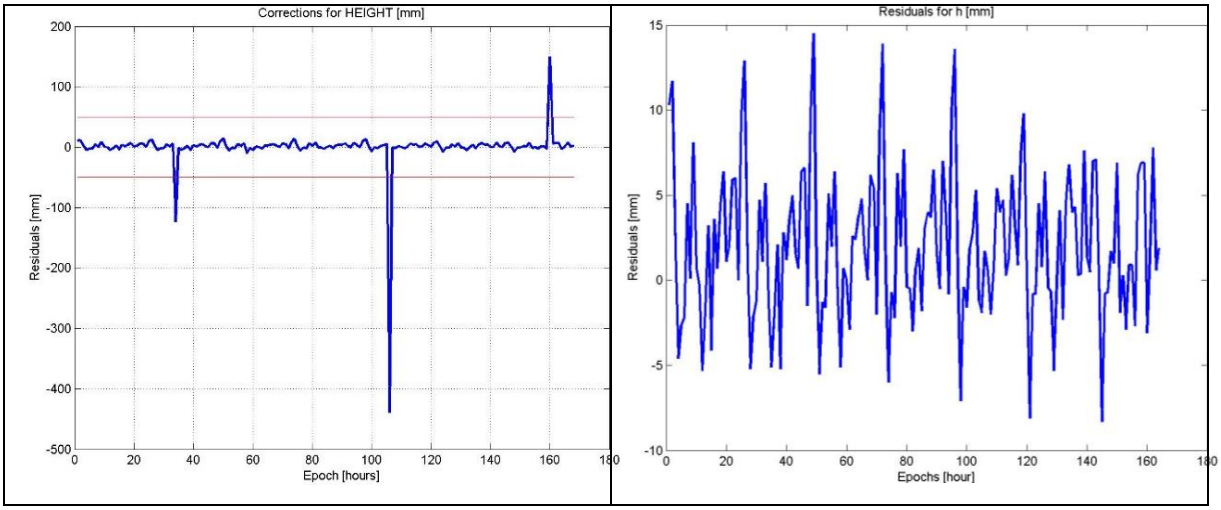

Fig. 6. 9: *Time series of height residuals, static method, 1 hour sessions – results with outliers (left side) and without outliers (right side).*

6.1.2.3. goGPS Processing and Results

For processing Milano Prova raw data, goGPS is used as well; the author is interested in observing the performance of this FOSS compared to strong powerful scientific software (Bernese GPS software) and commercial software (Leica Geo Office software).

With reference to the adopted post-processing strategy, Kalman filter is preferred to classical Leas-Square adjustment, which has been already used in LGO and BSW 5.2. The settings for Kalman filter are as follow:

- error standard deviation:
  - code: 2 m,

  - phase: 0.03 m,
  - initial state: 0.5 m.
- ambiguity resolution:
  - LAMBDA 2.0 – ILS, enumeration.
- float ambiguity restart after anomalies
  - Kalman: predicted code-phase difference.
- dynamic model: Static.

Additionally, GPS L1 code and phase double differencing, satellite elevation and SNR (weighting model) and 10º cut-off were assumed. The atmospheric delays were modelled by means of Klobuchar and Saastamoinen models while for ephemerides, the broadcast were used.

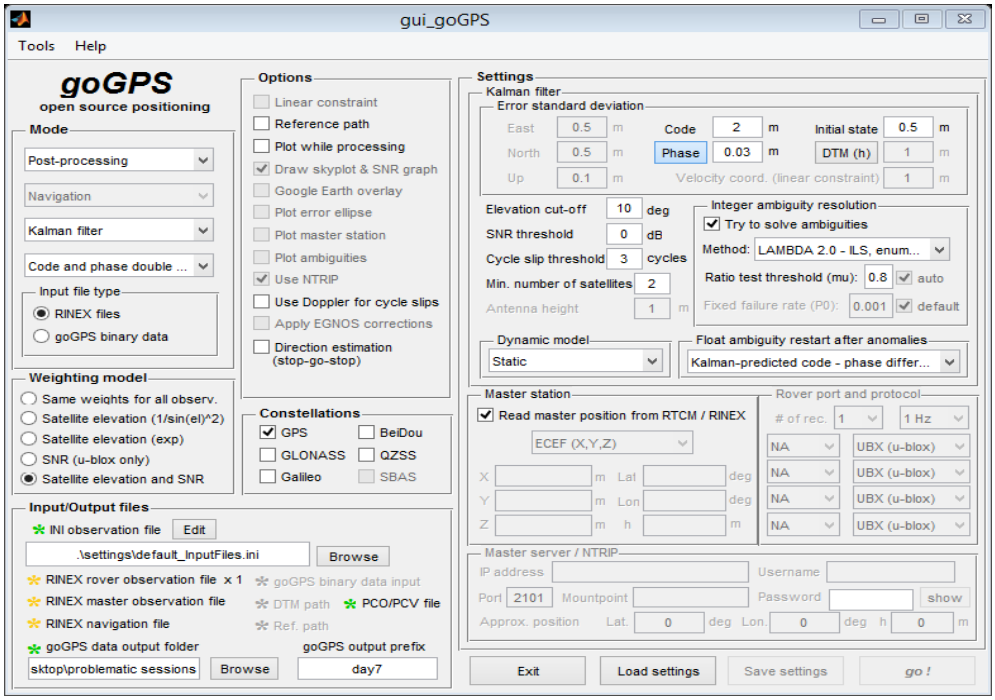

Fig. 6. 10: *goGPS user interface – processing strategy adopted for Milano Prova experiment.*

A slight increase in the number of results above the threshold of 5 cm is observed when compared to the performance of LGO and Bernese. In total, 14 outliers for East, 9 outliers for North and 12 outliers for height resulted (see Figures 6.11 – 6.13). Table 6.10 presents a short statistics of these outliers.

Parameter	dE [cm]	dN [cm]	dh [cm]
Max	22.5	58.5	109.2
Min	-81.3	-58.1	-84.8

Table 6. 10: *Maximum and minimum outlier for each of the position components.*

Table 6.11 shows the statistics of the non-problematic sessions. As expected the height residuals mean value is bigger than the mean for East and North, mostly because of the satellite geometry (it is impossible to track satellites below the horizon) and because of lack of antenna corrections (typically the PCO vertical component is the highest one). Moreover, it is expected to see bigger residuals for North than for East because of the same reason, poor satellite coverage along North – South axis.

Statistics	E [mm]	N [mm]	h [mm]
Min	-37	-14.4	-23.8
Max	11	32.6	34.2
Mean	-0.4	0.2	0.5
RMS	4.0	6.7	7.6

Table 6. 11: *Basic statistics of residuals.*

On one hand, it is very clear the size of the outliers identified in the problematic sessions. The reason for this is unknown yet but further investigation will be conducted.

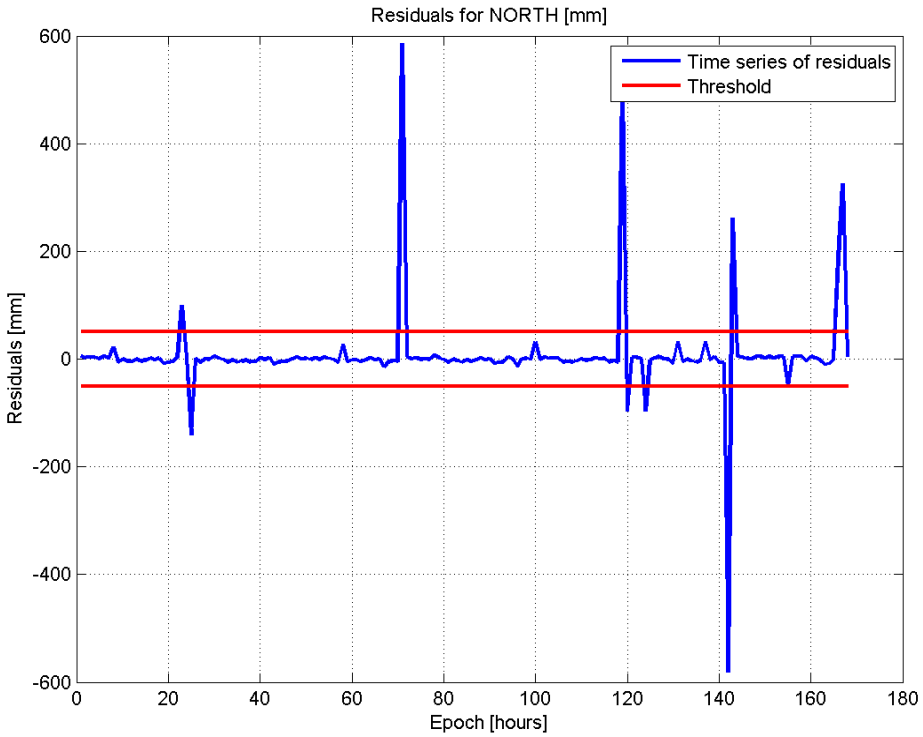

Fig. 6. 11: *Time series of North residuals, static method, 1 hour sessions.*

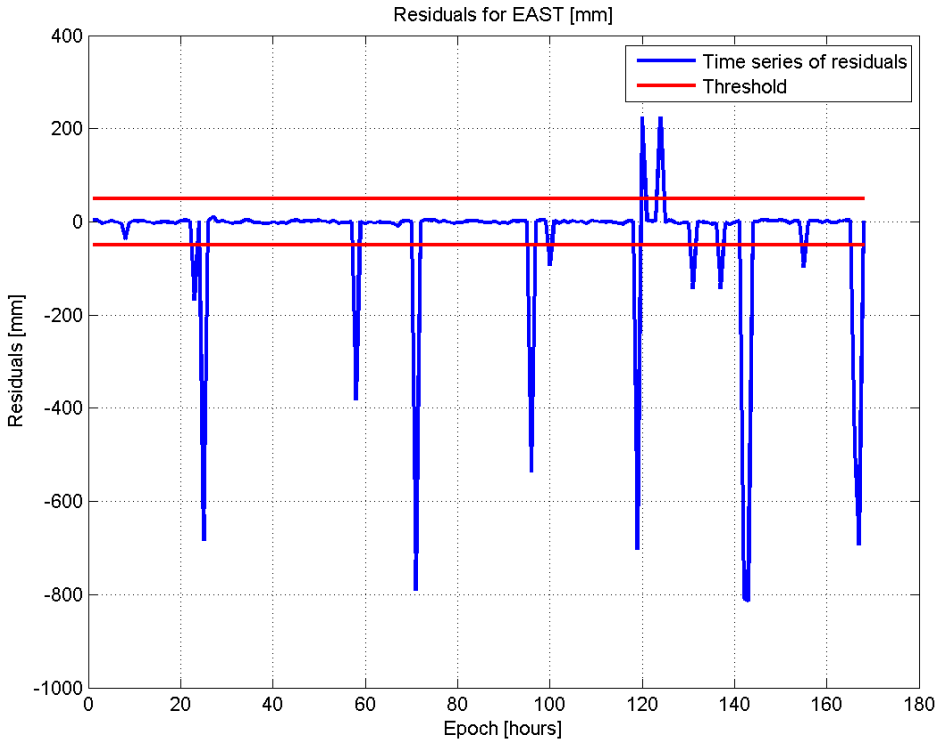

Fig. 6. 12: *Time series of East residuals, static method, 1 hour sessions.*

On the other hand, Kalman filter performed very well in the other sessions. For example, in 149 sessions the residuals were below 1 cm for East and North while for height, this threshold was not topped in 129 sessions. Again, there is the confirmation that more large residuals can be found for height than for planimetric components.

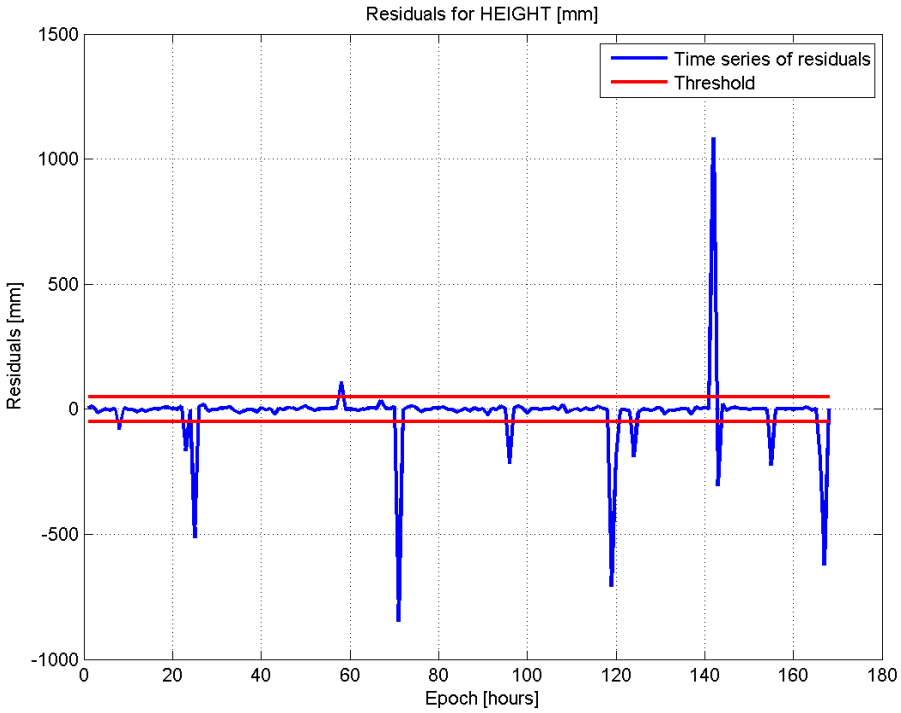

Fig. 6. 13: *Time series for East residuals, static method, 1 hour sessions.*

What is more, to assess even deeper the performance of the filter, residuals under 5 mm (with respect to the reference position) were searched: for North 117 out of 168 results (total number of estimations, good plus problematic) are below this threshold; for East the situation is even more encouraging, 148 sessions have residuals below 5 mm while for height, as expected, the number decreases to 96 sessions.

Error class	East [number of sessions]	North [number of sessions]	Height [number of sessions]
0 – 5 mm	148	117	96
5 – 10 mm	15	30	43
10 – 15 mm	5	21	29

Table 6. 12: *Number of residuals for different residual classes.*

To conclude the work of this experiment, a comparison had to be made between the results obtained with all software. In the following pictures two types of comparison are presented:

- First, the time series with u-blox absolute coordinates estimated by all three software without removing the outliers (see Figures 6.14 – 6.16).
- Secondly, the time series with residuals estimated by all three software – outliers have been omitted (see Figures 6.17 – 6.19).

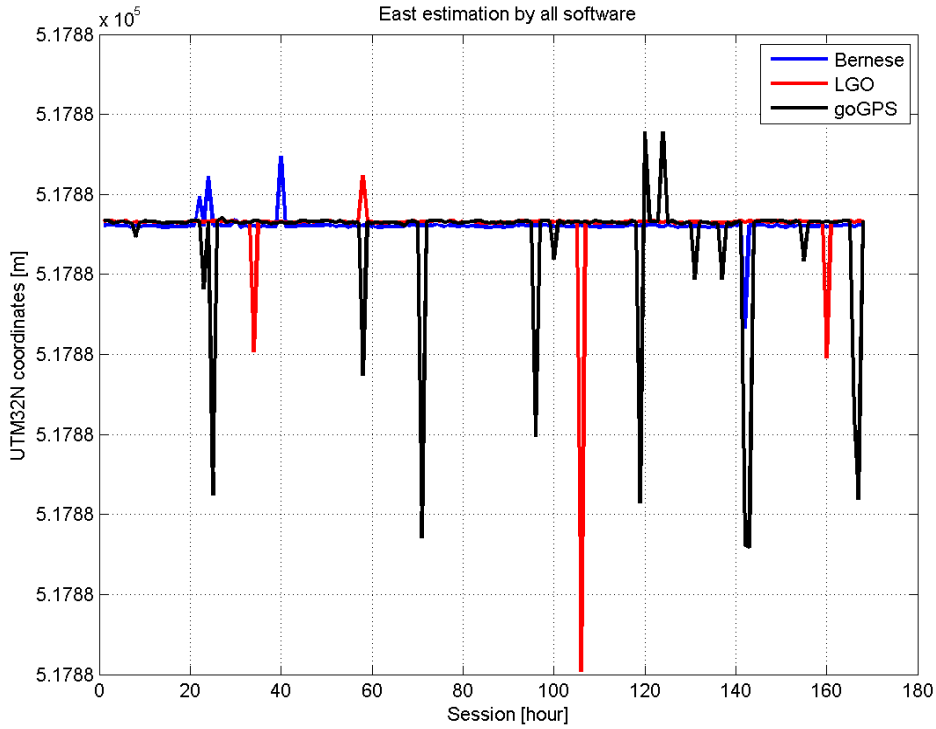

Fig. 6. 14: *Presence of outliers. East coordinates (UTM32N) for u-blox estimated with Bernese (blue), LGO (red) and goGPS (black).*

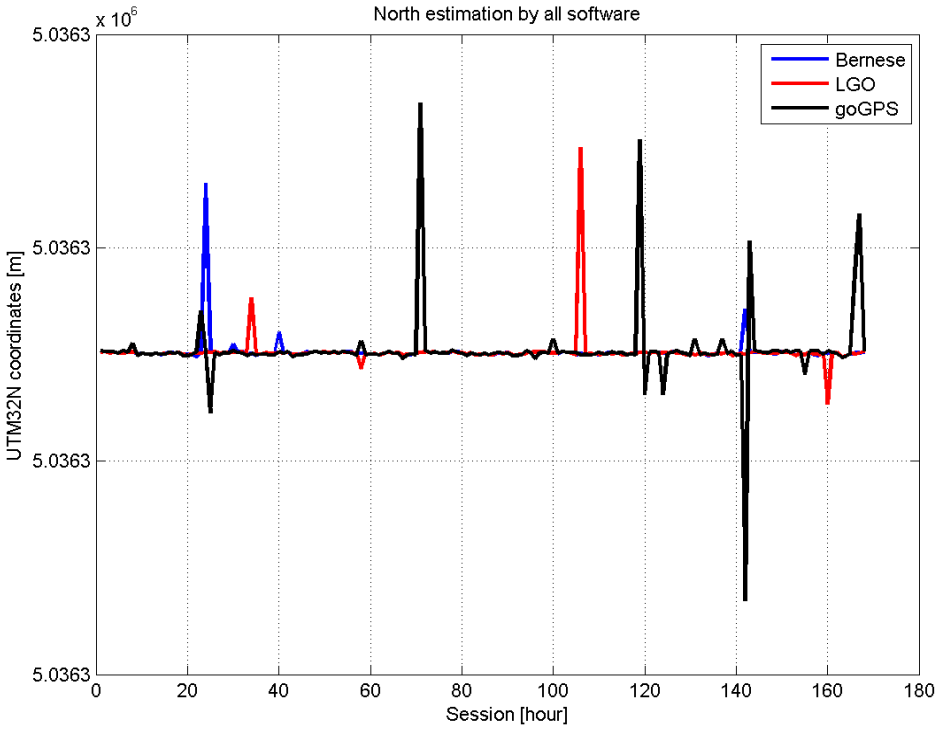

Fig. 6. 15: *Presence of outliers. North coordinates (UTM32N) for u-blox estimated with Bernese (blue), LGO (red) and goGPS (black).*

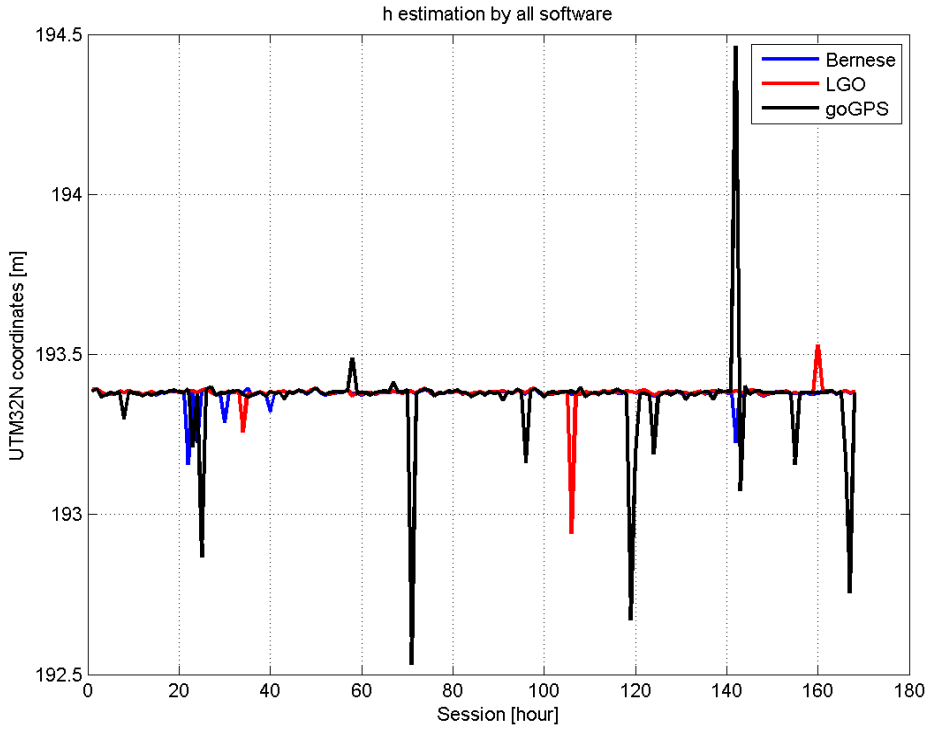

Fig. 6. 16: *Presence of outliers. h coordinates (UTM32N) for u-blox estimated with Bernese (blue), LGO (red) and goGPS (black).*

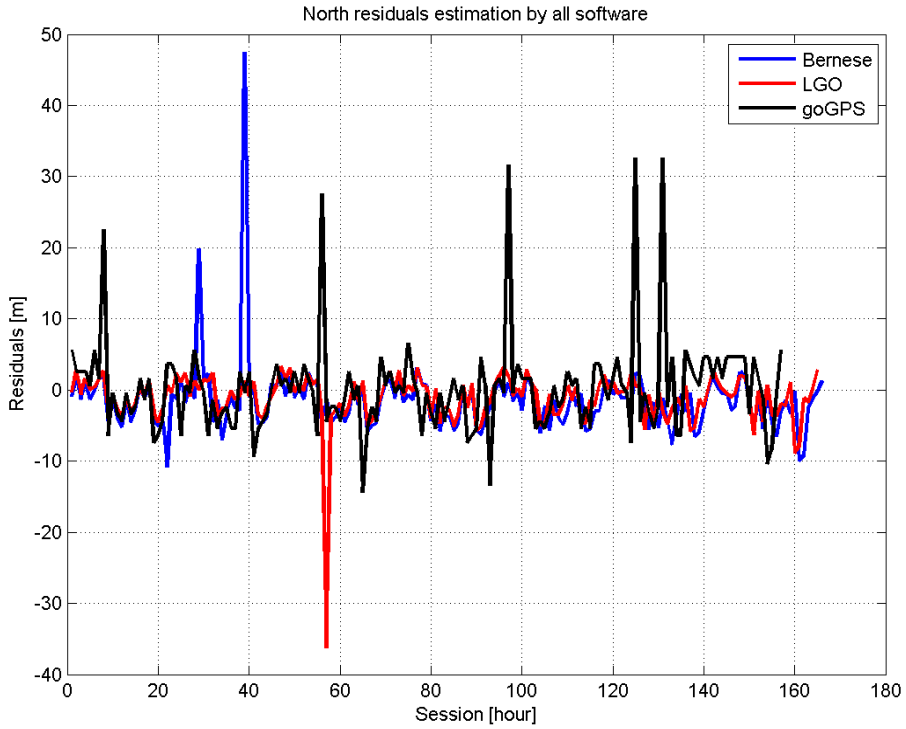

Fig. 6. 17: *North residuals for sessions without outliers (Bernese, in blue, LGO, in red and goGPS, in black).*

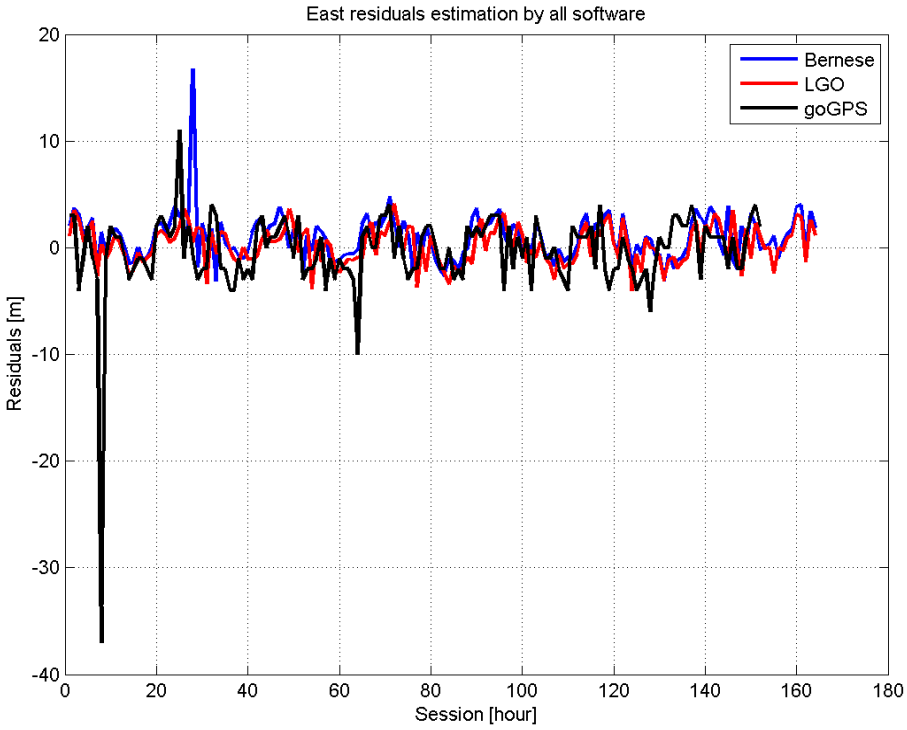

Fig. 6. 18: *East residuals for sessions without outliers (Bernese, in blue, LGO, in red and goGPS, in black).*

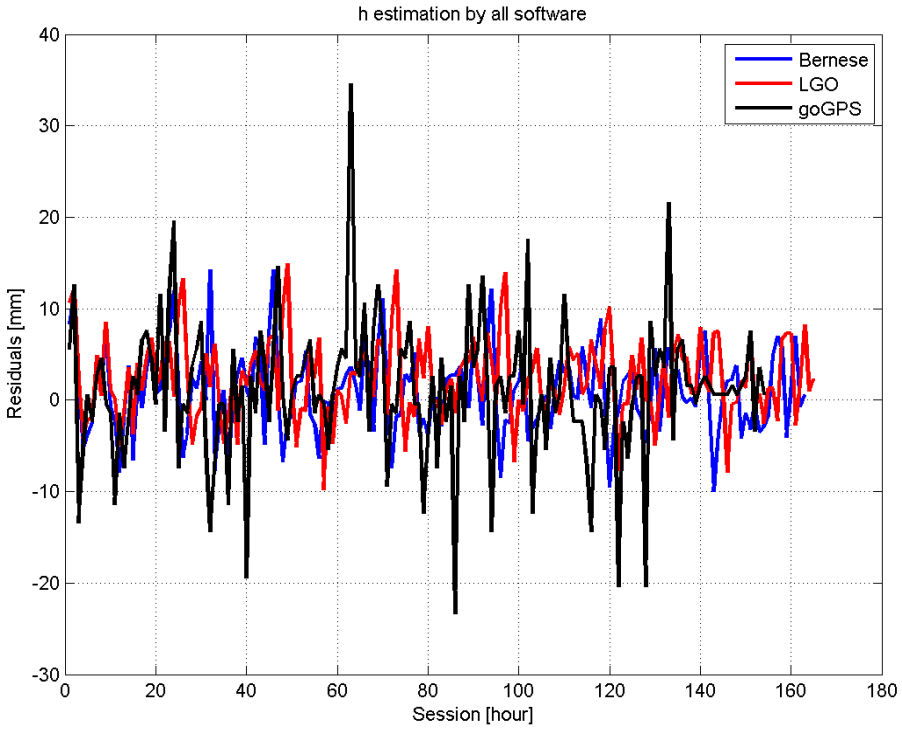

Fig. 6. 19: *h residuals for sessions without outliers (Bernese, in blue, LGO, in red and goGPS, in black).*

From the first three pictures related to results comparison it is easy to notice that each of the three software identifies different outliers (different sessions), with few exceptions. Regarding the plots of residuals of the good sessions, a consistency between software results can be observed for East and height, both in magnitude and sign while in North component there is a slightly disagreement for few of the estimates.

As a final conclusion of the comparison part, it can be easily accepted the idea that LGO provides optimal results when compared to BSW 5.2 software. Based on this and on the fact that LGO is much friendly user than BSW, from now on data processing will be carried out only in LGO.

6.2. Castelnuovo Test

The first test performed in Como, on the roof of Castelnuovo building (Politecnico di Milano) comprises one week of measurements, between May 8 and 15, 2015, or GPS Day 128 and Day 135.

The flowchart in Figure 6.20 summarizes the overall procedure to identify the differences of each individual, hourly solution with respect to the reference position.

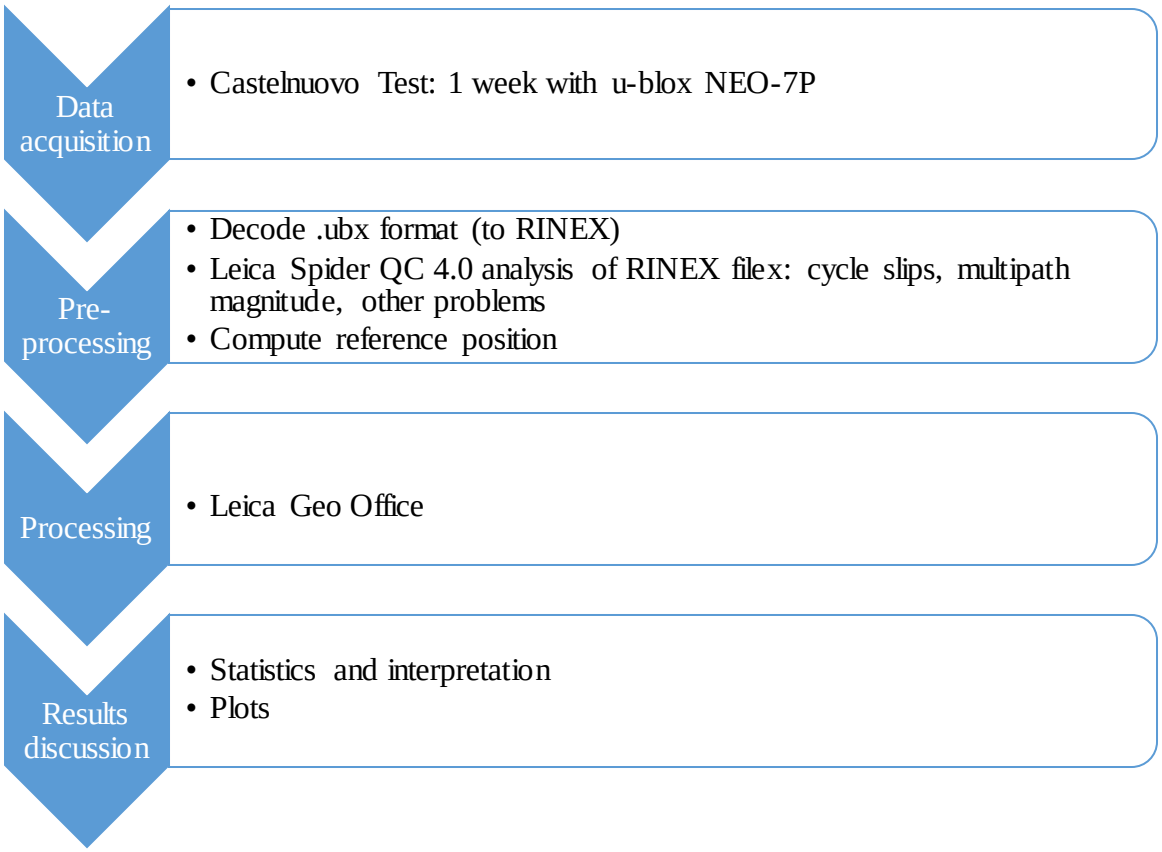

Fig. 6. 20: *Flowchart of the procedure adopted for Castelnuovo Test.*

6.2.1. Pre-processing stage

The goal is to have a better understanding of the analysed data and to discover in time if there were any serious problems that can make the experiment to fail. In total there is one week of data recorded without elevation mask (in processing phase an elevation cut off of 10^0 will be used), at a sampling rate of 1 Hz, in u-blox .ubx binary format.

With Milano Prova experiment it was proved that RTKLIB and goGPS provide as output identical RINEX files, without missing information. Therefore, from now on only RTKLIB will be used to convert .ubx format to RINEX 2.11. The user can decide (1) what the header of the RINEX file should contain: the receiver type, the antenna type and corrections, approximate position and comments and (2) which observations should be written: only GPS or mixed file, which of the signals (L1, L2, L5 and so on) and for each signal the observation type (code with/without phase).

As already said, u-blox NEO-7P is a single-frequency receiver capable of recording data on L1 only. Luckily, code and phase observations can be stored in the output file. In addition, SNR values and Doppler were checked as necessary outputs.

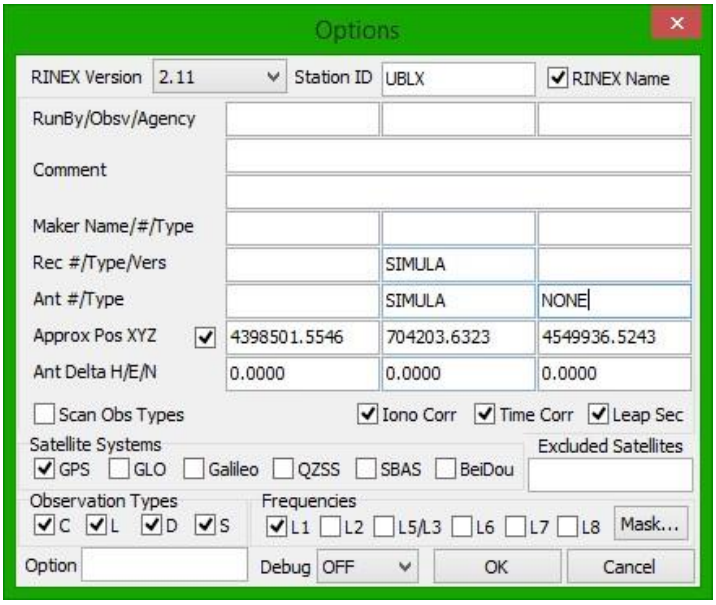

Fig. 6. 21: *Options for RINEX conversion.*

After conversion, the files were loaded and evaluated one by one in Spider QC, stressing the same quality indicators as in the case of Milan Prova experiment.

Before going to the statistics, it is worth mentioning that the last day of the campaign (GPS Day 135) is not complete because of a power failure, which turn off the PC and therefore, from that moment on there was no more power for the u-blox platform. About the quality check, it has been decided to begin the data investigation without using any elevation mask; in situations like this it is expected to see a big number of cycle slips and multipath due to the tracking of low elevation satellites. But the number of cycle slips found is too high, in average 10 300 per day (Day 1: 9042, Day2: 10 327, Day 3: 10 503, Day 3: 10 567, Day 5: 10 452, Day 6: 10 371, Day 7: 7 086); on the contrary multipath errors were better than expected, about 1.30 m (Day 1: 1.42 m, Day 2: 1.34 m, Day 3: 1.32 m; Day 4: 1.24 m; Day 5: 1.30 m; Day 6: 1.24 m; Day 7: 1.25). Basically, these numbers prove that site location was a good choice when it comes to multipath suppression but because of mountains and hills the visibility to low elevation satellites was obstructed and loss of lock was introduced.

The observation site is in a good environment, however as it can be seen in Figure 6.22 the visibility to satellites is obstructed to North by the mountain on top of which Brunate village is settled (approximately 1 000m above sea level). East of Castelnuovo building there is Parco Spina Verde, and close to the observation site the heights reach approximately 450 m. Even more, there is a mountain with an altitude of 480 m that blocks the view to satellites with low elevation on the South – East direction. Consequently, there is no surprise to see many cycle

slips when satellites are rising or setting in those line of sights. Because of the forests covering the mountains and other disturbances, loss of lock between satellites and receiver is expected to happen. Indeed, the result of the quality check confirmed this expectations.

Fig. 6. 22: *Site location and position of obstructions for low elevation satellites.*

Since the number of the cycle slips is not acceptable for the processing step, an appropriate cut off angle must be chosen and see if the numbers take a change for the better. As can be seen in Table 6.13, a mask of 10^{o} eliminates more than 80 % of the cycle slips and multipath is suppressed by 30 cm, in average. Although the improvement is optimal, the number of cycle slips is still high, about 1500 for 24 hours and more than 99 % of them are for satellites with elevation between 10 and 15 % (for example, for day 1, 1653 cycle slips out of 1663).

The necessity of an elevation mask was also stressed by the percentage of complete observations. The number of complete observations above the horizon drifts around 706 000 when the maximum possible is about 859 000; in percentage this is 82.2 %, which is an index of poor quality. With 10^{o} above the horizon the percentage increases to 98.9 % (646 000/653 000).

With 15^{0} elevation mask the number of cycle slips are decreased by 98 – 99 % and the percentage of complete observations becomes better but their absolute number (580 000) moves further away from the total number of maximum possible observations above horizon, 859 000 (when no mask is imposed). Besides, for each epoch, in average, a satellite is lost (from 8 to 7) and this is confirmed by the increase of GDOP value, from 3.8 to 4.7; therefore a slight deterioration of the satellites' geometry can be noticed. Lastly, this increase of the cut

off value has no eloquent influence on multipath effect; only some centimetre level improvements.

To conclude, it was decided to use 10^o as cut off angle because of the good balance between number of observations, on one side, and number of tracked satellites (GDOP), cycle slips and multipath, on the other side. Below, Table 6.13 presents the quality indicators value for a mask elevation of 10^o.

GPS complete obs $>10^0$ (out of theoretic)	GPS Data Completeness	Cycle Slips (cut off 10^0)	SNR [dB]	Data gaps [min]	Multipath [m]	PDOP	GDOP
320221/325331	98.4 %	824	46.2	3.8	1.03	3.2	3.8
724768/733281	98.8 %	1663	47.1	6.05	1.07	3.2	3.8
724972 /733313	98.9 %	1661	46.3	7.08	0.83	3.2	3.8
725440/733931	98.8 %	1529	46.8	6.3	1.06	3.2	3.8
725210/733609	98.9 %	1564	46.3	7.05	0.90	3.2	3.8
725373/733517	98.9 %	1786	46.3	6.5	0.96	3.2	3.8
725640/733571	98.9 %	1895	46.5	7.03	0.91	3.2	3.8
497237/502148	99.0 %	1252	45.5	4.9	0.83	3.2	3.8

Table 6. 13: *Daily quality indicators for u-blox Castelnuovo Test data.*

A remark has been already made in Chapter 5 regarding the reason for which a very short baseline was formed between Como u-blox and Como Geodetic (approximately 5 m). In the case of equally performing GPS platforms, when located close to each other, the raw data should have the same characteristics. In Table 6.14 the quality of L1 signal raw data logged by Leica GRX1200 geodetic receiver with an elevation mask of 10^0 can be found. Some surprising numbers can be seen: the number of complete observation is less than for u-blox NEO-7P, lower of about 120 000 for every 24 hours and the SNR values are insignificantly different. Not to mention that PDOP and GDOP values are almost identical with u-blox having a slightly advantage over Leica GRX1200 for GDOP values, 3.8 compared to 3.9. Even the multipath effect on u-blox is not so lousy, around 1 m compared to 0.2 m, when the prices of the two type of devices are taken into account. On the other hand, when it comes to cycle slips a geodetic receiver is second to none; for this experiment the total number of cycle slips reported for 24 hours do not exceed 100 with a maximum of 90 on GPS Day 134.

It should be noted the results of the quality checks for GPS Day 128 and Day 135 were not listed here because on this specific days the RINEX files from u-blox contain data for an interval smaller than 24 hours.

GPS complete obs $>10^0$ (out of theoretic)	GPS Data Completeness	Cycle Slips (cut-off 10^0)	SNR [dB]	Multipath [m]	PDOP	GDOP
-	-	-	-	-	-	-
603648/612134	98.6 %	69	47.5	0.16	3.2	3.9
604295/612679	98.6 %	69	47.6	0.16	3.2	3.9
604895/613259	98.6 %	76	47.6	0.15	3.2	3.9
604545/612843	98.6 %	74	47.6	0.15	3.2	3.9
577771/613638	94.2 %	69	47.6	0.16	3.2	3.9
606019/614406	98.6 %	90	47.6	0.16	3.2	3.9
-	-	-	-	-	-	-

Table 6. 14: *Quality indicators for Leica GRX1200 raw data (Day 128 and Day 135 are not presented – first and last row of the table above). Data gaps indicator is missing here because there were no gaps in the files.*

Compared to the test in Milano (u-blox LEA-4T) the numbers look much better: the values of the multipath, in average, did not move by a great deal from 1.0 m while the cycle slips diminished by few hundreds. The new measurement engine of u-blox NEO-7P proves to be more efficient in terms of tracking satellites, an average percentage of 98.8 % was obtained for data completeness (10^0 degrees above the horizon). Furthermore, the SNR values are comparable with those of geodetic receivers, with an average of 46.4 dB for the whole week. Finally, it must be taken into account that this discussion is not decisive in establishing which receiver performs better since two different sites are involved.

Table 6.15 contains the average statistics for the whole campaign giving a better idea of the setbacks and strong points of the data, which will be processed in the next step.

GPS obs $>10^0$ (out of theoretic)	GPS Data Completeness	Cycle Slips	SNR [dB]	Data gaps [min]	Multipath [m]	PDOP	GDOP
646108/653569	98.9 %	1522	46.4	6.07	0. 95	3.2	3.8

Table 6. 15: *Average quality indicators.*

For raw data logged by a low-cost GNSS sensor these numbers are satisfactory and any shortcomings can be largely removed in the processing phase of the project, based on data modelling techniques.

The last step of pre-processing was to prepare the 3-D reference coordinates by post-processing the raw data in LGO. A solution was estimated for every day of the campaign, in total 7, and then averaged in a final set of 3-D coordinates (see Table 6.16).

X [m]	Y [m]	Z [m]	E [m]	N [m]	h [m]
4398271.8352	704072.7789	4550188.7414	507359.9030	5072128.0637	284.5090
4398269.5162	704071.9437	4550193.1069	507359.4397	5072132.8402	285.9502

Table 6. 16: *Reference coordinates for u-blox and Pillar in ITRF2008 and UTM 32N.*

To summarize, up to this point RINEX files were created and checked for problems, statistics about quality indicators have been organized in tables and reference coordinates were computed.

6.2.2. Processing

In this case only LGO software is used for processing raw data. Experiment Milano Prova proved that LGO is trustworthy its results being very close to those obtained by BSW 5.2. However, it the future these data would be processed in BSW 5.2 as well for a more robust analysis.

6.2.2.2. LGO Processing and Results

The reference strategy used for this experiment is based on the following options:

Frequency: *L1*
Solution type: *Automatic*
Fix Ambiguities up to: *80 km (default)*
Cut-off: *10 degrees*
Ionospheric model: *Klobuchar*
Tropospheric model: *Saastamoinen*
Ephemerides: *broadcast*

Table 6. 17: *Processing parameters adopted in LGO.*

The ionospheric delay has a distinctive impact on the GNSS observations (Shagimuratov et al, 2002). Since the precise positioning is mostly performed relative, the impact of the ionospheric delays over very short baseline is greatly reduced by differencing techniques. In present case a

baseline of 100 m, phase double difference processing and Klobuchar model will be more than optimal to deal with ionosphere effect on GPS positioning accuracy.

LGO results are very encouraging, there is not even a single outlier identified in the processing phase: for each session all residuals are well below 5 cm blunder threshold.

The position of u-blox was estimated with respect to both of the geodetic receivers, Como Test and Como Geodetic.

For baseline Como Test – Como u-blox 172 results are different from the reference position with less than 5 mm for East coordinate, for North 148 of the estimates have residuals under 5 mm and only for one session (session 60) a residual larger than 10 mm was observed; for height component the residuals are slightly larger but well under the threshold: 92 sessions have residuals under 5 mm and only 5 sessions have errors bigger than 10 mm.

Error class	**East [number of sessions]**	**North [number of sessions]**	**Height [number of sessions]**
0 – 5 mm	172	148	92
5 – 10 mm	0	23	82
>10 mm	0	1	5

Table 6. 18: *Number of residuals for different residual classes.*

With this experiment an accuracy below cm level, required by most monitoring applications was reached proving the reliability of u-blox NEO-7P for such utilization.

Statistics	**E [mm]**	**N [mm]**	**h [mm]**
Min	-4	-13.7	-12.6
Max	4.4	7.3	13.6
Mean	-0.1	-1.0	0.1
RMS	1.7	3.4	5.9

Table 6. 19: *Basic statistics of residuals.*

Looking at Table 6.19 and Table 6.8 (LGO results for Milano Prova), seems like u-blox NEO-7P performed better than the old LEA-4T; this performance cannot be associate to the length of the baseline (both under 100m) or the processing parameters (the same strategy) but can be justify, on one side, by the upgraded measurement engine of the NEO-7P and on the other side, by the monitoring site location.

Graphical representations of the residuals for each 3-D coordinate are given in Figures 6.23 – 6.25.

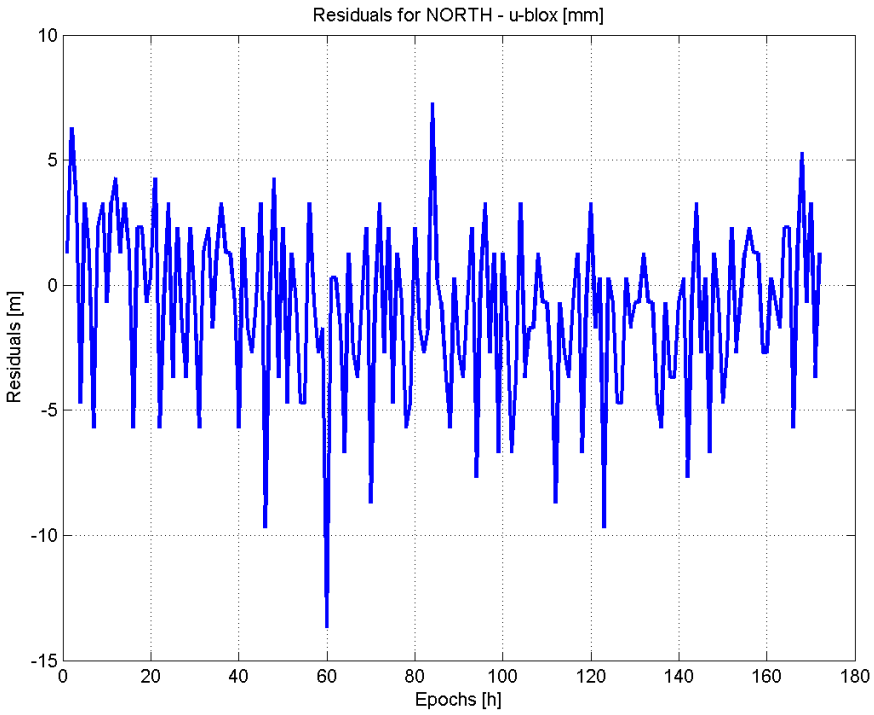

Fig. 6. 23: *Residuals for North, static method, 1 hour sessions.*

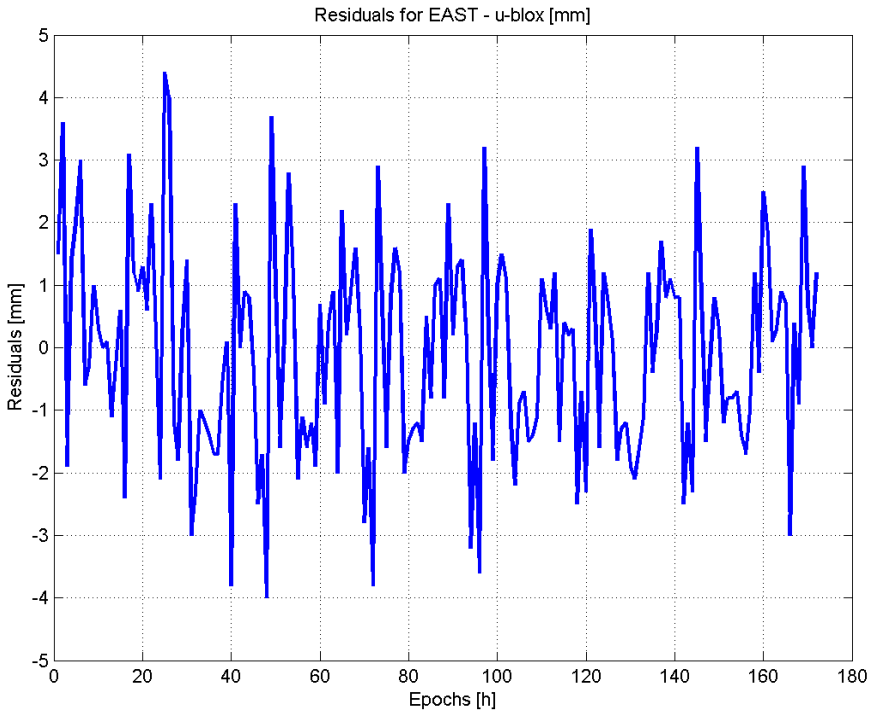

Fig. 6. 24: *Residuals for East, static method, 1 hour sessions.*

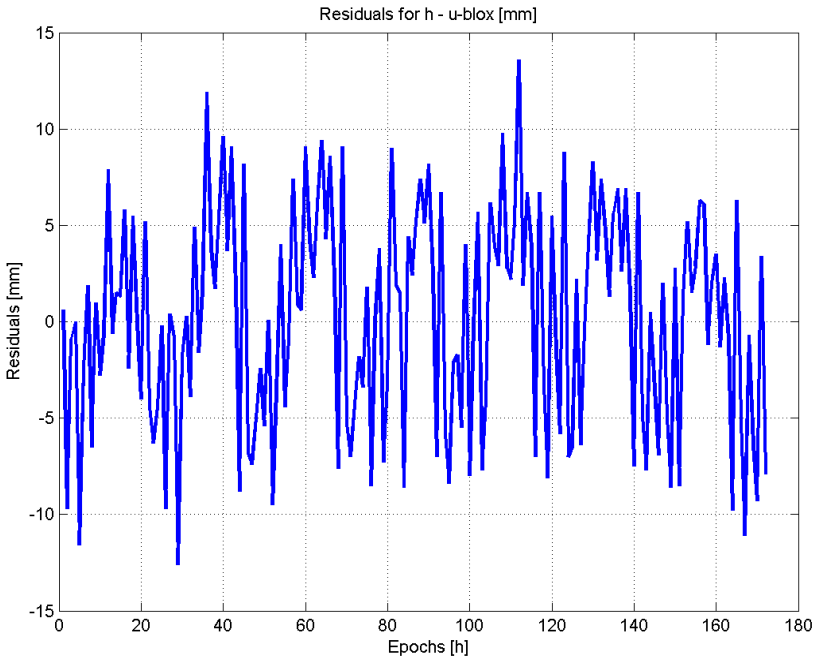

Fig. 6. 25: *Residuals for h, static method, 1 hour sessions.*

As already introduced, u-blox position was estimated with respect to Como Geodetic; thus, a new baseline Como Geodetic – Como u-blox (approximately 5 m) is processed. Even in this case there were no outliers but the residuals were slightly larger than for first baseline. For East component, again, all residuals are under 5 mm with one exception, session 25; for North 151 sessions are under 5mm while for height only 68 residuals are below 5mm. However, all 172 sessions presents residuals well under the 5 cm threshold. Table 6.20 shows the main statistic parameters for the residuals.

Statistics	E [mm]	N [mm]	h [mm]
Min	-4.2	-10.3	-11.6
Max	5.3	7.8	19.8
Mean	-0.2	-0.1	5.9
RMS	1.8	3.4	5.7

Table 6. 20: *Basic statistics of hourly residuals.*

A comparison between the estimated u-blox positions from processing the two baselines is presented graphically in Figures 6.26 – 6.28. It can be easily noticed the better accuracy obtained for North and East estimation by performing relative positioning with respect to Como Test rather to Como Geodetic (see Figures 6.26 and 6.27). For height, a particular effect had been observed: the mean of the residuals is 5.9233 mm; thus, for this component the residuals do not follow the normal distribution. To confirm this, the histogram (see Figure 6.29) of the

residuals has been generated and indeed a clear non-symmetric distribution around the expected 0 mean (skewed histogram). Moreover, this effect with unknown causes can be noticed in Figure 6.28 where there is a clear bias in u-blox height residuals for baseline Como Geodetic – Como u-blox with respect to baseline Como Test – Como u-blox.

Fig. 6. 26: *Comparisons of u-blox estimated residuals (North) based on two different baselines: Como Test – Como u-blox (in green) and Como Geodetic – Como u-blox (in red). Static method, 1 hour sessions.*

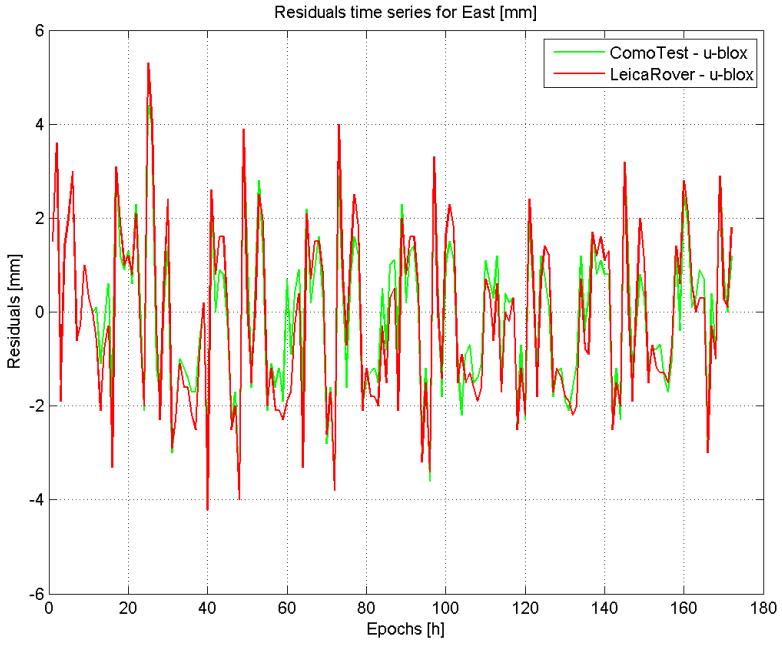

Fig. 6. 27: *Comparison of u-blox estimated residuals (East) based on two different baselines: Como Test – Como u-blox (in green) and Como Geodetic – Como u-blox (in red). Static method, 1 hour sessions.*

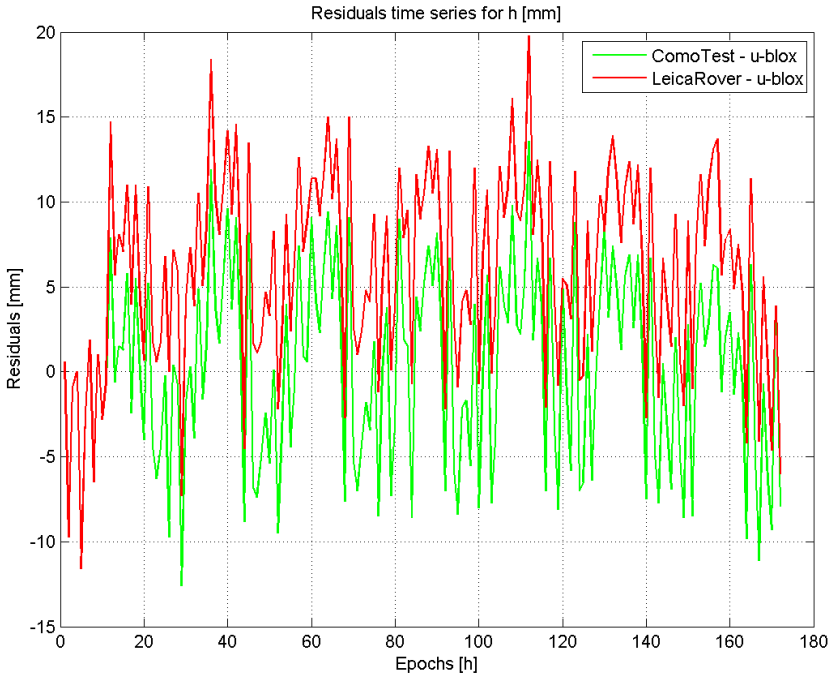

Fig. 6. 28: *Comparison of u-blox estimated residuals (height) based on two different baselines: Como Test – Como u-blox (in green) and Como Geodetic – Como u-blox (in red). Static method, 1 hour sessions.*

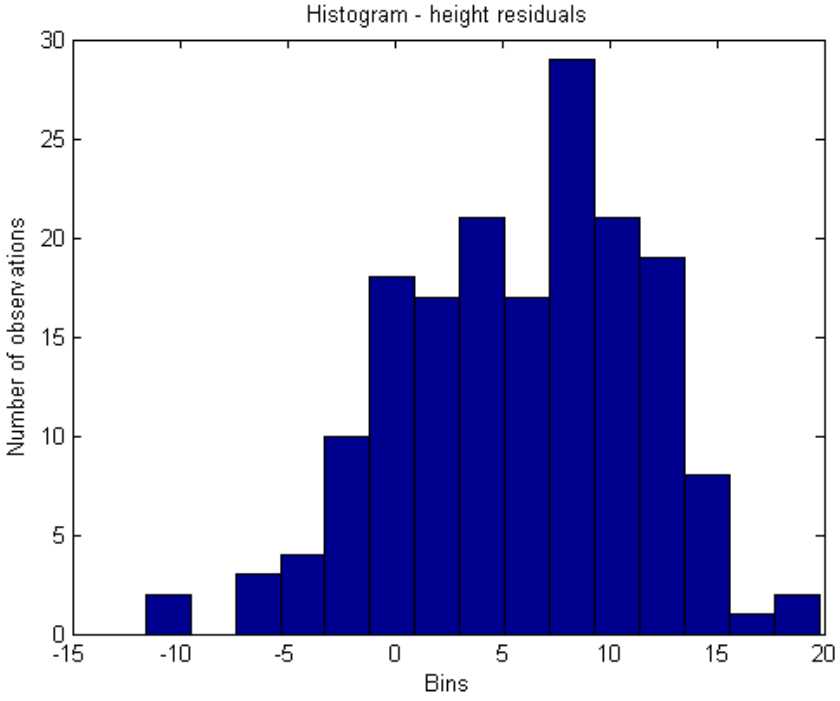

Fig. 6. 29: *Histogram of height residuals. Non-symmetric effect and not normal distribution.*

6.3. SIMU - SLIDE

The main goal of this test it to decide if u-blox low-cost sensor is capable of detecting position variations at centimetre and sub-centimetre level. Furthermore, it is very interesting to observe if the detected displacements are the same with the imposed ones. As noted, the device is composed of a 30 cm long metal rod over which the antenna is moving. Horizontal movements are allowed up to 10 cm while there is no possibility to move vertically the antenna.

SIMU - SLIDE project started on GPS Day 152 (1st of June, 2015) with two days of static acquisition to compute the reference start position of the antenna. Starting with GPS day 154 (3rd of June, 2015) antenna was shifted horizontally 5 mm every 3 hourly sessions (for each of the day 3 sessions were planned, therefore a movement of 1.5 cm).

The flowchart in Figure 6.30 summarizes the overall procedure to analyse the data.

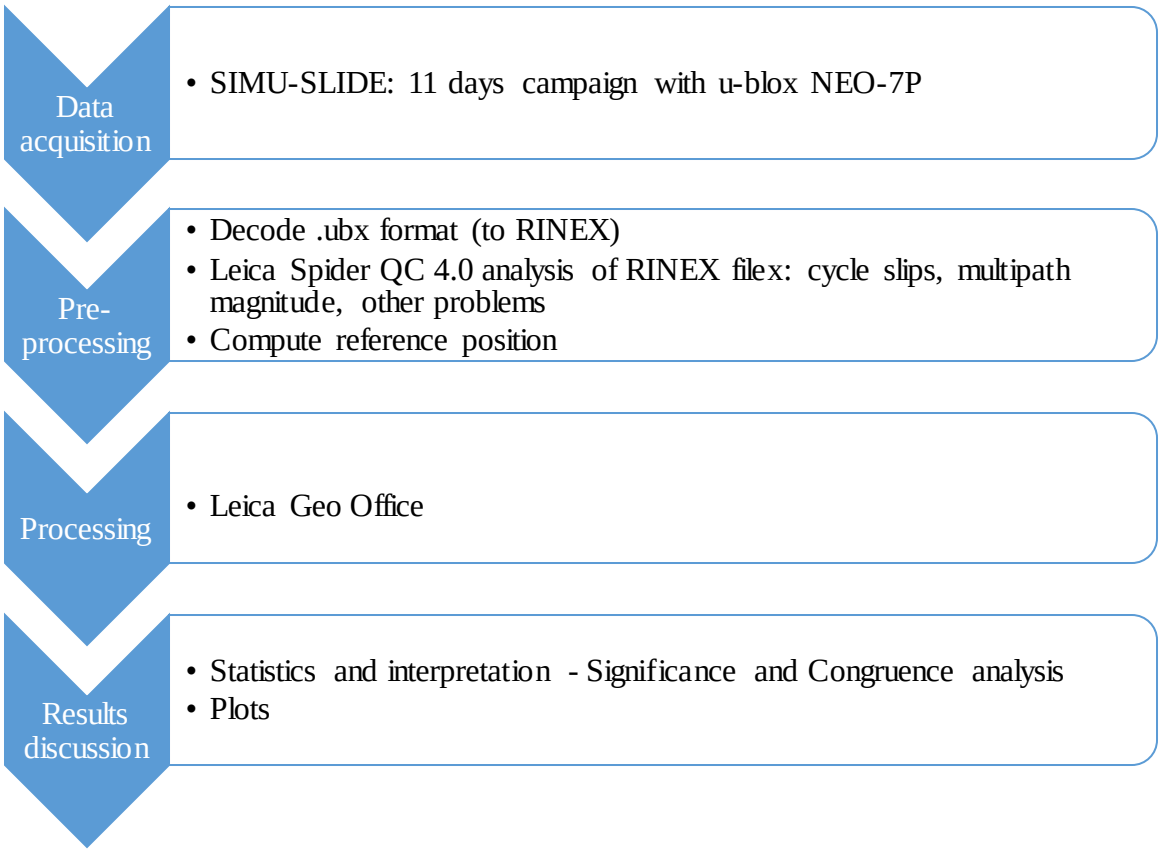

Fig. 6. 30: *Flowchart of the procedure adopted for SIMU-SLIDE project.*

6.3.1. Pre-processing stage

The goal is to have a better understanding of the analysed data and to discover any problem that could make the experiment to fail. In total there are 11 days of data recorded without

elevation mask (in processing phase an elevation cut off of 10^0 will be used), at a sampling rate of 1 Hz, in u-blox .ubx binary format.

RTKLIB is used to convert .ubx format to RINEX 2.11. As in the previous cases additional to correct header information the RINEX files contain at every epoch L1 signal observations: code, phase, SNR and Doppler for each satellite in view.

As for the other two experiments next step is to perform a preliminary data evaluation in Leica Spider QC, to discover if there are any issues. Table 6.21 summarizes the main qualitative findings related to the RINEX files of SIMU-SLIDE project. Each row of the table means one session, which as it was already reported in Chapter 5 last for 3 hours. Therefore, a first look at number GPS observations reveals a good percentage meaning that in terms of data completeness the low-cost unit used for this research performed very well. Besides this, SNR, PDOP and GDOP values display optimal values even from a geodetic receiver point of view. On the other hand, few problems were discovered.

First concern is related to the number of cycle slips. As it can be seen in table below there is a strange behaviour in the total number of cycle slips of the sessions. For example, a closer look at the first 3 rows which symbolize the 3 sessions of the first day of measurements reveals problems for the afternoon sessions. Between 11:00:00 and 14:00:00 GPS time – session number 2 of day 1 (13:00:00 and 16:00:00 local time) - 562 cycle slips occurred, even though a 10^0 mask elevation had been used. With the help of Spider QC the problem was identified and associated to satellite G6, responsible for 417 cycle slips.

GPS obs >10^0 (out of theoretic)	GPS Data Completeness	Cycle Slips	SNR [dB]	Data gaps [min]	Multipath [m]	PDOP	GDOP
83475/83529	99.9 %	42	44.8	1.03	1.08	3.4	4.1
79353/80585	98.5 %	562	45	1.03	1.04	3.2	3.8
88545/90739	97.6 %	500	45.2	1.03	0.97	3.1	3.7
86321/86423	99.9 %	21	44.8	1.05	1.19	3.4	4.1
79185/80202	98.7 %	194	44.7	1.07	0.88	3.3	3.9
85368/86861	98.3 %	568	44.5	0.9	0.91	3.2	3.8
83573/83667	99.9 %	55	44.3	1.08	1.08	3.4	4.0
78469/79803	98.3 %	539	44.9	0.9	1.19	3.2	3.8

89108/91634	97.2 %	594	43.9	0.9	0.99	3.2	3.8
83902/83960	99.9 %	73	44.6	1.03	1.15	3.4	4.0
78633/79968	98.3 %	513	44.5	1.05	1.01	3.2	3.8
88670/91422	97.0 %	580	43.6	1.07	0.94	3.2	3.8

Table 6. 21: *Quality indicators for each observation session.*

For session number 3 of day 1 – between 15:00:00 and 18:00:00 GPS Time (17:00:00 and 20:00:00 local time) – 500 cycle slips were counted, this time responsible for this value are satellites G2 and G5 while G6 was not tracked anymore. To summarize, more than 97 % of all cycle slips of each session are associated with elevation between 10 and 15 degrees (the preliminary analysis started with a mask of 10^0) and more than 85 % cycle slips are due to three satellites: G2, G5, G6.

This situation is consistent during the whole observation campaign, first session of every day (between 07:00:00 and 10:00:00 GPS Time) a small number of cycle slips is observed while for the remaining two sessions the number increases by ten times, in average. As it can be seen in Figure 6.31, satellites G2, G5 and G6 are masked by Brunate direction when they are below 15^o degrees and cycles slips are experienced based on the loss of lock.

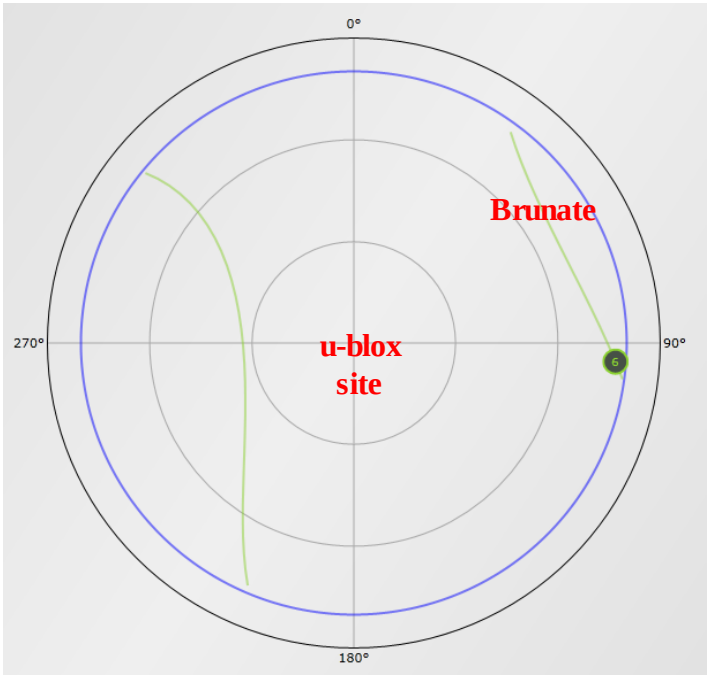

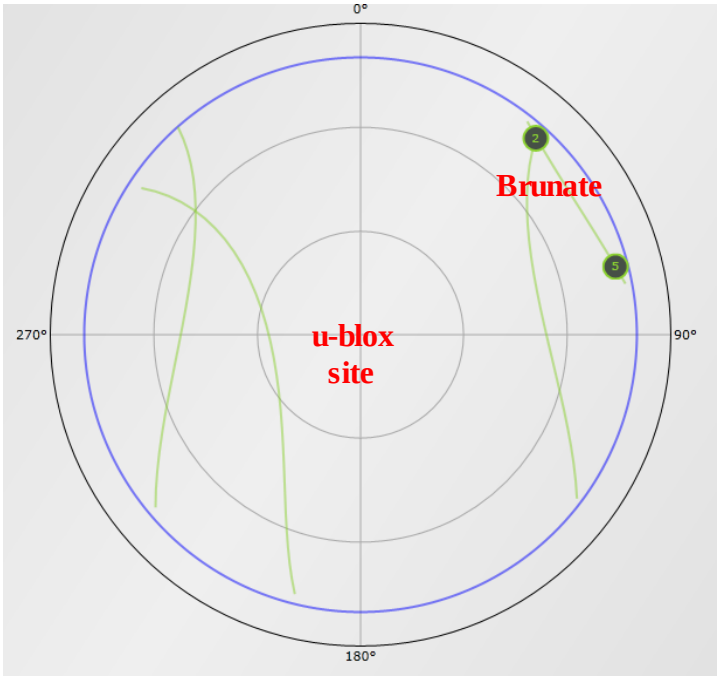

Fig. 6. 31: *SIMU-SLIDE project sky plots for problematic satellites. Trajectory followed by satellite G6 during Session 2 (up) and trajectories followed by G5 and G2 during Session 3 (below). Plots generated with Trimble planning online tool.*

Second issue is related to data gaps, in average for each 3 hours of observations (180 minutes) 1 minute, split in more short intervals of few seconds, is missing. This is not critical but is interesting to be mentioned because the same effect was noticed in Castelnuovo static experiment but not in Milano Prova, where 0 gaps were found. The intriguing part is that for Milano Prova a much older u-blox receiver was used (LEA-4T) while for Castelnuovo Test and SIMU-SLIDE project the u-blox NEO-7P represented the choice.

Lastly, the matter of multipath must be discussed although its values are not worrying. In average, for each session the multipath effect translates into a positioning error of 1 m while the threshold computed by QC is 0.5 m. For a low-cost GPS platform, with an antenna with no built-in groundplane or other multipath suppression technique these numbers are acceptable.

Table 6.22 recaps the average statistics for the whole campaign giving a better idea of the setbacks and strong points of the data, which will be processed in the next step.

GPS obs $>10^0$ (out of theoretic)	GPS Data Completeness	Cycle Slips	SNR [dB]	Data gaps [min]	Multipath [m]	PDOP	GDOP
83267/84306	98.8	333	44.7	1.00	1.04	3.3	3.9

Table 6. 22: *Averaged values of the quality indicators.*

The last step of pre-processing was to prepare the 3-D reference coordinates by post-processing the raw data in LGO. A solution was estimated for start position based on two days long files. These coordinates are in listed in Table 6.23:

X [m]	Y [m]	Z [m]	E [m]	N [m]	h [m]
4398272.3085	704069.4830	4550188.6031	507356.5755	5072128.0013	284.3722

Table 6. 23: *Reference coordinates in ITRF2008-WGS84 and UTM 32N.*

6.3.2. LGO Processing and Results

Based on aforementioned 3 processing strategies were compared:

- Processing strategy 1: for all sessions a cut-off angle of 10^0 was used and all satellites were enabled (see Figure 6.32).
- Processing strategy 2: for all sessions a cut-off angle of 15^0 was used with all satellites enabled. By increasing the elevation mask more than 95 % of the cycle slips were reduced but less satellites and observations are available.
- Processing strategy 3: a cut-off of 10^0 was imposed for all sessions. For first session – morning session - of each day (always characterized by a low number of cycle slips) all satellites were kept; for second session of each day, satellite G6 was disabled while for last session of each day, satellites G2 and G5 were disabled. As it was already stated these 3 satellites are responsible for the majority of cycle slips.

Based on the standard deviation of the results, strategy number 3 proved to be the best in this case and the results presented below are related to this option.

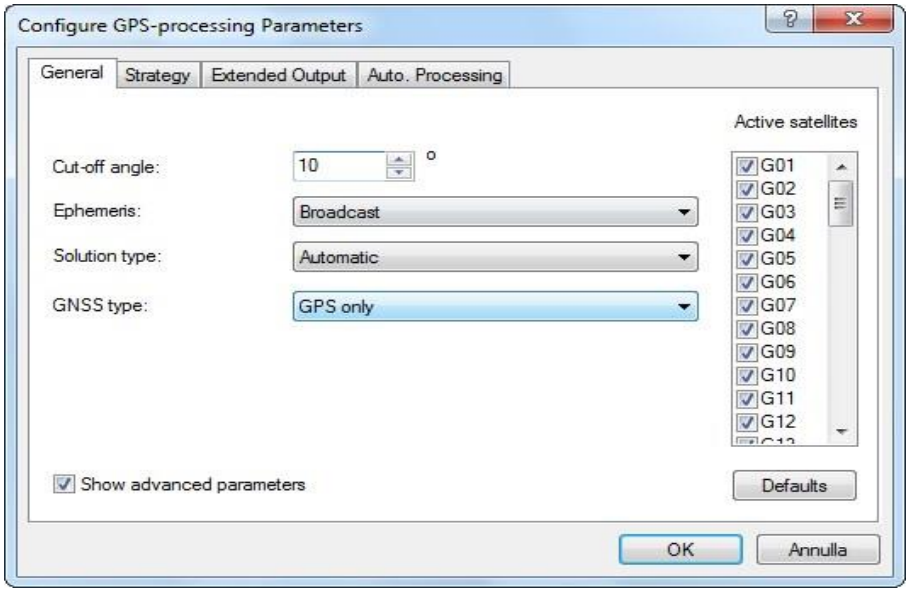

Fig. 6. 32: *Processing strategy number 1.*

Regarding the other processing parameters, broadcast ephemeris were always the choice, GPS L1 data, Saastamoinen tropospheric model and Klobuchar ionospheric model were adopted. Additionally, it was decided to estimate the position of the u-blox on hourly basis and not session. At the end, each of the 20 sessions is split in 3 hourly sub-sessions which are processed individually to estimate the 3-D position of the u-blox antenna.

In total, two baselines were estimated: Como Test – Como u-blox and Como Geodetic – Como u-blox.

1. Baseline Como Test – Como u-blox

Once the LGO output ($\Delta X^{CT\text{-}ublx}$, $\Delta Y^{CT\text{-}ublx}$ and $\Delta Z^{CT\text{-}ublx}$ in WGS-84) was available next step was to convert this into local coordinates with origin in Como Test. By doing so the horizontal and vertical component can be split and analysed separately.

To compute local coordinates of u-blox with respect to Como Test for each session *i*, the following rotation must be applied:

$$\underline{\Delta L_i}^{CT-ublx} = R * \underline{\Delta X_i}^{CT-ublx} \tag{6.4}$$

where R is the rotation matrix (see Appendix B), $\underline{\Delta L_i}^{CT-ublx}$ is a vector and contains the local coordinates of u-blox with respect to Como Test and $\underline{\Delta X_i}^{CT-ublx}$ is a vector and contains the WGS-84 coordinates of u-blox with respect to Como Test for each session *i*.

With theses new coordinates a mean East, mean N, mean height and mean baseline length were computed in the local systems:

$$\underline{\Delta L_{mean}} = (\underline{\Delta L_{start}}^{CT-ublx} + \underline{\Delta L_{end}}^{CT-ublx})/2 \tag{6.5}$$

These new quantities together with the known displacements were used to compute the theoretical East, North, height and baseline length:

$$\underline{\Delta L_i} = \underline{\Delta L_{mean}} + \delta i \begin{bmatrix} sin\Theta \\ cos\Theta \\ 0 \end{bmatrix} \tag{6.6}$$

where δi is the controlled displacements for each session, Θ is the orientation angle of Como Test – Como u-blox baseline and α is the slope angle between the two end points.

$$\Theta = \text{arctg}(\frac{\Delta E_{CT-ublx}}{\Delta N_{CT-ublx}}) = -0.9759\ rad \tag{6.7}$$

$$\alpha = \arcsin\left(\frac{\Delta h_{CT-ublx}}{D}\right) = 0.0880\ rad \qquad 6.8$$

where D is the slope distance between Como Test site and Como u-blox position.

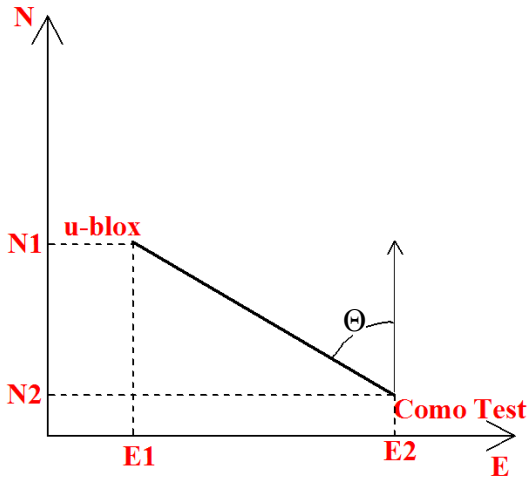

Fig. 6. 33: *Baseline scheme.*

At this point both the theoretical values and the actual displacements for each session (estimated in LGO) are available. Last thing to do is to compare these two sets of numbers (see Figures 6.34 – 6.37).

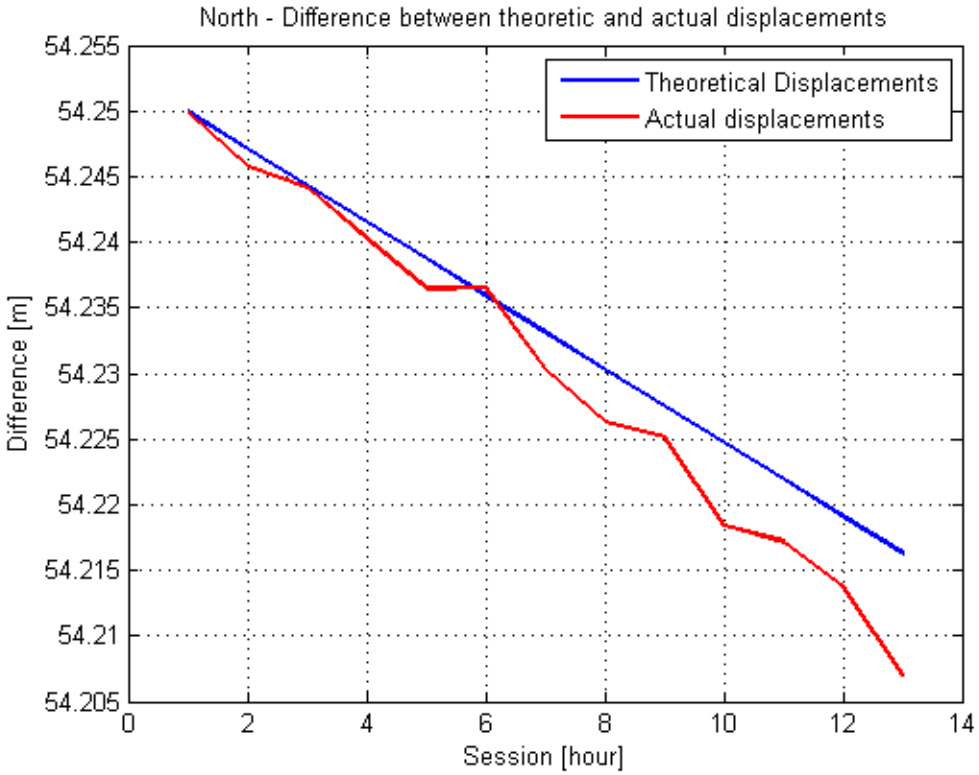

Fig. 6. 34: *Local North component of the baseline. Actual displacements (in red) from the theoretical ones (in blue).*

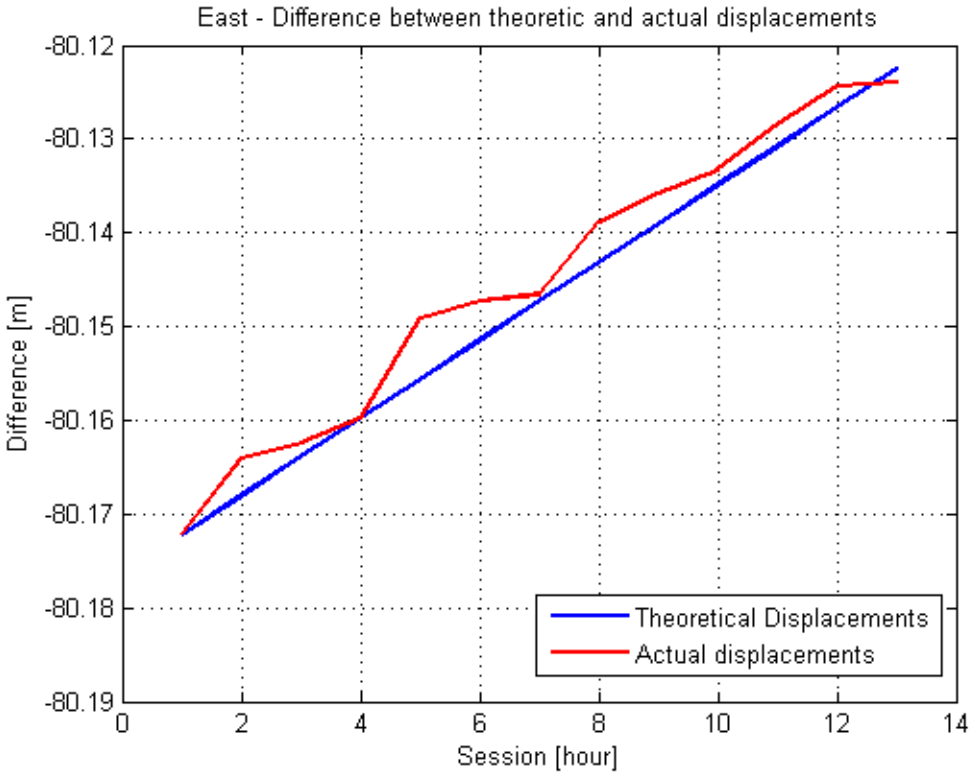

Fig. 6. 35: *Local East component of the baseline. Actual displacements (in red) from the theoretical ones (in blue).*

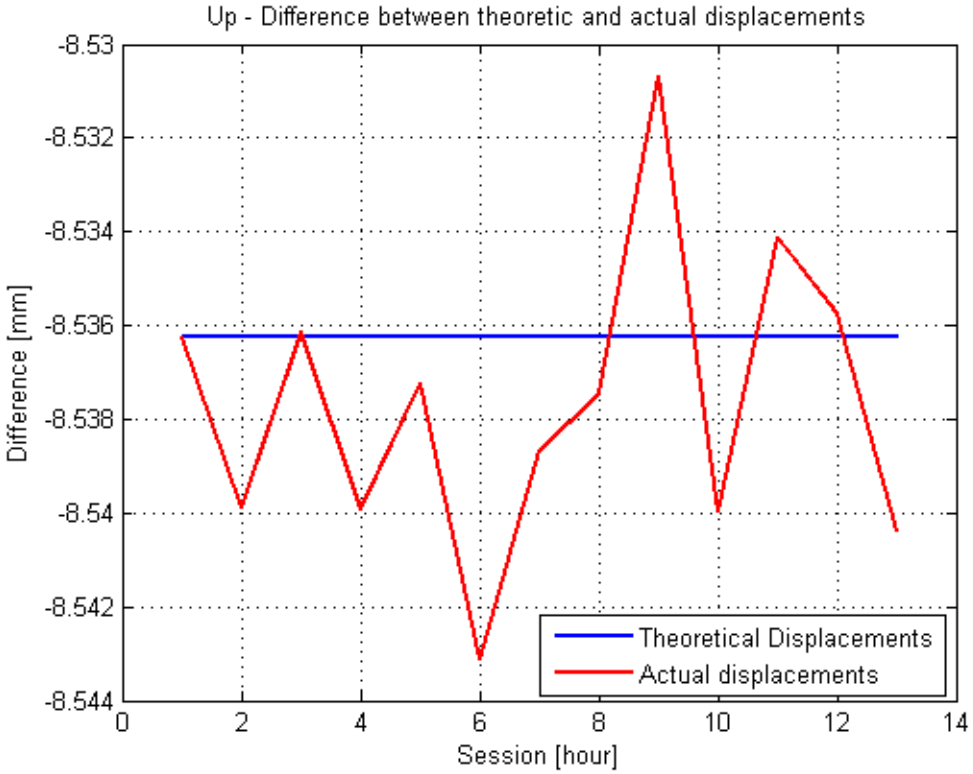

Fig. 6. 36: *Local height component of the baseline. Actual displacements (in red) from the theoretical ones (in blue).*

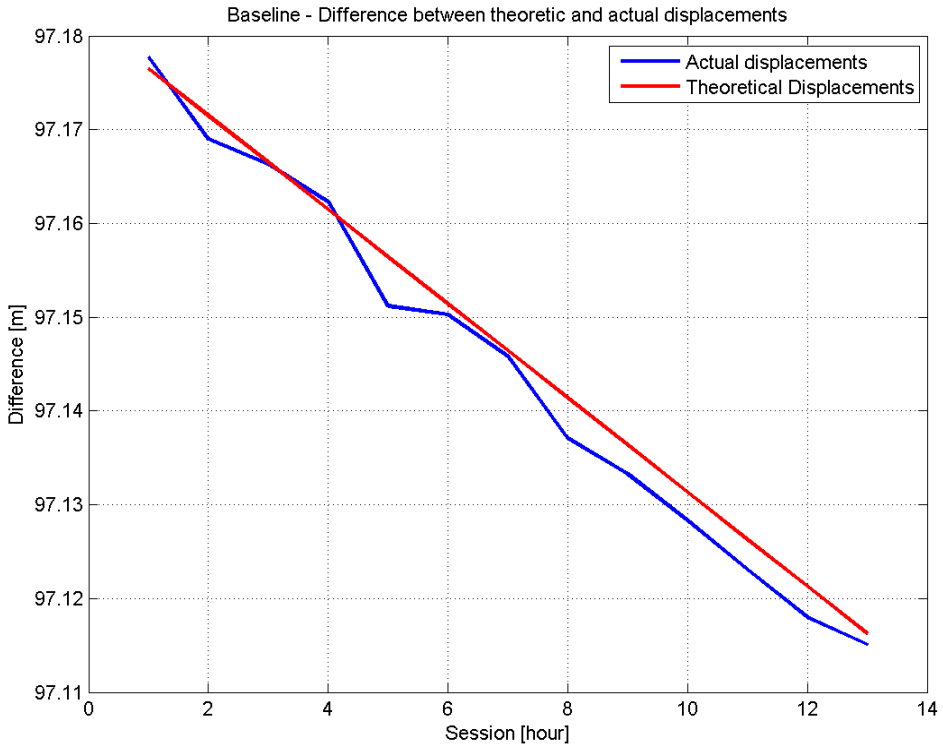

Fig. 6. 37: *Baseline length. Actual displacements (in red) from the theoretical ones (in blue).*

- Significance analysis

The significance analysis of the estimated coordinate differences between repeated surveys is an iterative procedure based on Chi test. This procedure allows a separation of the points into two groups: those whose coordinate estimates are significantly changed with repeated surveys and those whose coordinates are not changed (Biagi, L., et al., 1996).

It has to be assumed that the observations collected in the each session are independent to each other and the estimated coordinates and their residuals follow Gaussian distribution.

The null hypothesis is:

$$H_0: \hat{X}_\iota = \bar{X}_\iota \qquad 6.9$$

where $\hat{X}_\iota$ is the vector of estimated E, N and U coordinates and $\bar{X}_\iota$ is the vector composed by theoretical E, N and U in the local system.

If H_0 is true then the following statistic test holds, for an α of 5 %:

$$\frac{(\hat{X}_\iota - \bar{X}_\iota)^t C_i^{-1} (\hat{X}_\iota - \bar{X}_\iota)}{3} = \chi_0^2 < \chi^2_{0.05,m} \qquad 6.10$$

where C is the empirical covariance matrix computed by the author based on the results of experiment number 2, Castelnuovo Test and m is the number of unknown parameters to be tested (3 here). Thus, $\chi^2_{0.05,m} = 7.815$

If $\chi^2_0 < \chi^2_{0.05,\ 3}$ the null hypothesis is accepted as true, i.e. the coordinates do not show any significant differences at the chosen significance level, $\chi^2_0 > \chi^2_{0.05,\ 3}$ the null hypothesis is not accepted and the coordinates are significantly changed.

In total, just two outliers have been found and a summary of the analysis can be found in Table 6.24.

χ^2_0computed	Outlier
0	-
4.378987514	-
4.845170618	-
0.512707442	-
5.269396929	-
0.232671711	-
1.501184907	-
1.138176787	-
2.12026172	-
2.036340642	-
10.35818601	Yes
2.221765536	-
6.516935292	-
1.647437871	-
6.559182284	-
2.058631621	-
1.898069298	-
1.992240834	-
4.868265091	-
1.899870649	-
7.09734862	-
3.103562398	-
4.486844139	-
3.98733314	-
2.476413263	-
1.178000903	-
5.133285149	-
5.250654534	-
4.986741969	-
4.944666769	-
5.210388606	-

1.985454468	-
3.063246003	-
2.081040851	-
6.652847765	-
3.740538823	-
9.293574234	Yes

Table 6. 24: *Outlier detection based on χ_0^2 test with 3 unknowns and α = 5 %*

2. Baseline Como Geodetic – Como u-blox

To compute local coordinates of u-blox with respect to Como Geodetic, for each session *i* the steps from above must be followed. It is trivial to write again all the formulas; however based on the orientation angles of the two baselines, computed from the estimated coordinates, it was noticed that the two baseline are not perfectly perpendicular to each other. Thus, for the baseline Como Geodetic – Como u-blox corrections should be computed to take into account the extra β = 3.77238 gon. With the help of this corrections (ΔB_i) the imposed displacements and the measured distances can be projected on a line that makes a right angle with the current baseline (see Equation 6.9).

$$\Delta B_i = \delta_i \tan(\beta) \tag{6.11}$$

To shift the end points of the measured baselines on a line at 90^0 with respect to Como Geodetic – Como u-blox line of sight the following steps were performed:

1. All estimated baselines were reduced to horizontal plane:

$$L_i = B_i^{est} \cos(\alpha) \tag{6.12}$$

where α is the slope angle between Pillar and u-blox, computed based on Equation 6.8.

2. Project the end points of the estimated horizontal baseline of each session on a line 90^0 away from Pillar – u-blox the line of sight:

$$B_i^H = L_i - \Delta B_i \tag{6.13}$$

3. Compute the new slope angle between Como Geodetic and Como u-blox (now Como Geodetic – Como ublox vector and orientation of the sliding device are assumed to be orthogonally):

$$\alpha_i' = \Delta h / B_i^H \tag{6.14}$$

4. Last step, transform the estimated horizontal baseline of each session to a slope distance:

$$B_i^{final} = B_i^H / \cos(\alpha_i') \tag{6.15}$$

The same steps have been performed to compute the theoretical baseline lengths when the sliding device is oriented at a right angle from Como Geodetic – Como u-blox direction. Table 6.25 files the results obtained based on the above equations.

Session	Theoretic length [m] B_i^{theo}	Measured length [m] B_i^{final}
0	5.8426	5.8426
1	5.8426	5.839
2	5.8426	5.8389
3	5.8426	5.8412
4	5.8426	5.8376
5	5.8427	5.8377
6	5.8427	5.8411
7	5.8427	5.8394
8	5.8427	5.8377
9	5.8428	5.8437
10	5.8428	5.84
11	5.8429	5.8417
12	5.8429	5.8499

Table 6. 25: *Baseline lengths for each session. Theoretical values (column 2) versus measured values (column 3).*

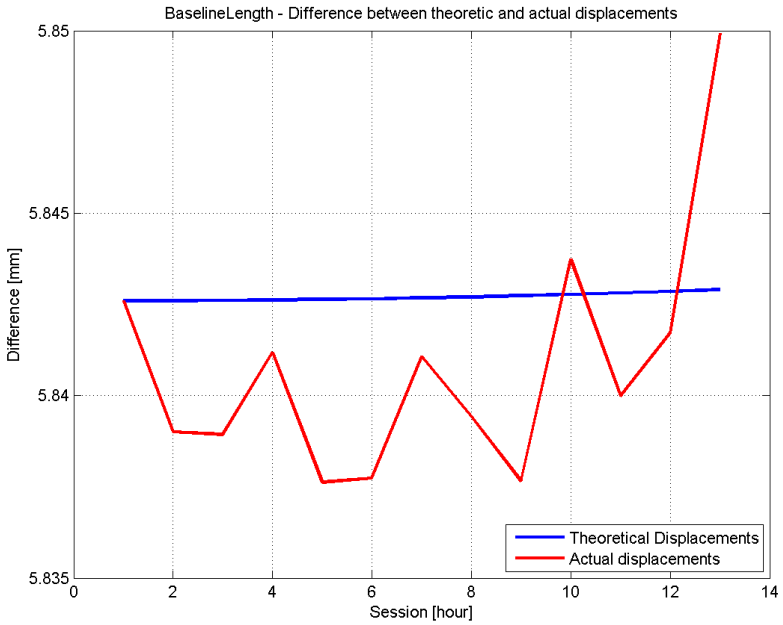

Fig. 6. 38: *Baseline length deviation (red), for each session, with respect to theoretical one (blue).*

Taking into account the precision of the sliding device, lack of antenna calibration and no knowledge about the antenna reference point, errors are expected to influence with few millimetres the estimated quantities. This is specially noticed for the height component; here

the values of residuals are bigger and this is due to lack of any information about antenna PCO (usually, this vector is mainly a vertical offset with very small East and North components). However, based on the results obtained and bearing in mind all shortcomings of u-blox this project comes in support of using u-blox NEO-7P in applications that require centimetre level accuracy, therefore landslide monitoring as well.

Chapter 7. Conclusion and Recommendations

This chapter outlines of the main conclusions obtained throughout the research conducted in the last months, and proposes recommendations for future work related to landslide monitoring by means of low-cost GNSS sensors.

7.1. Conclusions

The objective of this thesis is to investigate the feasibility of low-cost single-frequency GNSS sensors for landslides monitoring.

Landslides are a serious geologic hazard common to almost every country in the world. Globally, landslides are responsible for damages of billions of euro and hundreds of thousands of deaths and injuries each year. Due to the destruction and alarming number of casualties associated with landslide events, a closer monitoring of these natural risks must be ensured by all possible means.

The problem raised above can find its answer in GNSS low-cost sensors. These units can be integrated into complex control systems fully dedicated to collection and distribution of all forms of information related to landslides. To understand the potential of such type of platforms, two static experiments have been planned and performed. Then, one simulation of controlled displacement have been performed and the results have been analysed.

Before treating the experiments a series of conclusion can be drawn regarding u-blox position on today GNSS market:

- Two u-blox sensors of different generation have been tested during the research for this thesis, u-blox LEA-4T and u-blox NEO-7P. Both of them provide data of good quality. The latter presents some improvement in terms of multipath suppression, number of cycle slips and SNR values.
- Year by year u-blox company upgrades and innovates its products. Nowadays, u-blox sensors are capable of tracking more satellite systems in the same time (u-blox 8M model). Moreover, u-blox is capable of connecting and applying to its real - time solution RTCM 2.3 corrections broadcast by reference stations. NMEA streams can be sent out or received as well.

- Phase observations are required for caring out monitoring tasks as they are much more precise than code observations. u-blox gives as output in the raw message both code and phase observations, therefore meets the most basic requirement of any monitoring project.
- Dealing with a single-frequency receiver problems arise in post processing, especially for ionosphere modelling. A geodetic receiver offers the possibility of removing the ionosphere effect by combining the L1 and L2 observables into a new one, L3. Unfortunately, for u-blox this is not the case and final ionospheric global models and real-time corrections from augmentation systems become vital for applications that require cm level accuracy.
- Multipath can become a serious problem in sites with reflection sources leading to errors above the accepted threshold for monitoring applications. A solution can be to mount the antenna on a self-built ground-plane.
- For high accuracy applications antenna calibration is a must and cannot be neglected. The vertical component of the Phase Centre Offset is very important for an accurate estimate of antenna position.
- Commercial and scientific software do not decode u-blox binary format. A work around this is to use a FOSS software like goGPS or RTKLIB to convert the .ubx raw message to RINEX files.

Regarding the first topic of this research, i.e. static acquisition, the main conclusions of the results obtained are summarized below:

- LGO is a very good alternative to heavy scientific software. Milano Prova confirmed that LGO results are very close to Bernese results, both in magnitude and number of problematic sessions detected.
- Castelnuovo Test proved that u-blox can be trusted for to applications with sub-centimetre level accuracies

Regarding the second part of this thesis, the main conclusion of the results obtained are listed below:

- Results for SIMU-SLIDE projects are encouraging. A very cheap and not quite accurate sliding device had been designed and used to simulate displacements. For baseline the results are very satisfactory following the expected trend: baseline length modified for each session as planned.

- u-blox NEO-7P is able to single out horizontal displacements at sub centimetre level.

The practicable application of low cost GNSS equipment for landslide monitoring is proofed in three research projects already. Although accuracies in the sub-centimetre range are obtained which can be compared nearly with ordinary tachometric measurements, the full potential is not exploited yet. Recently the focus is made on a more sophisticated modelling and data handling.

7.2. Recommendations for Future Research

There are still some remaining issue related to monitoring applications by means of low-cost GNSS. Briefly, some of them will be reported in this last part of the thesis.

SIMU – SLIDE experiment provided promising results although a very rudimental sliding device had been used. Subsequently:

- More effort and resources should be guided towards this direction; once a more robust and accurate sliding device becomes available, the experiment should be repeated. The characteristics of the new support should be: possibility of force centring it on a pillar, levels for reaching a perfect horizontal position and a mechanism that can move the antenna 5 mm with very high accuracy on the intended directions. Moreover, a vertical induced displacement should be possible to investigate since errors are usually bigger for this component.

Multipath had been addressed only from a theoretical point of view.

- In future, the u-blox NEO-7P should be fixed on a ground-plane to shield against multipath. Would be an excellent test to perform a static acquisition for few days without a ground-plane and then to repeat the same test but with a ground-plane. The raw data coming from both sessions could be analysed for multipath effect in Spider QC and then processed with LGO. A comparison of results will show if and how much the multipath can affect the final position for a specific site.

The most important parameter in vertical ground deformation monitoring is the height coordinate of a monitored point, the knowledge of the mean antenna PCO and PCV with respect to the ARP (Stepniak et al., 2013). In addition, the main error source for the antenna phase centre is the vertical offset. Precise antenna PCO and PCV calibrations need to be applied (Rothacher, 2001). Therefore in the future the following work should be done:

- Relative antenna calibration of u-blox antenna. This type of calibration is easy to perform in a consistent manner. A very short baseline with accurately known end points must be first established. At one end, a reference antenna should be mounted and at the other end the u-blox NEO-7P antenna. 2 observation sessions of 24 hours are needed to collect the required raw data. Processing first session (without estimating PCO and PCV) the resulting relative position of both stations is corrupted by an unknown mean PCO. Before second session antennas must be swamp between each other; the result of this session will be distorted by the same mean PCO but with opposite sign. Therefore, the mean position deriving from processing both sessions together is correct (because of the opposite sign the PCO cancels). At this moment PCV can be estimated.

The quality of moving receivers should be investigated. u-blox NEO-7P should be tested also for kinematic positioning:

- The author already has planned few experiments for monitoring the platform of Como Borghi train station and a metallic bridge crossed by train. Due to lack of time to properly investigate the results it was decided not to present them in this research but in future works. However, at a first glance it was noticed clearly that u-blox could capture the displacements caused by a train in movement over the bridge; the question that remains is if this displacements are the real vibrations of the train or they are too corrupted by errors. Consequently, further investigations can be conducted in this direction before drawing any conclusion.

For static processing the length of one session should be decreased:

- a time interval of 15 min can be considered (Heunecke et al., 2011) for having a higher sampling rate of the landslide area. Therefore, the Castelnuovo Test raw data can be broke down in 15 min long observation sessions and analysed.
- Once the previous work is done and the results are validated, it is recommended to perform a monitoring of a real landslide site for a period of time.

Appendix A. Spider QC reports

This appendix contains examples of Spider QC final reports. For each of the projects a report was added here. First, is the report for GPS Day 75, 2014 (Milano Prova), then a report for u-blox NEO-7P data and Leica GRX1200 data (GPS Day 130) acquired during Castelnuovo Test. At last, a report for one of the sessions of DRFIT project concludes this appendix.

Milano Prova Example of QC Report

Leica SpiderQC v4.0 (Free Version) Quality Report

Program Run:	2015/06/20 07:06:23.14

File Details:

Observation File:	UBLX0750.14O
GPS Navigation File:	MILA0750.14N
Quality Testing:	**Fail (See below for details)**

Station Details:

Marker Name/Number:	UBLX0750	UBLX0750	
Observer/Agency:			
Receiver #/Type/Vers:			
Antenna #/Type:		SIMULA NONE	
Antenna Offsets (HEN):	0.026	0.000	0.000
Approx Position (XYZ):	4421892.598	718469.940	4525016.357
Approx Position (plh):	45° 28' 46.50083" N	9° 13' 43.60905" E	193.405m
Diff. Est-Header:	-0.1 m dX	-6.0 m dY	1.3 m dZ
Diff. Est-Header:	6.1 m (86398 estimates)		

Session Summary:

Time of first obs:	2014/03/16 00:00:02.00 GPS
Time of last obs:	2014/03/16 23:59:59.00 GPS
Session length:	24.00 hours
GPS week:	1784, day 0
Observation interval:	1.00 seconds
UTC leap seconds:	16 seconds
Num SVs with obs:	31
Num SVs with nav:	32
Total GPS orbits:	410
Total GLONASS orbits:	0
Total Galileo orbits:	0
SVs with obs:	G1 G2 G3 G4 G5 G7 G8 G9 G10 G11 G12 G13 G14 G15 G16 G17 G18 G19 G20 G21 G22 G23 G24 G25 G26 G27 G28 G29 G30 G31 G32
SVs without obs:	G6 R1 R2 R3 R4 R5 R6 R7 R8 R9 R10 R11 R12 R13 R14 R15 R16 R17 R18 R19 R20 R21 R22 R23 R24 R25 E1 E2 E3 E4 E5 E6 E7 E8 E9 E10 E11 E12 E13 E14 E15 E16 E17 E18 E19 E20 E21 E22 E23 E24 E25 E26 E27 E28 E29 E30 E31 E32 E33 E34 E35 E36 E37 E38 E39 E40 E41 E42 E43 E44 E45 E46 E47 E48 E49 E50 E51 E52 E53 E54

	E55 S1 S2 S3 S4 S5 S6 S7 S8 S9 S10 S11 S12 S13 S14 S15 S16 S17 S18 S19 S20 S21 S22 S23 S24 S25 S26 S27 S28 S29 S30 S31 S32 S33 S34 S35 S36 S37 S38 S39 S40 S41 S42 S43 S44 S45 S46 S47 S48 S49 S50
SVs with nav:	G1 G2 G3 G4 G5 G6 G7 G8 G9 G10 G11 G12 G13 G14 G15 G16 G17 G18 G19 G20 G21 G22 G23 G24 G25 G26 G27 G28 G29 G30 G31 G32
SVs without nav:	
User Disabled SVs:	R1 R2 R3 R4 R5 R6 R7 R8 R9 R10 R11 R12 R13 R14 R15 R16 R17 R18 R19 R20 R21 R22 R23 R24 R25

Quality Testing:

	Pass/Fail	Details
General Tests		
Epochs With Data:	Pass	Value 100.0 %, Threshold 99.0 %
File Format:	Pass	
RX Clock:	Pass	
Other:	**Fail**	**(See Error Messages)**
GPS Specific Tests		
Cycle Slips:	Pass	Value 0 slips, Threshold 1418 slips
Multipath:	**Fail**	**Value 3.73m MP1, Threshold 0.5 m**
Data Completeness:	**Fail**	**Value 94.8 %, Threshold 95.0 %**
Navigation Data:	**Fail**	

General Quality Indicators:

Tracking

Num obs > 0°:	932463
Num possible obs > 0°:	1004975
Num obs with invalid nav:	**336**
Num obs without nav:	0
Num obs to unhealthy SV:	30877
Num obs with WLF change:	708881
Num obs GPS > 0°:	932463
Num obs GLONASS > 0°:	0
Num obs Galileo > 0°:	0
Num obs All > 0°:	932463
Epochs with < 5 SV > 10°:	0 (0.0 %)
Epochs with all SV > 10°:	48990 (56.7 %)
Epochs with full data > 10°:	48990 (56.7 %)

Satellite Geometry

DOP	Minimum	Maximum	Average
PDOP	2.5	5.9	3.3
GDOP	2.9	7.4	3.9

Data Gaps

Num epochs with data:	86398
Num epochs without data:	0
Data Gaps:	0.00 seconds

List of Data Gaps (-)

Duration	Start Time	End Time
None		

Non-tracked satellites > 10° (^):

SV	Time (minutes)	Epoch Range	Elevation Range	Azimuth Range
G32	14.717	9217 / 10100	10.00° / 16.43°	202.60° / 203.45°
G1	6.350	9856 / 10237	10.01° / 12.16°	261.98° / 263.76°
G6	309.633	1 / 18579	33.16° / 10.00°	132.93° / 158.49°
G6	209.717	41400 / 53983	67.41° / 15.92°	183.49° / 73.42°
G6	101.300	57411 / 63489	10.00° / 10.00°	321.95° / 282.29°
Total:	641.717 (38502 observations)			

Receiver Clock

Clock Slips > 10°:	9
Max RX clock offset:	0.500155 ms (at 2014/03/16 01:35:31.00)
Num of RX clock resets:	0
Total clock drift:	+0.000000 ms
Rate of clock drift:	+0.000 ms/hr
Av time between resets:	0.000 minute(s)

Quality Indicators by Satellite System:

	Total	GPS	GLONASS	Galileo
Tracking				
Num obs > 10°:	708881	708881	-	-
% obs > 10°:	94.8 %	94.8 %	-	-
Num possible obs > 10°:	747570	747570	-	-
Num complete obs > 10°:	708881	708881	-	-
% complete obs > 10°:	94.8 %	94.8 %	-	-
Average # SV per Epoch:	8.2	8.2	-	-
Obs L2 : Obs L1:	-	-	-	-
Obs L5 : Obs L1:	-	-	-	-
Cycle Slips				
Num cycle slips > 10°:	-	-	-	-
% slips per complete obs:	-	-	-	-
Num complete obs per slip:	-	-	-	-
IOD Slips > 10°:	708687	708687	-	-
Outliers > 10°:	-	-	-	-
LLI L1 : Obs L1:	-	-	-	-
LLI L2 : Obs L2:	-	-	-	-
LLI L5 : Obs L5:	-	-	-	-
Multipath				
MP1 RMS:	3.728 m	3.728 m	-	-
MP2 RMS:	-	-	-	-
MP5 RMS:	-	-	-	-

General Error Messages:

-	Loss	of	power	after	epoch		2014/03/16	00:00:01.00
-	Change	in	observation	interval	detected	at	2014/03/16	01:35:32.00
-	Change	in	observation	interval	detected	at	2014/03/16	03:32:58.00
-	Change	in	observation	interval	detected	at	2014/03/16	05:21:31.00
-	Change	in	observation	interval	detected	at	2014/03/16	07:06:43.00
-	Change	in	observation	interval	detected	at	2014/03/16	09:05:51.00
-	Change	in	observation	interval	detected	at	2014/03/16	11:35:06.00
-	Change	in	observation	interval	detected	at	2014/03/16	14:21:13.00
-	Change	in	observation	interval	detected	at	2014/03/16	20:53:19.00

- Change in observation interval detected at 2014/03/16 23:49:31.00

Castelnuovo Test Example Reports

Leica SpiderQC v4.0 (Free Version) Quality Report

Program Run:	2015/06/20 07:56:43.86

File Details:

Observation File:	UBLOX1300.15O
GPS Navigation File:	cots1300.15n
Quality Testing:	**Fail (See below for details)**

Station Details:

Marker Name/Number:	UBLOX	UBLOX	
Observer/Agency:			
Receiver #/Type/Vers:		SIMULA	
Antenna #/Type:		SIMULA	
Antenna Offsets (HEN):	0.000	0.000	0.000
Approx Position (XYZ):	4398270.321	704070.202	4550190.525
Approx Position (plh):	45° 48' 9.71413" N	9° 05' 40.86146" E	284.461m
Diff. Est-Header:	1.7 m dX	-2.3 m dY	-0.6 m dZ
Diff. Est-Header:	3.0 m (85936 estimates)		

Session Summary:

Time of first obs:	2015/05/10 00:00:00.00 GPS
Time of last obs:	2015/05/10 23:59:59.00 GPS
Session length:	24.00 hours
GPS week:	1844, day 0
Observation interval:	1.00 seconds
UTC leap seconds:	16 seconds
Num SVs with obs:	32
Num SVs with nav:	32
Total GPS orbits:	196
Total GLONASS orbits:	0
Total Galileo orbits:	0
SVs with obs:	G1 G2 G3 G4 G5 G6 G7 G8 G9 G10 G11 G12 G13 G14 G15 G16 G17 G18 G19 G20 G21 G22 G23 G24 G25 G26 G27 G28 G29 G30 G31 G32
SVs without obs:	R1 R2 R3 R4 R5 R6 R7 R8 R9 R10 R11 R12 R13 R14 R15 R16 R17 R18 R19 R20 R21 R22 R23 R24 R25 E1 E2 E3 E4 E5 E6 E7 E8 E9 E10 E11 E12 E13 E14 E15 E16 E17 E18 E19 E20 E21 E22 E23 E24 E25 E26 E27 E28 E29 E30 E31 E32 E33 E34 E35 E36 E37 E38 E39 E40 E41 E42 E43 E44 E45 E46 E47 E48 E49 E50 E51 E52 E53 E54 E55 S1 S2 S3 S4 S5 S6 S7 S8 S9 S10 S11 S12 S13 S14 S15 S16 S17 S18 S19 S20 S21 S22 S23 S24 S25 S26 S27 S28 S29 S30 S31 S32 S33 S34 S35 S36 S37 S38 S39 S40 S41 S42 S43 S44 S45 S46 S47 S48 S49 S50
SVs with nav:	G1 G2 G3 G4 G5 G6 G7 G8 G9 G10 G11 G12 G13 G14 G15 G16 G17 G18 G19 G20 G21 G22 G23 G24 G25 G26 G27 G28 G29 G30 G31 G32
SVs without nav:	
User Disabled SVs:	R1 R2 R3 R4 R5 R6 R7 R8 R9 R10 R11 R12 R13 R14 R15 R16 R17 R18 R19 R20 R21 R22 R23 R24 R25

Quality Testing:

	Pass/Fail	Details
General Tests		
Epochs With Data:	Pass	Value 99.5 %, Threshold 99.0 %
File Format:	Pass	
RX Clock:	Pass	
Other:	**Fail**	**(See Error Messages)**
GPS Specific Tests		
Cycle Slips:	**Fail**	**Value 1661 slips, Threshold 1450 slips**
Multipath:	**Fail**	**Value 0.83m MP1, Threshold 0.5 m**
Data Completeness:	Pass	Value 98.9 %, Threshold 95.0 %
Navigation Data:	Pass	

General Quality Indicators:

Tracking

Num obs > 0°:	816853
Num possible obs > 0°:	969518
Num obs with invalid nav:	0
Num obs without nav:	0
Num obs to unhealthy SV:	21739
Num obs with WLF change:	8225
Num obs GPS > 0°:	816853
Num obs GLONASS > 0°:	0
Num obs Galileo > 0°:	0
Num obs All > 0°:	816853
Epochs with < 5 SV > 10°:	0 (0.0 %)
Epochs with all SV > 10°:	78601 (91.5 %)
Epochs with full data > 10°:	78601 (91.5 %)

Satellite Geometry

DOP	Minimum	Maximum	Average
PDOP	2.5	4.2	3.2
GDOP	3.0	5.2	3.8

Data Gaps

Num epochs with data:	85936
Num epochs without data:	**464**
Data Gaps:	**7.73 minutes**

List of Data Gaps (-)

Duration	Start Time	End Time
9.00 seconds	2015/05/10 00:15:17.00	2015/05/10 00:15:27.00
---	---	---
10.00 seconds	2015/05/10 23:26:46.00	2015/05/10 23:26:57.00
Total:	7.73 minutes	

Non-tracked satellites > 10° (^):

SV	Time (minutes)	Epoch Range	Elevation Range	Azimuth Range
G14	9.633	6005 / 6573	13.55° / 10.00°	40.06° / 39.24°
G31	16.750	13282 / 14277	14.87° / 10.00°	37.30° / 33.10°
G16	16.850	23511 / 24512	13.28° / 10.00°	36.87° / 30.96°

G28	6.067	42893 / 43257	12.23° / 10.00°	51.48° / 52.26°
G17	9.633	48636 / 49214	13.56° / 10.00°	39.92° / 39.18°
G6	6.833	55443 / 55853	11.94° / 10.00°	35.62° / 33.86°
G2	12.033	61463 / 62185	14.30° / 10.00°	42.03° / 40.84°
G5	4.383	66117 / 66380	14.35° / 13.64°	42.80° / 41.18°
G20	19.517	66058 / 67229	14.03° / 10.00°	43.34° / 36.90°
G5	13.767	66650 / 67476	12.85° / 10.00°	39.58° / 35.05°
G18	7.967	82727 / 83205	12.95° / 10.00°	51.58° / 52.08°
Total:	123.433 (7405 observations)			

Receiver Clock

Clock Slips > 10°:	257
Max RX clock offset:	0.724035 ms (at 2015/05/10 00:00:00.00)
Num of RX clock resets:	0
Total clock drift:	+0.000000 ms
Rate of clock drift:	+0.000 ms/hr
Av time between resets:	0.000 minute(s)

Quality Indicators by Satellite System:

	Total	GPS	GLONASS	Galileo
Tracking				
Num obs > 10°:	724972	724972	-	-
% obs > 10°:	98.9 %	98.9 %	-	-
Num possible obs > 10°:	733313	733313	-	-
Num complete obs > 10°:	724972	724972	-	-
% complete obs > 10°:	98.9 %	98.9 %	-	-
Average # SV per Epoch:	8.4	8.4	-	-
Obs L2 : Obs L1:	-	-	-	-
Obs L5 : Obs L1:	-	-	-	-
Cycle Slips				
Num cycle slips > 10°:	1661	1661	-	-
% slips per complete obs:	0.229 %	0.229 %	-	-
Num complete obs per slip:	43647	43647	-	-
IOD Slips > 10°:	721083	721083	-	-
Outliers > 10°:	-	-	-	-
LLI L1 : Obs L1:	0.0023	0.0023	-	-
LLI L2 : Obs L2:	-	-	-	-
LLI L5 : Obs L5:	-	-	-	-
Multipath				
MP1 RMS:	0.833 m	0.833 m	-	-
MP2 RMS:	-	-	-	-
MP5 RMS:	-	-	-	-

Leica SpiderQC v4.0 (Free Version) Quality Report

Program Run:	2015/06/20 08:04:53.16

File Details:

Observation File:	LEICA1300.15O
GPS Navigation File:	003_1300.15n
Quality Testing:	**Fail (See below for details)**

Station Details:

Marker Name/Number:	003	003	
Observer/Agency:			
Receiver #/Type/Vers:	471463	LEICA GX1230GG	8.10
Antenna #/Type:		LEIAX1202GG	
Antenna Offsets (HEN):	0.000	0.000	0.000
Approx Position (XYZ):	4398268.712	704071.968	4550194.051
Approx Position (plh):	45° 48' 9.82415" N	9° 05' 40.95398" E	286.076m
Diff. Est-Header:	2.5 m dX	-4.2 m dY	3.0 m dZ
Diff. Est-Header:	5.7 m (73800 estimates)		

Session Summary:

Time of first obs:	2015/05/10 00:00:00.00 GPS
Time of last obs:	2015/05/10 23:59:59.00 GPS
Session length:	24.00 hours
GPS week:	1844, day 0
Observation interval:	1.00 seconds
UTC leap seconds:	16 seconds
Num SVs with obs:	31
Num SVs with nav:	31
Total GPS orbits:	217
Total GLONASS orbits:	0
Total Galileo orbits:	0
SVs with obs:	G1 G2 G3 G4 G5 G6 G7 G9 G10 G11 G12 G13 G14 G15 G16 G17 G18 G19 G20 G21 G22 G23 G24 G25 G26 G27 G28 G29 G30 G31 G32
SVs without obs:	G8 R1 R2 R3 R4 R5 R6 R7 R8 R9 R10 R11 R12 R13 R14 R15 R16 R17 R18 R19 R20 R21 R22 R23 R24 R25 E1 E2 E3 E4 E5 E6 E7 E8 E9 E10 E11 E12 E13 E14 E15 E16 E17 E18 E19 E20 E21 E22 E23 E24 E25 E26 E27 E28 E29 E30 E31 E32 E33 E34 E35 E36 E37 E38 E39 E40 E41 E42 E43 E44 E45 E46 E47 E48 E49 E50 E51 E52 E53 E54 E55 S1 S2 S3 S4 S5 S6 S7 S8 S9 S10 S11 S12 S13 S14 S15 S16 S17 S18 S19 S20 S21 S22 S23 S24 S25 S26 S27 S28 S29 S30 S31 S32 S33 S34 S35 S36 S37 S38 S39 S40 S41 S42 S43 S44 S45 S46 S47 S48 S49 S50
SVs with nav:	G1 G2 G3 G4 G5 G6 G7 G9 G10 G11 G12 G13 G14 G15 G16 G17 G18 G19 G20 G21 G22 G23 G24 G25 G26 G27 G28 G29 G30 G31 G32
SVs without nav:	G8
User Disabled SVs:	R1 R2 R3 R4 R5 R6 R7 R8 R9 R10 R11 R12 R13 R14 R15 R16 R17 R18 R19 R20 R21 R22 R23 R24 R25

Quality Testing:

	Pass/Fail	Details
General Tests		

Epochs With Data:	Pass	Value 100.0 %, Threshold 99.0 %
File Format:	Pass	
RX Clock:	Pass	
Other:	Pass	

GPS Specific Tests

Cycle Slips:	Pass	Value 69 slips, Threshold 1209 slips
Multipath:	Pass	Value 0.16m MP1 / 0.27m MP2, Threshold 0.5 m
Data Completeness:	Pass	Value 98.6 %, Threshold 95.0 %
Navigation Data:	**Fail**	

General Quality Indicators:

Tracking

Num obs > 0°:	785851
Num possible obs > 0°:	908022
Num obs with invalid nav:	0
Num obs without nav:	**128474**
Num obs to unhealthy SV:	0
Num obs with WLF change:	0
Num obs GPS > 0°:	785851
Num obs GLONASS > 0°:	0
Num obs Galileo > 0°:	0
Num obs All > 0°:	785851
Epochs with < 5 SV > 10°:	12600 (14.6 %)
Epochs with all SV > 10°:	79237 (91.7 %)
Epochs with full data > 10°:	79237 (91.7 %)

Satellite Geometry

DOP	Minimum	Maximum	Average
PDOP	2.5	4.2	3.2
GDOP	3.0	5.2	3.9

Data Gaps

Num epochs with data:	86400
Num epochs without data:	0
Data Gaps:	0.00 seconds

List of Data Gaps (-)

Duration	Start Time	End Time
None		

Non-tracked satellites > 10° (^):

SV	Time (minutes)	Epoch Range	Elevation Range	Azimuth Range
G16	27.650	22988 / 24647	14.82° / 10.00°	41.08° / 30.96°
G7	2.550	33666 / 33819	10.92° / 10.00°	66.10° / 66.66°
G28	8.617	42970 / 43487	13.18° / 10.00°	51.17° / 52.26°
G17	11.950	48757 / 49474	14.41° / 10.00°	40.15° / 39.18°
G6	17.883	55079 / 56152	14.84° / 10.00°	38.82° / 33.86°
G2	13.567	61699 / 62513	14.84° / 10.00°	42.22° / 40.84°
G20	24.933	66090 / 67586	14.92° / 10.00°	45.33° / 36.90°
G5	24.450	66366 / 67833	14.61° / 10.00°	43.47° / 35.05°

G18	7.967	83171 / 83649	12.95° / 10.00°	51.58° / 52.08°
Total:	139.567 (8373 observations)			

Receiver Clock

Clock Slips > 10°:	0
Max RX clock offset:	0.000044 ms (at 2015/05/10 13:32:48.00)
Num of RX clock resets:	0
Total clock drift:	+0.000000 ms
Rate of clock drift:	+0.000 ms/hr
Av time between resets:	0.000 minute(s)

Quality Indicators by Satellite System:

	Total	GPS	GLONASS	Galileo
Tracking				
Num obs > 10°:	604295	604295	-	-
% obs > 10°:	98.6 %	98.6 %	-	-
Num possible obs > 10°:	612679	612679	-	-
Num complete obs > 10°:	604295	604295	-	-
% complete obs > 10°:	98.6 %	98.6 %	-	-
Average # SV per Epoch:	7.0	7.0	-	-
Obs L2 : Obs L1:	1.000	1.000	-	-
Obs L5 : Obs L1:	-	-	-	-
Cycle Slips				
Num cycle slips > 10°:	69	69	-	-
% slips per complete obs:	0.011 %	0.011 %	-	-
Num complete obs per slip:	875790	875790	-	-
IOD Slips > 10°:	243	243	-	-
Outliers > 10°:	-	-	-	-
LLI L1 : Obs L1:	-	-	-	-
LLI L2 : Obs L2:	0.0001	0.0001	-	-
LLI L5 : Obs L5:	-	-	-	-
Multipath				
MP1 RMS:	0.163 m	0.163 m	-	-
MP2 RMS:	0.267 m	0.267 m	-	-
MP5 RMS:	-	-	-	-

SIMU-SLIDE QC Model Report

Leica SpiderQC v4.0 (Free Version) Quality Report

Program Run:	2015/06/20 08:10:02.43

File Details:

Observation File:	ublx5.15O
GPS Navigation File:	cots5.15n
Quality Testing:	**Fail (See below for details)**

Station Details:

Marker Name/Number:			
Observer/Agency:	GFL	POLIMI	
Receiver #/Type/Vers:		SIMULA	
Antenna #/Type:		SIMULA	
Antenna Offsets (HEN):	0.000	0.000	0.000
Approx Position (XYZ):	4398270.321	704070.202	4550190.525
Approx Position (plh):	45° 48' 9.71413" N	9° 05' 40.86146" E	284.461m
Diff. Est-Header:	2.7 m dX	-4.5 m dY	0.9 m dZ
Diff. Est-Header:	5.3 m (10736 estimates)		

Session Summary:

Time of first obs:	2015/06/04 10:00:00.00 GPS
Time of last obs:	2015/06/04 12:59:59.00 GPS
Session length:	3.00 hours
GPS week:	1847, day 4
Observation interval:	1.00 seconds
UTC leap seconds:	16 seconds
Num SVs with obs:	14
Num SVs with nav:	32
Total GPS orbits:	54
Total GLONASS orbits:	0
Total Galileo orbits:	0
SVs with obs:	G2 G6 G12 G13 G14 G15 G17 G18 G22 G24 G25 G28 G29 G31
SVs without obs:	G1 G3 G4 G5 G7 G8 G9 G10 G11 G16 G19 G20 G21 G23 G26 G27 G30 G32 R1 R2 R3 R4 R5 R6 R7 R8 R9 R10 R11 R12 R13 R14 R15 R16 R17 R18 R19 R20 R21 R22 R23 R24 R25 E1 E2 E3 E4 E5 E6 E7 E8 E9 E10 E11 E12 E13 E14 E15 E16 E17 E18 E19 E20 E21 E22 E23 E24 E25 E26 E27 E28 E29 E30 E31 E32 E33 E34 E35 E36 E37 E38 E39 E40 E41 E42 E43 E44 E45 E46 E47 E48 E49 E50 E51 E52 E53 E54 E55 S1 S2 S3 S4 S5 S6 S7 S8 S9 S10 S11 S12 S13 S14 S15 S16 S17 S18 S19 S20 S21 S22 S23 S24 S25 S26 S27 S28 S29 S30 S31 S32 S33 S34 S35 S36 S37 S38 S39 S40 S41 S42 S43 S44 S45 S46 S47 S48 S49 S50
SVs with nav:	G1 G2 G3 G4 G5 G6 G7 G8 G9 G10 G11 G12 G13 G14 G15 G16 G17 G18 G19 G20 G21 G22 G23 G24 G25 G26 G27 G28 G29 G30 G31 G32
SVs without nav:	
User Disabled SVs:	R1 R2 R3 R4 R5 R6 R7 R8 R9 R10 R11 R12 R13 R14 R15 R16 R17 R18 R19 R20 R21 R22 R23 R24 R25

Quality Testing:

	Pass/Fail	Details
General Tests		
Epochs With Data:	Pass	Value 99.4 %, Threshold 99.0 %
File Format:	Pass	
RX Clock:	Pass	
Other:	**Fail**	**(See Error Messages)**
GPS Specific Tests		
Cycle Slips:	**Fail**	**Value 194 slips, Threshold 158 slips**
Multipath:	**Fail**	**Value 0.88m MP1, Threshold 0.5 m**
Data Completeness:	Pass	Value 98.7 %, Threshold 95.0 %
Navigation Data:	Pass	

General Quality Indicators:

Tracking

Num obs > 0°:	88233
Num possible obs > 0°:	102265
Num obs with invalid nav:	0
Num obs without nav:	0
Num obs to unhealthy SV:	0
Num obs with WLF change:	806
Num obs GPS > 0°:	88233
Num obs GLONASS > 0°:	0
Num obs Galileo > 0°:	0
Num obs All > 0°:	88233
Epochs with < 5 SV > 10°:	0 (0.0 %)
Epochs with all SV > 10°:	9719 (90.5 %)
Epochs with full data > 10°:	9719 (90.5 %)

Satellite Geometry

DOP	Minimum	Maximum	Average
PDOP	2.9	3.8	3.3
GDOP	3.3	4.5	3.9

Data Gaps

Num epochs with data:	10736
Num epochs without data:	**64**
Data Gaps:	**1.07 minutes**

List of Data Gaps (-)

Duration	Start Time	End Time
10.00 seconds	2015/06/04 10:27:37.00	2015/06/04 10:27:48.00
11.00 seconds	2015/06/04 10:57:52.00	2015/06/04 10:58:04.00
11.00 seconds	2015/06/04 11:28:07.00	2015/06/04 11:28:19.00
10.00 seconds	2015/06/04 11:58:22.00	2015/06/04 11:58:33.00
11.00 seconds	2015/06/04 12:28:36.00	2015/06/04 12:28:48.00
11.00 seconds	2015/06/04 12:58:52.00	2015/06/04 12:59:04.00
Total:	1.07 minutes	

Non-tracked satellites > 10° (^):

SV	Time (minutes)	Epoch Range	Elevation Range	Azimuth Range

G28	6.650	1006 / 1405	12.45° / 10.00°	51.51° / 52.37°
G17	10.033	6864 / 7456	13.72° / 10.00°	40.09° / 39.35°
Total:	16.683 (1001 observations)			

Receiver Clock

Clock Slips > 10°:	59
Max RX clock offset:	0.754661 ms (at 2015/06/04 10:00:00.00)
Num of RX clock resets:	0
Total clock drift:	+0.000000 ms
Rate of clock drift:	+0.000 ms/hr
Av time between resets:	0.000 minute(s)

Quality Indicators by Satellite System:

	Total	GPS	GLONASS	Galileo
Tracking				
Num obs > 10°:	79185	79185	-	-
% obs > 10°:	98.7 %	98.7 %	-	-
Num possible obs > 10°:	80202	80202	-	-
Num complete obs > 10°:	79185	79185	-	-
% complete obs > 10°:	98.7 %	98.7 %	-	-
Average # SV per Epoch:	7.4	7.4	-	-
Obs L2 : Obs L1:	-	-	-	-
Obs L5 : Obs L1:	-	-	-	-
Cycle Slips				
Num cycle slips > 10°:	194	194	-	-
% slips per complete obs:	0.245 %	0.245 %	-	-
Num complete obs per slip:	40817	40817	-	-
IOD Slips > 10°:	78552	78552	-	-
Outliers > 10°:	-	-	-	-
LLI L1 : Obs L1:	0.0024	0.0024	-	-
LLI L2 : Obs L2:	-	-	-	-
LLI L5 : Obs L5:	-	-	-	-
Multipath				
MP1 RMS:	0.882 m	0.882 m	-	-
MP2 RMS:	-	-	-	-
MP5 RMS:	-	-	-	-

Notes:

(*) Signal strength is mapped between 1 (worst) and 9 (best), 5 is the threshold for good SNR, 0 indicates value is unknown

(#) A complete GPS observation contains non-zero L1 code and phase measurements with a SNR of at least 4

(#) A complete GLONASS observation contains non-zero code and phase measurements with a SNR of at least 4

(#) A complete Galileo observation contains non-zero code and phase measurements with a SNR of at least 4

(-) The minimum duration of a data gap to be reported is 5 seconds

(^) A satellite has to be above the elevation mask with no observations recorded for at least 120 seconds to be reported

- The elevation mask is set at 10°
- Abbreviations: Av=Average, IOD=Ionospheric delay, Num=Number, Obs=Observations, MP=Multipath, SV=Satellite vehicle, Elev=Elevation, Nav=Navigation data (ephemeris), WLF=Wavelength factor
- It took 3.3 seconds to process this file
- This file was processed using version 4.0.0.49

Appendix B. Local coordinates transformation

To compute local coordinates of a point with respect to an arbitrary origin, the following rotation must be applied.

$$l_1 = \begin{vmatrix} E \\ N \\ U \end{vmatrix} = R\Delta X_{O-1}$$

where R is the rotation matrix

$$R = \begin{vmatrix} -sin\lambda_o & cos\lambda_o & 0 \\ -sin\varphi_o cos\lambda_o & -sin\varphi_o sin\lambda_o & cos\varphi_o \\ cos\varphi_o cos\lambda_o & cos\varphi_o sin\lambda_o & sin\varphi_o \end{vmatrix}$$

with λ_o and φ_o are the latitude and longitute of the point set as origin of the newly formed local coordinate system.

Bibliography

Awange, J.L, Environmental Monitoring using GNSS, Environmental Science and Engineering, 2012

Bălteanu, D., Chendeş, V., Sima, M., Enciu, P., A country-wide spatial assessment of landslide susceptibility in Romania, Geomorphology, volume 124, issues 3-4, 15 December 2010,

BeiDou Navigation Satellite System Signal In Space Interface Control Document Open Service Signal B1I (Version 1.0), China Satellite Navigation Office, December 2012

Bernese GPS Software user manual, 2007

Betti, B., Biagi, L., Crespi, M., Riguzzi, F., GPS sensitivity analysis applied to non-permanent deformation control networks, Journal of Geodesy, 1999

Bilban, G., Vulic, M., Ganic, A., The use of Leica Geo Office in mine surveying, RMZ Materials and Geoenvironment, Vol.54, No.4, December 2007

Blewitt, G., Basic of GPS technique, appears in the textbook Geodetic Applications of GPS, 1997

Braasch, M.S., Multipath Effects, Global Positioning Systems: Theory and Applications, American Institute of Aeronautics and Astronautics, Vol.1, 1996

Brown, R.G., Hwang, P.Y.C., Introduction to Random Signals and Applied Kalman Filtering, second edition, 1992

Carcanague, S., Low-cost GPS/GLONASS Precise Positioning Algorithm in Constrained Environment

Carrier phase and its measurement for GNSS, Cillian O'Driscoll, Inside GNSS, July/August 2010

Cruden, D.M., 1991, A Simple Definition of a Landslide. Bulletin of the International Association of Engineering Geology, No. 43, pp. 27-29

Dodson, A.H., Meng, X., Roberts, G.W., Adaptive Method for Multipath Mitigation and Its Applications for Structural Deflection Monitoring, 2001)

European Commission and European Space Agency (2002) Galileo mission high level definition, 3rd issue.http://ec.europa.eu/dgs/energy transport/Galileo/doc/Galileo hld v3 23 09 02.pdf. Accessed 11 Nov 2008

Federal Aviation Administration [FAA]), FAQ on WAAS

Galileo Open Service, Singnal in Space Interface Control Document, OS SIS ICS, Issue 1, European Commission, September 2010

Gassner, G., Wieser, A., Brunner, F.K., GPS Software Development for Monitoring of Landslides, FIG XXII International Congress, Washington, D.C. USA, April 2002

Gili, J.A, Corominas, J., Rius, J., Using Global Positioning System techniques in landslide monitoring, ELSEVIER, Engineering Geology, 2000

GLONASS Interface Control Document, Navigational radiosignal L1, L2, Rusian Institute of Space Device Engineering, January 2008

GPS, GLONASS; Galileo and more. Springer, Wien

Gunther, J., Heunecke, O., Pink, S., Schuhback, S., Development towards a low-cost GNSS based sensor network for the monitoring of landslides, May 2008

Hartinger H (2002), Development of a continuous GPS deformation monitoring system, Shaker Verlag Aachen

Heunecke, O., Glabsch, J., Schuhbacl, S., Landslide Monitoring Using Low Cost GNSS Equipment – Experiences from Two Alpine Testing Sites, Journal of Civil Engineering and Architecture, Volume 5, No.8, August 2011

Hofman-Wellenhof B, Lichtenegger H, Wasle E (2008) GNSS global navigation satellite system:

Im, S.B, Hurlebaus, S., Kang, Y.J, Summary Review of GPS Technology for Structural Health Monitoring, Journal of Structural Engineering, October 2013

Jayanta, K.R., Use of Multiple Antennas to Mitigate Carrier Phase Multipath in Reference Stations, ION GPS-99, September 1999

Jo, H., Sim, S-H., Tatkowski, A., Spencer Jr., B.F., Nelson M.E, Feasibility of displacement monitoring using low-cost GPS receivers, Structural Control and Health Monitoring, 2012, DOI: 10.1002/stc.1532

K.N. Suryanarayana Rao and S. Pal. The Indian SBAS System – GAGAN. Abstract from the India-United States Conference on Space Science, Applications, and Commerce. June 2004.

Klobuchar, J., 1987. Ionospheric Time-Delay Algorithms for Single-Frequency GPS Users. IEEE Transactions on Aerospace and Electronic Systems (3), pp. 325-331.

Langley, R.B., The GPS receiver: An introduction, GPS World, Vol. 2, No. 1, January 1991, pp. 50-53

Larocca, A.P.C, Schaal, R.E., Santos, M.C, Langley, R.B, Kim, D., Dynamic Monitoring of Structures at the Milimeter Level: GPS versus Displacement Transducers and Accelerometers – A Summary, ION GNSS 18th International Technical Meeting of the Satellite Division, Sepetmber 2005.

Leick A (1995), GPS satellite surveying, 2nd edition, John Wiley & Sons, Inc., New York

Li, B., Teunissen, P.J.G, High Dimensional Integer Ambiguity Resolution: A First Comparison between LAMBDA and Bernese, The Journal of Navigation, 2011

Li, X., The Advantage of an Integrated RTK-GPS System in Monitoring Structural Deformation, Journal of Global Positioning Systems, 2004, Vol.3

Magged, K.M.A., Assessment of the accuracy of Processing GPS Static Baselines up to 40 km using single and dual frequency GPS receivers, International Journal of Modern Engineering Research (IJMER), Vol. 4, Issue 1, January 2014

Navstar GPS Space Segment/Navigation User Segment Interfaces IS-GPS-200F, GPS Directorate, March 2012

Petovello, M., Absolutely Relative Positioning, Inside GNSS, May/June 2011

Prasad R, Ruggieri M (2005) Applied satellite navigation using GPS, GALILEO and augmentation systems. Artech House, Boston/London

Rawat, M.S., Joshi, V., Rawat, B.S., Kumar, K, Landslide movement monitoring using GPS technology: A case study of Bakthang lanslide, Gangtok, East Sikkim, India, Journal of Development and Agricultural Economics, Vol.3, May 2011

Reid, M.E., LaHusen, G., Baum, R.L, Kean, J.W., Schulz, W.H., Highland, L.M., Real-Time Monitoring of Landslides, USGS, 2006

Rodriguez, J-A., Hein, G.W., GNSS Signals and Spectra, in Proceedings of the 2nd meeting of the international Committee on Global Navigation Satellite System (IGC-02), Bangalore, India, Spetmeber, 2007

RTKLIB ver. 2.4.2 Manual

Salvati, P., Bianchi, C., Rossi, M., Guzzetti, F., Societal landslide and flood risk in Italy, March, 2010

Schwieger, V., Accurate High-Sensitivity GPS for Short Baselines, FIG Working Week 2009, Surveyors Key Role in Accelerated Development, Eilat, Israel, 3-8 May 2009

Schwieger, V., Glaser, A., Possibilities of Low Cost GPS Technology for Precise Geodetic Applications, From Pharaohs to Geoinformatics, FIG Working Week 2005, Cairo, Egypt, April 16-21, 2005

Schwieger, V., High-Sensitivity GPS – an Availability, Reliability and Accuracy Test, FIG Working Week 2008, Sweden, 14-19 June 2008

Schwieger, V., High-Sensitivity GPS – the Low Cost Future of GNSS ?!, International Federation of Surveyors, August, 2007

Şanlioglu, I., Zeybek, M., Investigation on GPS heighting accuracy with use of tropospheric models in commercial GPS softwares for different heights, FIG Working Week 2012, Italy, May 2012

Stepniak, K., Baryla, R., Wielgosz, P., Kurpinski, G., Optimal Data Processing Strategy in Precise GPS Levelling Networks, Acta Geodeyn. Geomater, Vol.10, N0.4, 2013, DOI: 10.13168/AGG.2013.0044

Tawk, Y., Advanced Algorithmic and Architecture Designs for Future Satellite Navigation Receivers, April, 2013

Teunissen, P.J.G., 1993, Least-Squares Estimation of the Integer GPS Ambiguities, Delft Geodetic Computing Centre (LGR), Delft University of Technology.

The policy issue of landslide in Romania, 2005

Wells, D.E., et al., Guide to GPS Positioning, Fredericton, New Brunswick: Canadian GPS Associates, 1987

Wieser, A., Gaggl, M., Hartinger, H., Improved Positioning Accuracy with High-Sensivity GNSS Receivers and SNR Aided Integrity Monitoring of Pseudo-Range Observations,

Wisniewski, B., Bruniecki, K., Moszynski, M., Evaluation of RTKLIB's Positioning Accuracy Using low-cost GNSS receiver and ASG-EUPOS, The International Journal on Marne Navigation and Safety of Sea Transportation, Volume 7, Number 1, March 2013

Zhang, J., Li, B., Dempster, A.G., Rizos, C., Evaluation of High Sensitivity GPS Receivers, International Symposium on GPS/GNSS, Taipei, October , 2010